

Wilfrid Laurier University

Scholars Commons @ Laurier

Theses and Dissertations (Comprehensive)

2014

Relative Equilibria of Isosceles Triatomic Molecules in Classical Approximation

Damaris Miriam McKinley

Wilfrid Laurier University, damaris.mckinley@gmail.com

Follow this and additional works at: <https://scholars.wlu.ca/etd>



Part of the [Chemistry Commons](#), [Dynamical Systems Commons](#), [Non-linear Dynamics Commons](#), [Numerical Analysis and Computation Commons](#), [Ordinary Differential Equations and Applied Dynamics Commons](#), and the [Physics Commons](#)

Recommended Citation

McKinley, Damaris Miriam, "Relative Equilibria of Isosceles Triatomic Molecules in Classical Approximation" (2014). *Theses and Dissertations (Comprehensive)*. 1686.
<https://scholars.wlu.ca/etd/1686>

This Thesis is brought to you for free and open access by Scholars Commons @ Laurier. It has been accepted for inclusion in Theses and Dissertations (Comprehensive) by an authorized administrator of Scholars Commons @ Laurier. For more information, please contact scholarscommons@wlu.ca.

RELATIVE EQUILIBRIA OF ISOSCELES TRIATOMIC
MOLECULES
IN CLASSICAL APPROXIMATION

by

DAMARIS MCKINLEY

THESIS

Submitted to the Department of Mathematics

Faculty of Science

in partial fulfilment of the requirements for the

Master of Science in Mathematics

Wilfrid Laurier University

September, 2014

(Damaris McKinley) 2014©

Abstract

In this thesis we study relative equilibria of di-atomic and isosceles tri-atomic molecules in classical approximations with repulsive-attractive interaction. For di-atomic systems we retrieve well-known results. The main contribution consists of the study of the existence and stability of relative equilibria in a three-atom system formed by two identical atoms of mass m and a third of mass m_3 , constrained in an isosceles configuration at all times.

Given the shape of the binary potential only, we discuss the existence of equilibria and relative equilibria. We represent the results in the form of energy-momentum diagrams. We find that fixing the masses and varying the potential defining parameters could lead to no spatial, one family of spatial, or two families of spatial relative equilibria. We also observe that varying the value of m leads to a shift in the relative equilibria, and that varying m_3 has no effect on the existence of relative equilibria, but may change their stability. We specialize the existence results to Lennard-Jones models and further study stability by performing numerical experiments.

Acknowledgements

I would like to deeply thank my supervisor, Dr. Cristina Stoica, for her patience and guidance throughout my Undergraduate and Graduate studies. She has immensely broadened my view on the field of Mathematics, and has truly made this (at times overwhelming) experience, more enjoyable. Cristina has been a dear friend and without her support I would not have accomplished the things that I have.

I am grateful to all of my instructors, lab coordinators and those who have contributed to my learning and growing throughout my studies. To my committee members, thank you for taking the time to read and provide constructive feedback for the work encompassed in these covers.

To my wonderful parents and siblings, for all of the laughter, love and support. I greatly cherish our talks, Sunday lunches and family events.

Finally to my loving husband Sean, whose unconditional support, advice and belief in my abilities, has inspired me to continue on my quest for knowledge, and achieve my dreams. Whose confidence is a daily inspiration to push further than I ever thought possible.

Contents

Abstract	i
Acknowledgements	ii
Contents	iii
List of Figures	vi
1 Introduction	1
1.1 General Theory	1
1.2 Outline of Thesis and Results	6
2 Diatomic molecules	9
2.1 Two point-mass systems	9
2.2 Analytical solution	11
2.3 Relative equilibria, the Energy-Momentum diagram and Hill regions .	13
2.4 Diatomic Lennard-Jones molecules	16
3 Isosceles three point-mass systems	25
3.1 Three point-mass systems in Jacobi coordinates	25

3.2	Isosceles configurations	28
4	Relative equilibria for molecular-type interactions	34
4.1	Planar equilibria and relative equilibria ($z = 0$)	36
4.1.1	The qualitative approach	36
4.1.2	The analytical approach	39
4.2	Spatial equilibria and relative equilibria ($z \neq 0$)	40
4.2.1	The qualitative approach	40
4.2.2	The analytical approach	45
4.3	Stability	48
4.3.1	Lyapunov stability	49
4.3.2	Spectral Stability	51
5	Numerical Simulations for Lennard-Jones Type Interactions	52
5.1	General set-up	52
5.2	Numerical Simulations	54
6	Conclusion	63
A	Equilibria and stability for autonomous ODEs	66
B	Mathematical formulation of conservative mechanical N-point mass systems	71
B.1	Newtonian N -Body Systems	71
B.2	Lagrangian Formulation	81
B.3	The Legendre transform and Hamiltonian mechanics	86
B.4	Cyclic Coordinates	91

B.5	Equilibria and relative equilibria	94
B.6	Hill regions of motion	98
C	Matlab code used for Numerical Simulations	99
	Bibliography	117

List of Figures

1.1	A typical shape of a repulsive-attractive inter-atomic potential. The parameters r_e and D_e are the distance at which the potential reaches its minimum and the depth of the potential well, respectively, and are determined experimentally.	2
2.1	The reduced potential $V_{\text{red}}(r; c) = \frac{c^2}{2Mr^2} - \frac{A}{r^6} + \frac{B}{r^{12}}$ for various values of the angular momentum c . The lowest curve corresponds to $c = 0$. The constants are taken as $A = 1$, $B = 32$ and $M = 1$	17
2.2	The reduced Lennard-Jones potential diagram when $c = 0$, i.e. when $V_{\text{red}}(r; 0) = V(r)$	18
2.3	The phase plane diagram when $c = 0$	19
2.4	The reduced Lennard-Jones potential diagram when $0 < c < c_{cr}$	20
2.5	The phase plane diagram when $0 < c < c_{cr}$	20
2.6	The reduced Lennard-Jones potential diagram with $c = c_{cr}$	21
2.7	The phase plane diagram when $c = c_{cr}$	22
2.8	The reduced Lennard-Jones potential diagram when $c > c_{cr}$	22
2.9	The phase plane diagram when $c > c_{cr}$	23
2.10	The Energy-Momentum diagram for a diatomic molecule.	24

3.1	The three point mass system with a change of coordinates, \mathbf{r} and \mathbf{s}	26
3.2	The three point mass system with change of coordinates.	29
4.1	The sum $F'(r) + G'\left(\frac{r}{2}\right)$, pictured in dark blue, displaying one maximum. The curves $\frac{c^2}{Mr^3}$ can intersect it in two points (the purple and light blue curves), which corresponds to angular momenta $0 < c < c_{0,p}$ or in one point (the black curve), which corresponds to an angular momentum $c = c_{0,p}$. For momenta $c > c_{0,p}$ there are no intersections.	37
4.2	The sum $F'(r) + G'\left(\frac{r}{2}\right)$, pictured in dark blue, displaying two maxima. The curves $\frac{c^2}{Mr^3}$ can intersect it in four points, three points (the brown curve), two points (the light blue curve), or in one point (the black curve).	38
4.3	Diagram of $F'(r)$ depicting $\frac{c^2}{Mr^3}$ for $c = c_{0,s}$ and $c = c_{1,s}$	41
5.1	Dependency of the distance $m_1 - m_2$ on the angular momentum, for planar RE of an H_3 -type molecule.	55
5.2	Dependency of the distance $m_1 - m_2$ on the angular momentum for spatial RE of an H_3 -type molecule.	56
5.3	Dependency of the “height” distance m_3 to the origin on the angular momentum for spatial RE of an H_3 -type molecule.	56
5.4	The Energy-Momentum diagram for H_3 -type molecules. At low momenta there are three families of RE: two planar and one spatial. As the momentum increases, the spatial family meets the planar family and it bifurcates	57
5.5	Close-up of the spatial RE bifurcation	57

5.6	Dependency of the distance $m_1 - m_2$ on the angular momentum c , for planar RE molecules for an H_2D -type molecule ($m = 0.5$). As m increases, planar RE are present for higher momenta.	58
5.7	Dependency of the distance $m_1 - m_2$ on the angular momentum c , for planar RE molecules for an D_2H -type molecule ($m = 1.5$). As m increases, planar RE are present for higher momenta.	58
5.8	Dependency distance $m_1 - m_2$ on the angular momentum c for spatial RE of an H_2D -type molecule ($m = 0.5$)	59
5.9	Dependency distance $m_1 - m_2$ on the angular momentum c for spatial RE of an D_2H -type molecule ($m = 1.5$)	59
5.10	The dependency of the “height” distance m_3 to the origin on the angular momentum c for spatial RE of an H_2D -type molecule ($m = 0.5$)	60
5.11	The dependency of the “height” distance m_3 to the origin on the angular momentum c for spatial RE of a D_2H -type molecule ($m = 1.5$)	60
5.12	The Energy-Momentum diagram for H_2D -type molecule ($m = 0.5$) .	61
5.13	H_2D -type molecule ($m = 0.5$)	61
5.14	The Energy-Momentum diagram for D_2H -type molecule ($m = 1.5$) .	62
5.15	A close-up of the bifurcation for a D_2H -type molecule ($m = 1.5$) . .	62

Chapter 1

Introduction

1.1 General Theory

In Molecular Dynamics, classical approximations are often employed in order to reduce the computational effort that is required when using the corresponding quantum-based models. These approximations consist in modelling the atoms in the realm of classical mechanics as mass points which interact via a potential determined experimentally.

Within the classical mechanics framework, the simplest atomic models assume that the atoms are in binary interactions only, and that the mutual potential is defined by a *repulsive-attractive* reciprocal action as follows (Figure 1.1):

- atoms in close proximity repel each other;
- at medium range, the atoms attract, and there exists a unique distance at which the atoms are in a stable equilibrium;
- at large distances, the atoms do not interact.

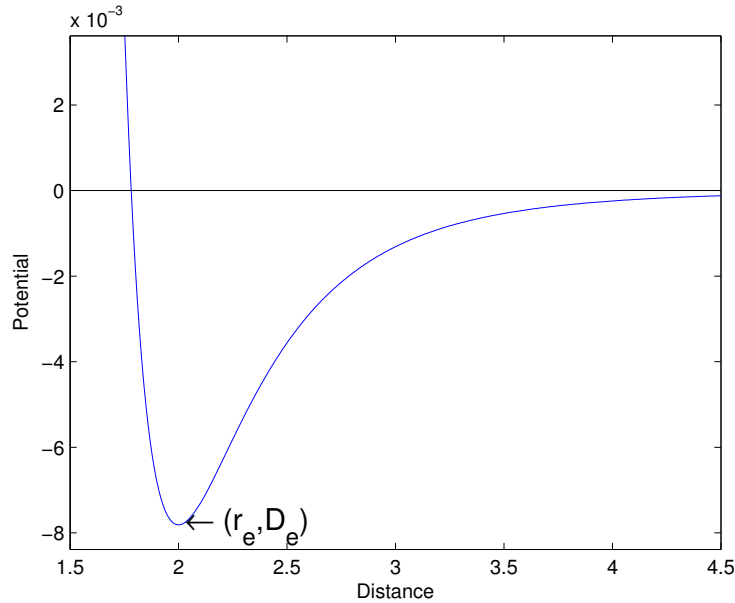


Figure 1.1: A typical shape of a repulsive-attractive inter-atomic potential. The parameters r_e and D_e are the distance at which the potential reaches its minimum and the depth of the potential well, respectively, and are determined experimentally.

The most common functional relation expressing the atomic repulsive-attractive interaction is the 12–6 *Lennard-Jones* potential. Denoting r as the distance between atoms, the Lennard-Jones potential is given by

$$V(r) = -\frac{A}{r^6} + \frac{B}{r^{12}}$$

where $A = 4D_e r_e^6$ and $B = 4D_e r_e^{12}$. The Lennard-Jones potential is known for providing a particularly accurate model for neutral atoms and molecules, as well as noble gas atoms. The parameters in the equation are derived from either “second-virial” or “viscosity coefficients” [Bird & al. (1967)]. However, the use of the powers 6 and 12 of the inverse of the distance in the potential is due to a computational convenience; a discussion on the validity of classical approximations for interatomic

and intermolecular interactions may be found in [Brush (1970)]. In fact, chemists determined that the power of the repulsive inverse of the distance term is slightly different from one gas to another, taking values in between (12) and (13). Thus, a qualitative analysis of an atomic model within the framework of classical mechanics need not be restricted to the 12 – 6 potential. Consequently, it is important to study properties of the inter-atomic dynamics which are not necessarily based on the potential’s mathematical (analytical) formula, but rather on its shape, as given by a generic graphical representation.

The approximations of the atomic systems considered here belong to the class of mechanical systems which are of the form “kinetic plus potential,” conserve energy and are invariant under rotations. In the present study, the systems are invariant with respect to planar rotations. The classical program of investigation which applies to this subclass entails:

1. Applying a reduction procedure which, by exploiting the rotational invariance, leads to a *reduced system* with a lower number of degrees of freedom. The potential is augmented by the centrifugal term and the reduced dynamics takes the form “kinetic plus reduced potential”. The reduced system has two (internal) parameters: the total angular momentum c , and the total energy h . The case $c = 0$ describes motions for which the system does not rotate.
2. The description of the *Hill* (or permissible) regions of motion, that is, the domains of the configurations space occupied by possible motions as the level of the total energy varies. The latter are obtained as a consequence of the energy conservation and the form “kinetic plus reduced potential” of the system. Essentially, the Hill regions are subsets of the configuration space where the

potential energy is under a (fixed) level of the energy.

3. Finding the equilibria and determine their stability. Also, for rotating systems ($c \neq 0$), finding the relative equilibria, that is, the equilibria of the reduced system, and determine their stability modulo rotations.
4. Representing the set of equilibria and relative equilibria in the *Energy-Momentum diagram*, where each plotted point represents a relative equilibrium with energy h and momentum c .

For molecules, relative equilibria take the form of steady rotations about stationary axes during which the “shape” of the system does not change. As described in the physical-chemistry literature [Pavlichenkov & al. (1988), Kozin & al. (1996), Kozin & al. (2000)], they can be used to explain and predict features of quantum spectra.

In this thesis, we study equilibria and relative equilibria of diatomic and isosceles triatomic molecules in the framework of classical mechanics. The atoms are modelled as mass points which interact via molecular-type potentials, that is, smooth functions of shapes as in Figure 1.1, or Lennard-Jones functions.

For diatomic systems we retrieve some well-known results (see [Kozin & al. (1999)]), including the description of the Hill regions of motion and the Energy-Momentum diagram.

We further study of the existence and stability of relative equilibria in a three-point mass system formed by two particles m_1 and m_2 with identical parameters of the potential and equal masses ($m_1 = m_2 = m$), and a third, m_3 . The configurations

and the velocities are constrained such that the atoms form an isosceles configuration at all times such that the identical atoms m may rotate about an axis on which m_3 is located. Depending on the mass ordering, we call this three point-mass system to be of type H_3 (three identical atoms), H_2D ($m < m_3$), and D_2H ($m > m_3$).

The relative equilibria study of isosceles triatomic systems develops on three levels: first, we deduce results using qualitative analysis in which case the inter-particle interaction is modelled by a general repulsive-attractive “well”-shaped potential with parameters given by the coordinates of their critical points. Second, we perform an analytical investigation, in which case the inter-particle interaction is given by the generalized Lennard-Jones potential; third, we perform numerical experiments using a code which we designed and implemented.

In describing the dynamics, we use the Lagrangian-Hamiltonian formalism. Specifically, the atomic system is initially modelled in Lagrangian formulation, which we convert to polar coordinates, and observe that the Lagrangian displays a cyclic coordinate. This is due to the dynamics invariance with respect to rotations and leads to the conservation of angular momentum. Applying the Legendre transform, we formulate the problem as a Hamiltonian system. The conservation of angular momentum becomes immediate and it allows the reduction of the dynamics by one degree of freedom. The reduced Hamiltonian is then defined as the original Hamiltonian in which the momentum corresponding to the angular momentum becomes a parameter. In addition, the reduced Hamiltonian takes the form “kinetic plus reduced potential”, where the reduced potential is the potential augmented by an (inertia) angular-momentum dependent term. The relative equilibria are defined as equilibria of the reduced Hamiltonian system. Thus for each fixed angular momentum (now

a parameter) we determine the relative equilibria. In the original system, these are uniform rotations about a stationary axis.

Each relative equilibrium is then tested to determine its stability modulo rotations. The Lyapunov test classifies (relative) equilibria as stable if a certain real-valued *Lyapunov* function fulfills certain conditions. For systems with Hamiltonian structure it can be shown that the Lyapunov function can be taken the Hamiltonian itself. Moreover, for systems of the form “kinetic plus reduced potential”, the Lyapunov stability test is reduced to testing the definiteness of the Hessian at the relative equilibrium of the reduced potential. If the Hessian is positive definite, then the relative equilibrium is stable. If the the Hessian is undefined, the stability can be classified using the linearization method. From the linearization matrix, we find the eigenvalues of each solution. If all of the eigenvalues are purely complex, the relative equilibria is spectrally stable, otherwise it is unstable.

1.2 Outline of Thesis and Results

In Chapter 2 we study diatomic systems. We present the general dynamical theory of a two point-mass system with a potential which depends on the inter-particle distance only. We give the criteria for the existence and stability of relative equilibria and include the definitions of the Hill (permissible) regions of motion and the Energy-Momentum diagram. We specify the theory to the case of the 12-6 Lennard-Jones potential. As previously mentioned, most of the results in this chapter are well-known (see [Kozin & al. (1999)]).

In Chapter 3 we model a three point-mass system with a general inter-particle

distance dependent potential. We define isosceles configurations and write the Lagrangian of the system in cartesian and polar coordinates. We determine Hamilton's equations of motion by performing the Legendre Transform on the Lagrangian in polar coordinates and deduce the reduced Hamiltonian and the reduced potential. We write the equations of motion of the reduced systems and the equilibria and relative equilibria existence conditions.

In Chapter 4, we analyze the existence and stability of relative equilibria (RE). We discuss qualitatively the existence of the RE, by considering only the shape of the inter-particle potential. The number of planar and spatial families of RE is found as a function of the total angular momentum and the ordering of the critical points of the potential. We observe that the number of families of RE is independent of the mass m_3 on the isosceles' triangle vertical. We find that there can be at least two and at most four families of planar RE. In Proposition (4.2.1) we establish conditions which provide the number of families of spatial RE. To our knowledge, this is the first time that such conditions are deduced. We further specialize the inter-particle interaction to a generalized Lennard-Jones potential of the form

$$V(r) = -\frac{A}{r^a} + \frac{B}{r^b}, \quad 2 < a < b, \quad A > 0, B > 0, \quad (1.1)$$

and we prove that there are always two planar RE. In Corollary (4.2.3) we establish the analytic conditions equivalent to those in Proposition (4.2.1). We also show that H_3 -type molecules always display one family of spatial RE at low angular momenta, which, as the momentum increases, bifurcates into two families. At high momenta all RE cease to exist. The chapter ends by establishing the RE stability criteria.

In Chapter 5, we perform numerical experiments using a Matlab[®] code which

we designed and implemented. We calculate diagrams for an H_3 -type molecule and compare H_2D - and D_2H -type molecules by varying the mass of the two identical atoms. We present the results in “distance versus angular momentum” and Energy-Momentum diagrams. The numerical experiments are all in agreement with the theoretical predictions of the preceding chapter.

The last Chapter concludes over our work and presents some possible future research.

The Appendices provide the theoretical prerequisites required in this thesis. Appendix A briefly reviews notions of dynamical systems theory applicable to nonlinear ODEs in general. Appendix B presents notions of classical mechanics in general, and in the Lagrangian-Hamiltonian formalism.

Chapter 2

Diatomic molecules

2.1 Two point-mass systems

We study a planar two point-mass system with a potential which depends on the inter-particle distance within the framework of the general classical mechanics and dynamical systems theory.

Consider a system in \mathbb{R}^2 , formed by two mass points m_1 and m_2 with mutual interaction given by a smooth potential

$$V : D \rightarrow \mathbb{R}, \quad D \subset \mathbb{R} \text{ open.}$$

The evolution in time of the relative vector between the mass points is given by the trajectories of the Lagrangian

$$L(x, y, v_x, v_y) = \frac{1}{2}M (v_x^2 + v_y^2) - V \left(\sqrt{x^2 + y^2} \right), \quad (2.1)$$

where $M := \frac{m_1 m_2}{m_1 + m_2}$ denotes the relative mass of the two mass points. Passing to polar coordinates, we have

$$L(r, \theta, v_r, v_\theta) = \frac{1}{2}M (v_r^2 + (r v_\theta)^2) - V(r). \quad (2.2)$$

Applying the Legendre transform we obtain the Hamiltonian

$$H(r, \theta, p_r, p_\theta) = \frac{1}{2M} \left(p_r^2 + \frac{p_\theta^2}{r^2} \right) + V(r) \quad (2.3)$$

with the equations of motion given by

$$\dot{r} = \frac{p_r}{M} \quad (2.4)$$

$$\dot{p}_r = \frac{p_\theta^2}{Mr^3} - V'(r) \quad (2.5)$$

$$\dot{\theta} = \frac{p_\theta}{Mr^2} \quad (2.6)$$

$$\dot{p}_\theta = 0. \quad (2.7)$$

From above it is immediate that, given initial conditions $(r(t_0), \theta(t_0), p_r(t_0), p_\theta(t_0))$, we obtain

$$p_\theta(t) = \text{const.} = p_\theta(t_0) =: c, \quad (2.8)$$

a relation which expresses the conservation of angular momentum. In addition, the Hamiltonian system defined by (2.3) benefits from the energy integral; that is, for any solution $(r(t), \theta(t), p_r(t), p_\theta(t))$, we have

$$H(r(t), \theta(t), p_r(t), p_\theta(t)) = \text{const.} = H(r(t_0), \theta(t_0), p_r(t_0), p_\theta(t_0)) =: h. \quad (2.9)$$

Substituting (2.8) into (2.3), we reduce the Hamiltonian by one degree of freedom and obtain the *reduced Hamiltonian*

$$H_{\text{red}}(r, p_r; c) = \frac{1}{2M} p_r^2 + \frac{c^2}{2Mr^2} + V(r), \quad (2.10)$$

for which the equations of motion are given by

$$\dot{r} = \frac{p_r}{M} \quad (2.11)$$

$$\dot{p}_r = \frac{c^2}{Mr^3} - V'(r). \quad (2.12)$$

Note that H_{red} depends parametrically on the angular momentum c . By conservation of energy, we have

$$H_{\text{red}}(r(t), p_r(t); c) = \text{const.} = H(r(t_0), p_r(t_0); c(t_0)) =: h, \quad (2.13)$$

so the phase-space (r, p_r) of the system (2.10) is fully described by the level sets

$$\frac{1}{2M} p_r^2 + \frac{c^2}{2Mr^2} + V(r) = h. \quad (2.14)$$

2.2 Analytical solution

To obtain the analytical solution of (2.4) - (2.7) we use the reduced dynamics of (2.10). Consider an initial condition $(r(t_0), \theta(t_0), p_r(t_0), p_\theta(t_0))$. From (2.8) we have

$$p_\theta(t) = p_\theta(t_0) = c. \quad (2.15)$$

Further, from (2.14) we have

$$\frac{1}{2M}p_r^2(t) + \frac{c^2}{2Mr^2(t)} + V(r(t)) = \frac{1}{2M}p_r^2(t_0) + \frac{c^2}{2Mr^2(t_0)} + V(r(t_0)) = h, \quad (2.16)$$

and so

$$p_r = \pm \sqrt{2M \left(h - \frac{c^2}{2Mr^2} - V(r) \right)} \quad (2.17)$$

(where, for simplifying the notation, we dropped the explicit dependency of time).

Let us assume that $p_r(t_0) > 0$ and so we retain the plus sign in the expression above (if $p_r(t_0) < 0$, then we choose the minus sign). Then, using (2.11) we have

$$\frac{dr}{dt} = \frac{1}{M} \sqrt{2M \left(h - \frac{c^2}{2Mr^2} - V(r) \right)} \quad (2.18)$$

and thus

$$\frac{dr}{\frac{1}{M} \sqrt{2M \left(h - \frac{c^2}{2Mr^2} - V(r) \right)}} = dt. \quad (2.19)$$

It follows that

$$\int_{r(t_0)}^{r(t)} \frac{ds}{\frac{1}{M} \sqrt{2M \left(h - \frac{c^2}{2Ms^2} - V(s) \right)}} = t - t_0, \quad (2.20)$$

from where, provided the integral above is computed, we obtain $r(t)$. Further, $p_r(t)$ is immediately given by a direct substitution of $r(t)$ into (2.17). It remains to solve $\theta(t)$. Using (2.6) we have

$$\frac{d\theta}{dt} = \frac{c}{Mr^2(t)} \quad (2.21)$$

or

$$d\theta = \frac{c}{Mr^2(t)} dt. \quad (2.22)$$

Thus

$$\theta(t) = \theta(t_0) + \int_{t_0}^t \frac{c}{Mr^2(\tau)} d\tau. \quad (2.23)$$

where $r(t)$ is the solution of (2.20).

Remark 2.2.1. *For most potentials, the integral (2.20) cannot be expressed by quadratures. However, using the energy integral (2.14) the understanding of the global dynamics can be obtained from the phase-space diagrams.*

2.3 Relative equilibria, the Energy-Momentum diagram and Hill regions

As defined in Appendix B.5, the equilibria of the reduced Hamiltonian (2.10) are relative equilibria of the full (un-reduced) system. For the two point-mass system (2.11)-(2.12) relative equilibria are solutions of the form $(r_e(c), 0)$, where $r_e(c)$ is a critical point of the *reduced potential*:

$$V_{\text{red}}(r; c) = \frac{c^2}{2Mr^2} + V(r) \quad (2.24)$$

and so the reduced Hamiltonian reads

$$H_{\text{red}}(r, p_r; c) = \frac{1}{2M} p_r^2 + V_{\text{red}}(r; c). \quad (2.25)$$

Given the conservation of energy, the phase-space is determined by the level curves

$$\frac{1}{2M} p_r^2 + V_{\text{red}}(r; c) = h. \quad (2.26)$$

Physically, relative equilibria for two point-mass systems are motions in which the two masses are following circular and uniform motions around their common centre of mass. Given an equilibrium $(r_e(c), 0)$ of (2.11)-(2.12), then (2.23) becomes

$$\theta(t) = \frac{c}{Mr_e^2(c)}(t - t_0) + \theta(t_0), \quad (2.27)$$

and thus the polar angle θ evolves linearly in time with constant angular velocity $\dot{\theta} = \frac{c}{Mr_e^2(c)}$. Note that the usual equilibria of the un-reduced system are obtained by taking $c = 0$; in this case, the mass points are in a fixed position, with $\theta(t) = \theta_0$.

A relative equilibrium $(r_e(c), 0)$ is stable if the second derivative

$$V''_{\text{red}}(r_e(c); c) > 0. \quad (2.28)$$

If this fails to be true, then one tests for linear or spectral stability by finding the eigenvalues of the linearization matrix of (2.11)-(2.12):

$$\begin{pmatrix} 0 & \frac{1}{M} \\ -V''_{\text{red}}(r_e(c); c) & 0 \end{pmatrix}. \quad (2.29)$$

A direct calculation shows that $(r_e(c), 0)$ is spectrally stable if $V''_{\text{red}}(r_e(c); c) > 0$ which ensures that all of the eigenvalues have zero real part. We note that for this class of systems, testing for spectral stability coincides to testing for Lyapunov stability.

The Energy-Momentum diagram (that is, the set of points in the (c, h) plane where each plotted point represents a relative equilibrium with momentum c and energy h ;

see Appendix B.5) is obtained by substituting (r, p_r) by $(r_e(c), 0)$ in (2.14):

$$h - V_{\text{red}}(r_e(c); c) = 0. \quad (2.30)$$

Thus the Energy-Momentum graph is given by:

$$\mathcal{EM} := \{(c, h) \mid h = V_{\text{red}}(r_e(c); c)\}. \quad (2.31)$$

As pointed out in Appendix B.6, for each fixed energy level h , the configurations \mathbf{q} of a Newtonian N -body potential system with potential V , are restricted to be in the domain $\{\mathbf{q} \mid V(\mathbf{q}(t)) \leq h\}$ and so one may partition the configuration space in the Hill regions of motion

$$\mathcal{H}(h) := \{\mathbf{q} \mid V(\mathbf{q}) \leq h\}. \quad (2.32)$$

For a two point-mass system, the Hill regions of motion corresponding to the reduced Hamiltonian $H_{\text{red}}(r, p_r; c)$ are parametrized by c . Specifically, for each fixed c , we determine the Hill regions

$$\mathcal{H}_c(h) := \{r \mid V_{\text{red}}(r; c) \leq h\}. \quad (2.33)$$

For each fixed set of parameters (c, h) , the Hill region designates the allowed range for the inter-particle distance. The phase-space of the reduced system (2.11)-(2.12) is fully depicted by the curves in Equation (2.26).

2.4 Diatomic Lennard-Jones molecules

We now specialize the potential $V(r)$ to the 12 – 6 Lennard-Jones case. Recall the molecular 12 – 6 Lennard-Jones potential is given by

$$V(r) = -\frac{A}{r^6} + \frac{B}{r^{12}}. \quad (2.34)$$

In this case, the reduced Hamiltonian (2.10) becomes

$$H_{\text{red}}(r, p_r; c) = \frac{1}{2M}p_r^2 + \frac{c^2}{2Mr^2} - \frac{A}{r^6} + \frac{B}{r^{12}} \quad (2.35)$$

or, equivalently,

$$H_{\text{red}}(r, p_r; c) = \frac{p_r^2}{2M} + V_{\text{red}}(r; c), \quad (2.36)$$

where

$$V_{\text{red}}(r; c) = \frac{c^2}{2Mr^2} - \frac{A}{r^6} + \frac{B}{r^{12}}. \quad (2.37)$$

The relative equilibria configurations $(r_e(c))$ are found as the critical points of $V_{\text{red}}(r; c)$. It can be observed that since

$$V'_{\text{red}}(r; c) = -\frac{c^2}{Mr^3} + \frac{6A}{r^7} - \frac{12B}{r^{13}}, \quad (2.38)$$

we cannot find explicit expressions for $(r_e(c))$. Graphing the reduced potential (see Figure 2.1), we observe that as the value of the angular momentum increases from zero, the number of relative equilibria in the system varies. Following an elementary calculus analysis of the function $y = V_{\text{red}}(r; c)$, we have the following cases:

1. $c = 0$;

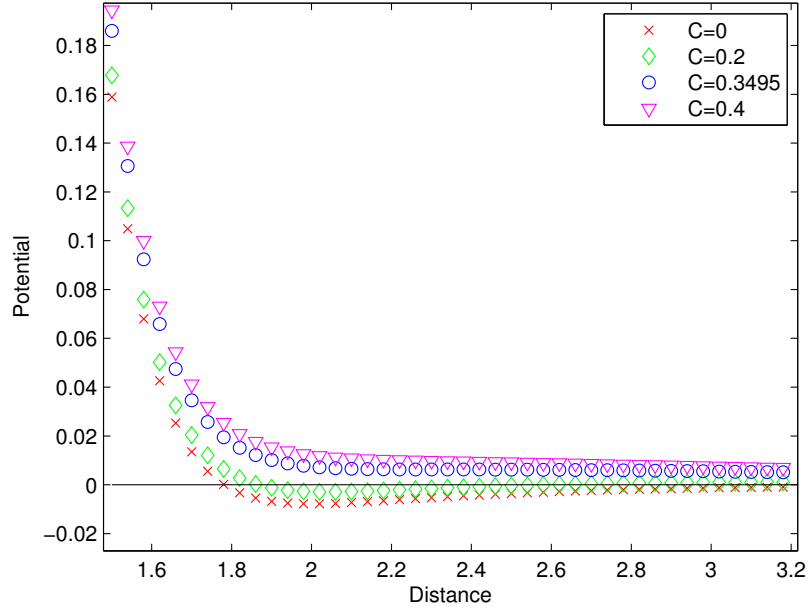


Figure 2.1: The reduced potential $V_{\text{red}}(r; c) = \frac{c^2}{2Mr^2} - \frac{A}{r^6} + \frac{B}{r^{12}}$ for various values of the angular momentum c . The lowest curve corresponds to $c = 0$. The constants are taken as $A = 1$, $B = 32$ and $M = 1$.

2. $0 < c < c_{cr}$;
3. $c = c_{cr}$;
4. $c > c_{cr}$.

where

$$c_{cr} = \frac{3\sqrt{2MB}}{5^{\frac{5}{6}}B^{\frac{1}{3}}}.$$

Case 1:

When $c = 0$, the motion is linear and the potential energy takes the form

$$V_{\text{red}}(r; 0) = -\frac{A}{r^6} + \frac{B}{r^{12}} = V(r).$$

The diagram in Figure 2.2 shows that there exists a single equilibrium point which is found at a critical value $h = h_{cr}$. The Hill Regions are given by (see Figure 2.3):

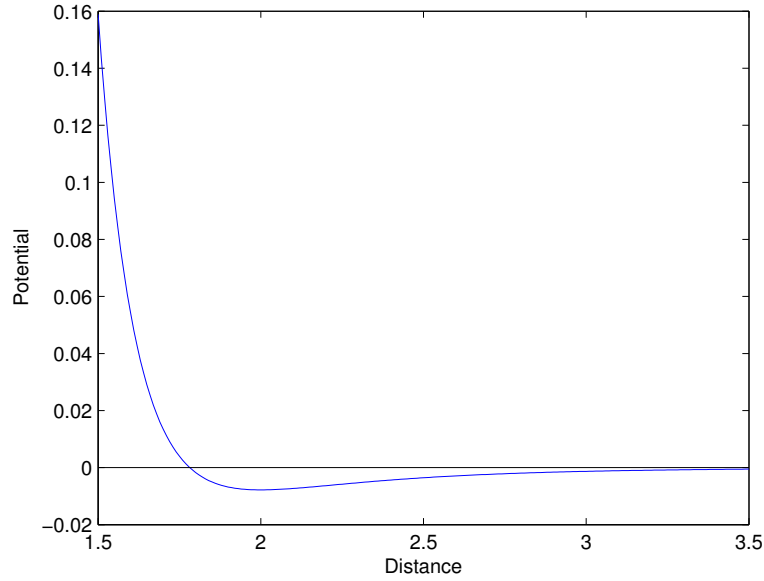


Figure 2.2: The reduced Lennard-Jones potential diagram when $c = 0$, i.e. when $V_{\text{red}}(r; 0) = V(r)$.

- $h < h_{cr} \implies \mathcal{H}_c(h) = \emptyset$ (the void set);
- $h = h_{cr} \implies \mathcal{H}_c(h) = r_e$, where the distance between the atoms is constant (the system is in an equilibrium);
- $h_{cr} < h < 0 \implies \mathcal{H}_c(h) = (r_{min}, r_{max})$;
- $h \geq 0 \implies \mathcal{H}_c(h) = (r_{min}, \infty)$.

Case 2:

When $0 < c < c_{cr}$, there exists two equilibrium points (see Figure 2.4). The Hill Regions are as follows:

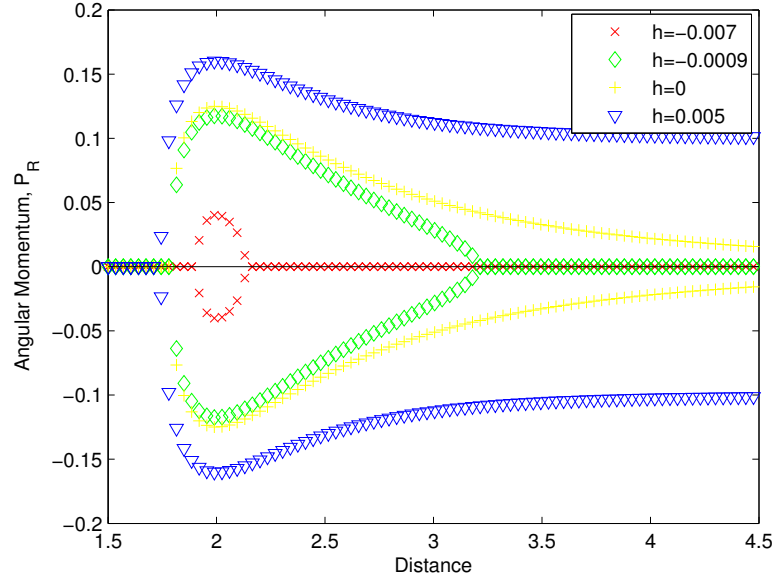


Figure 2.3: The phase plane diagram when $c = 0$.

- $h < h_{cr1} \implies \mathcal{H}_c(h) = \emptyset$;
- $h = h_{cr1} \implies \mathcal{H}_c(h) = r_{e1}$ (equilibrium);
- $h_{cr1} < h < 0 \implies \mathcal{H}_c(h) = (r_{min}, r_{max})$;
- $h = 0 \implies \mathcal{H}_c(h) = (r_{min}, r_{max})$;
- $0 < h < h_{cr2} \implies \mathcal{H}_c(h) = (r_1, r_2) \cup (r_3, \infty)$;
- $h = h_{cr2} \implies \mathcal{H}_c(h) = (r_1, \infty)$, including the equilibrium r_{e2} ;
- $h > h_{cr2} \implies \mathcal{H}_c(h) = (r_{min}, \infty)$.

The phase plane is graphed in Figure 2.5.

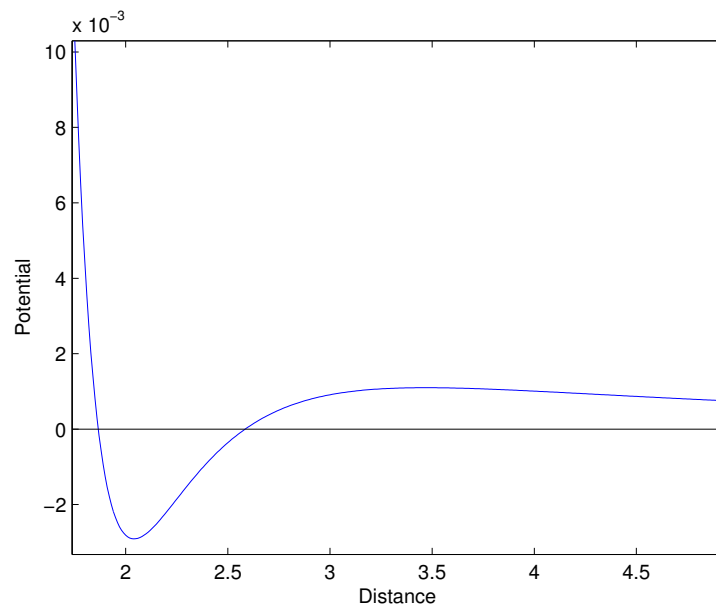


Figure 2.4: The reduced Lennard-Jones potential diagram when $0 < c < c_{cr}$.

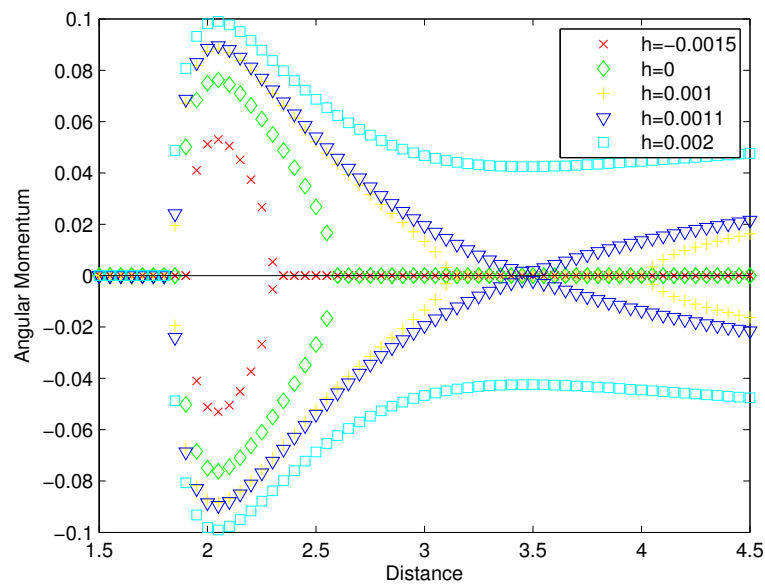


Figure 2.5: The phase plane diagram when $0 < c < c_{cr}$.

Case 3:

When $c = c_{cr}$, there is a unique relative equilibrium (see Figure 2.6). The Hill Regions are:

- $h \leq 0 \implies \mathcal{H}_c(h) = \emptyset$;
- $0 < h < h_{cr} \implies \mathcal{H}_c(h) = (r_{min}, \infty)$;
- $h = h_{cr} \implies \mathcal{H}_c(h) = (r_{e_1}, \infty)$, (for r_{e_1} equilibrium);
- $h > h_{cr} \implies \mathcal{H}_c(h) = (r_{min}, \infty)$.

The phase plane is graphed in Figure 2.7.

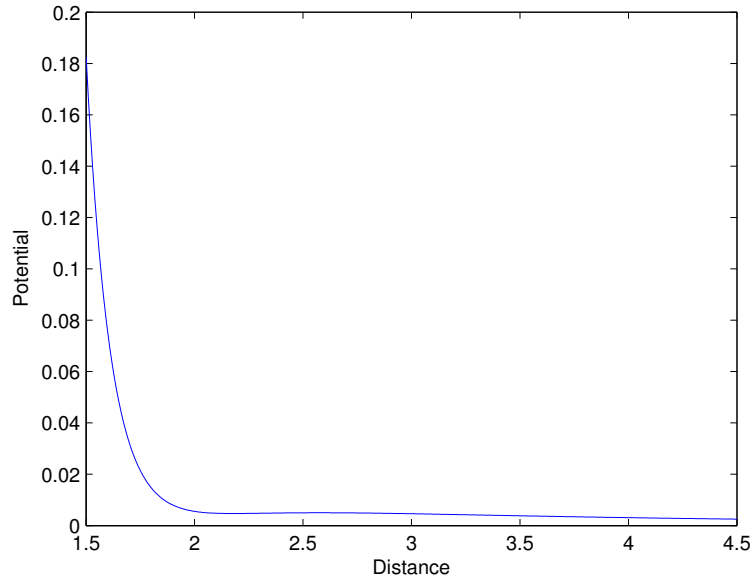
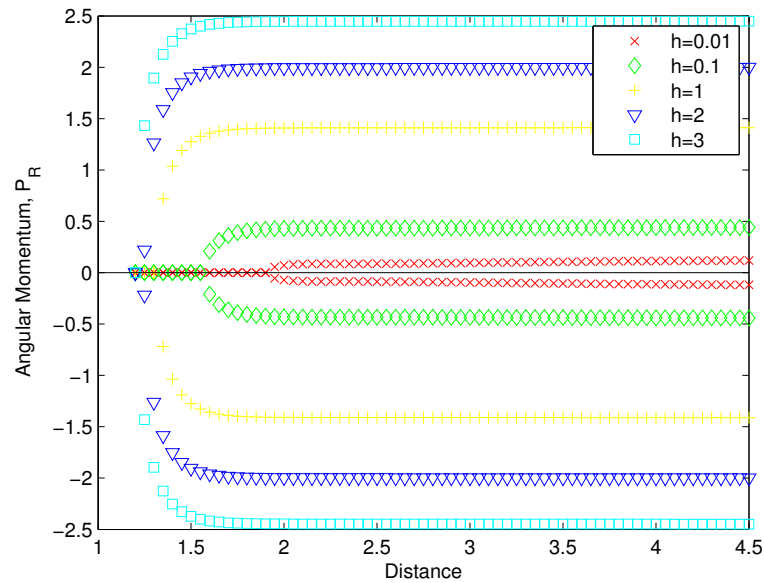
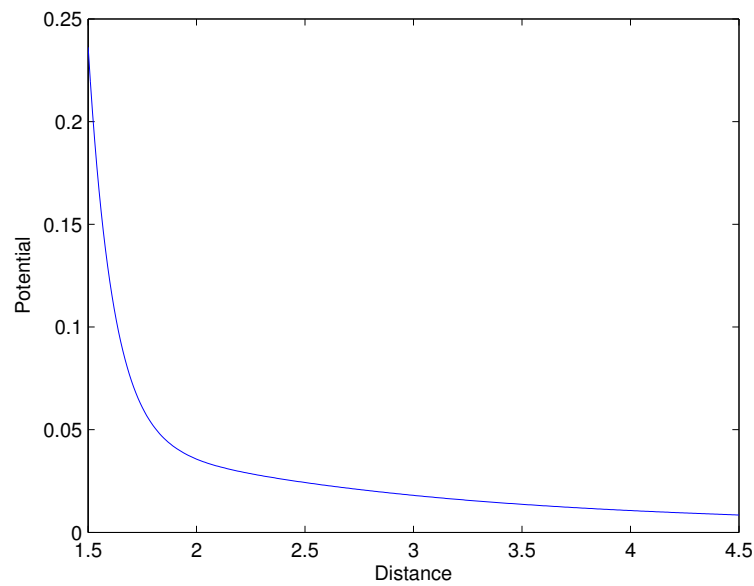


Figure 2.6: The reduced Lennard-Jones potential diagram with $c = c_{cr}$.

Case 4: When $c > c_{cr}$, there are no equilibrium points as seen in Figure 2.8. The Hill Regions are:

Figure 2.7: The phase plane diagram when $c = c_{cr}$.Figure 2.8: The reduced Lennard-Jones potential diagram when $c > c_{cr}$.

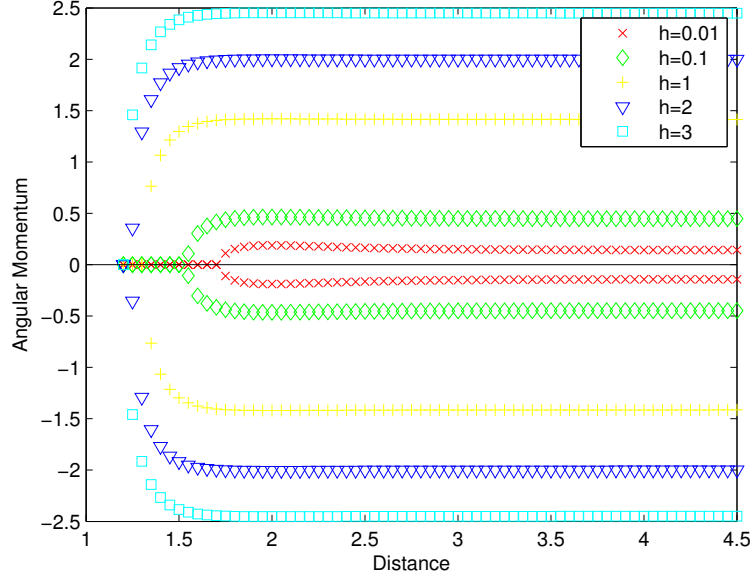


Figure 2.9: The phase plane diagram when $c > c_{cr}$.

- $h \leq 0 \implies \mathcal{H}_c(h) = \emptyset$;
- $h > 0 \implies \mathcal{H}_c(h) = (r_{min}, \infty)$;

The phase plane is graphed in Figure 2.9.

Recall that relative equilibria are stable for values of c such that $V''_{red}(r_e(c); c) > 0$ (see relation (2.28)). For the Lennard-Jones potential this condition becomes

$$V''_{red}(r_e(c); c) = \frac{3c^2}{Mr_e^4(c)} - \frac{42A}{r_e^8(c)} + \frac{156B}{r_e^{14}(c)} > 0. \quad (2.39)$$

Next we determine numerically the Energy-Momentum diagram - see Figure 2.10, where we have marked the stable and unstable relative equilibria, as denoted in the legend. We distinguish the following cases:

- there exists one unique equilibria when $c = 0$ and it is stable;
- there exists two equilibria when $c \in (0, c_{cr})$. The stability can be observed from the diagram;
- at $c = c_{cr}$, the two equilibria merge into one unique (stable) equilibrium.
- for $c > c_{cr}$, no equilibrium exists.

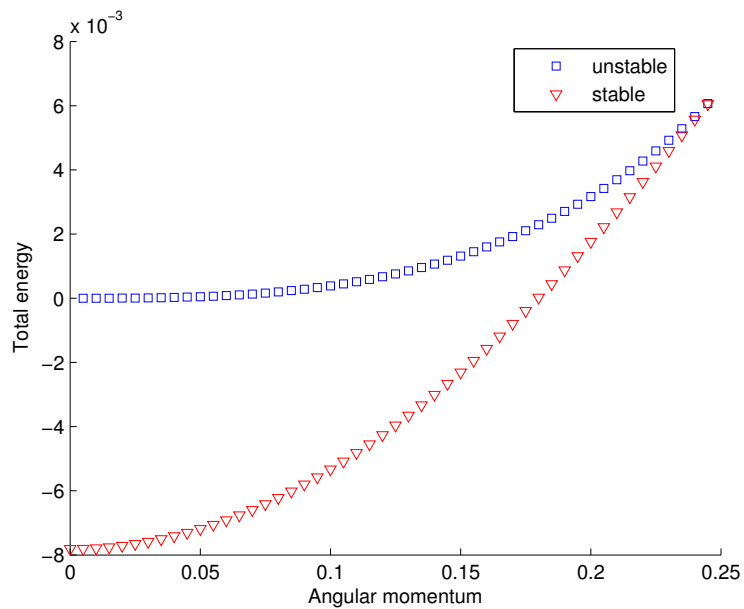


Figure 2.10: The Energy-Momentum diagram for a diatomic molecule.

Chapter 3

Isosceles three point-mass systems

3.1 Three point-mass systems in Jacobi coordinates

The three point-mass problem (or the three-body problem) consists of finding the positions and velocities in time, for a system formed by three mass points with binary distance-dependent interactions. The dynamics is given by a first order differential system formed with 18 equations. The number of equations is reduced to 12, using the linear momentum integral and choosing the centre of mass at the origin of the coordinate system.

The Lagrangian of a three point-mass system formed by the masses is given by

$$L(\mathbf{R}, \dot{\mathbf{R}}) = \frac{m_1}{2} \dot{\mathbf{R}}_1^2 + \frac{m_2}{2} \dot{\mathbf{R}}_2^2 + \frac{m_3}{2} \dot{\mathbf{R}}_3^2 - V_{12}(|\mathbf{R}_1 - \mathbf{R}_2|) - V_{23}(|\mathbf{R}_2 - \mathbf{R}_3|) - V_{13}(|\mathbf{R}_3 - \mathbf{R}_1|) .$$

3.1. THREE POINT-MASS SYSTEMS IN JACOBI COORDINATES 26

where $\mathbf{R} = (\mathbf{R}_1, \mathbf{R}_2, \mathbf{R}_3)$ and $\dot{\mathbf{R}} = (\dot{\mathbf{R}}_1, \dot{\mathbf{R}}_2, \dot{\mathbf{R}}_3)$ are the m_1 , m_2 and m_3 coordinates and velocities, respectively, and $V_{ij} : D_{ij} \rightarrow \mathbb{R}$, $D_{ij} \in \mathbb{R}$ open, $1 \leq i < j \leq 3$ are smooth binary potentials. We follow a similar procedure as in [Meyer & al. (1992)] and perform a change of coordinates in accordance with Figure (3.1), by defining

$$\mathbf{r} = \mathbf{R}_2 - \mathbf{R}_1 \quad (3.1)$$

$$\mathbf{s} = -\frac{m_1}{m_1 + m_2} \mathbf{R}_1 - \frac{m_2}{m_1 + m_2} \mathbf{R}_2 + \mathbf{R}_3 \quad (3.2)$$

$$\mathbf{T} = \frac{m_1 \mathbf{R}_1 + m_2 \mathbf{R}_2 + m_3 \mathbf{R}_3}{m_1 + m_2 + m_3}. \quad (3.3)$$

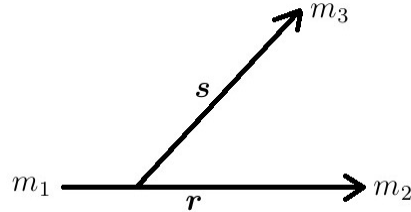


Figure 3.1: The three point mass system with a change of coordinates, \mathbf{r} and \mathbf{s} .

Notice that the vector \mathbf{r} is the relative vector between \mathbf{R}_1 and \mathbf{R}_2 , \mathbf{s} is the relative vector between the centre of mass of m_1 and m_2 , and \mathbf{R}_3 . By definition, the new coordinates are called *Jacobi coordinates*. Performing this change of coordinates in the Lagrangian, we obtain

$$L(\mathbf{r}, \mathbf{s}, \dot{\mathbf{r}}, \dot{\mathbf{s}}) = \frac{1}{2} M_1 \dot{\mathbf{r}}^2 + \frac{1}{2} M_2 \dot{\mathbf{s}}^2 + \frac{1}{2 M_3} \dot{\mathbf{T}}^2 - V_{12}(|\mathbf{r}|) - V_{23}(|\mathbf{s} + \alpha_1 \mathbf{r}|) - V_{13}(|\mathbf{s} - \alpha_2 \mathbf{r}|), \quad (3.4)$$

3.1. THREE POINT-MASS SYSTEMS IN JACOBI COORDINATES 27

where

$$\alpha_1 := \frac{m_1}{m_1 + m_2} \quad \text{and} \quad \alpha_2 := \frac{m_2}{m_1 + m_2}, \quad (3.5)$$

and M_1 , M_2 and M_3 are given by

$$M_1 = \frac{m_1 m_2}{m_1 + m_2}, \quad M_2 = \frac{m_3(m_1 + m_2)}{m_1 + m_2 + m_3} \quad \text{and} \quad M_3 = m_1 + m_2 + m_3. \quad (3.6)$$

Using the Lagrange equations of motion (see Appendix B), the equation for \mathbf{T} integrates trivially and leads to

$$\mathbf{T}(t) = \mathbf{c}_1 t + \mathbf{c}_2 \quad (3.7)$$

where \mathbf{c}_1 and \mathbf{c}_2 are constants of motion fixed by the initial conditions:

$$\mathbf{c}_2 = \mathbf{T}(t_0) = m_1 \mathbf{R}_1(t_0) + m_2 \mathbf{R}_2(t_0) + m_3 \mathbf{R}_3(t_0), \quad (3.8)$$

$$\mathbf{c}_1 = \dot{\mathbf{T}}(t_0) = m_1 \dot{\mathbf{R}}_1(t_0) + m_2 \dot{\mathbf{R}}_2(t_0) + m_3 \dot{\mathbf{R}}_3(t_0). \quad (3.9)$$

In fact, the evolution of \mathbf{T} , which is that of the centre of mass of the system (normalized by the total mass), is due to the conservation of linear momentum. The motion of \mathbf{T} is known since \mathbf{r} and \mathbf{s} don't depend on it (see formula (3.4)), so without loss of generality we can consider

$$L(\mathbf{r}, \mathbf{s}, \dot{\mathbf{r}}, \dot{\mathbf{s}}) = \frac{1}{2} M_1 \dot{\mathbf{r}}^2 + \frac{1}{2} M_2 \dot{\mathbf{s}}^2 - V_{12}(|\mathbf{r}|) - V_{23}(|\mathbf{s} + \alpha_1 \mathbf{r}|) - V_{13}(|\mathbf{s} - \alpha_2 \mathbf{r}|). \quad (3.10)$$

Applying the Legendre transform $(\mathbf{r}, \mathbf{s}, \dot{\mathbf{r}}, \dot{\mathbf{s}}) \rightarrow (\mathbf{r}, \mathbf{s}, \mathbf{p}_r, \mathbf{p}_s)$ we obtain the Hamiltonian

$$H(\mathbf{r}, \mathbf{s}, \mathbf{p}_r, \mathbf{p}_s) = \frac{1}{2M_1} \mathbf{p}_r^2 + \frac{1}{2M_2} \mathbf{p}_s^2 + V_{12}(|\mathbf{r}|) + V_{23}(|\mathbf{s} + \alpha_1 \mathbf{r}|) + V_{13}(|\mathbf{s} - \alpha_2 \mathbf{r}|). \quad (3.11)$$

3.2 Isosceles configurations

Consider now that two of the masses are equal, say $m_1 = m_2 = m$, and that $V_{23}(x) = V_{13}(x)$ for any $x \in D$. In this case one can prove directly that isosceles configurations, i.e., the set of solutions with

$$r_z = s_x = s_y = p_{rz} = p_{sx} = p_{sy} = 0, \quad \text{for all } t$$

form an invariant submanifold under the flow of the system. For such motions, \mathbf{r} is confined to the horizontal plane, whereas \mathbf{s} moves on the vertical axis only. This invariant submanifold is evident from a physical standpoint (i.e. since the forces balance). Thus isosceles motions are described by a three degree of freedom mechanical system with the configuration space given by (r_x, r_y, s_z) and momenta (p_{rx}, p_{ry}, p_{sz}) . The Lagrangian is given by

$$L(\mathbf{r}, \mathbf{s}, \dot{\mathbf{r}}, \dot{\mathbf{s}}) = \frac{1}{2} M_1 \dot{\mathbf{r}}^2 + \frac{1}{2} M_2 \dot{\mathbf{s}}^2 - F(|\mathbf{r}|) - G\left(\left|\mathbf{s} + \frac{\mathbf{r}}{2}\right|\right) - G\left(\left|\mathbf{s} - \frac{\mathbf{r}}{2}\right|\right) \quad (3.12)$$

where, to ease notation, we denoted $F := V_{12}$ and $G := V_{23} = V_{13}$.

We convert to cylindrical coordinates and change the notation for s_z (as shown in

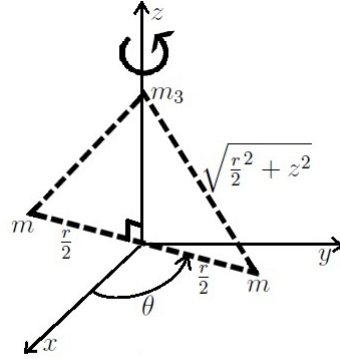


Figure 3.2: The three point mass system with change of coordinates.

Figure (3.2))

$$r_x = r \cos \theta, \quad r_y = r \sin \theta, \quad s_z = z$$

and calculate further

$$\begin{cases} \dot{r}_x = \dot{r} \cos \theta - r \sin \theta \dot{\theta} \\ \dot{r}_y = \dot{r} \sin \theta + r \cos \theta \dot{\theta} \end{cases}$$

to obtain the Lagrangian

$$L(r, \theta, z, \dot{r}, \dot{\theta}, \dot{z}) = \frac{1}{2} M_1 (\dot{r}^2 + r^2 \dot{\theta}^2) + \frac{1}{2} M_2 \dot{z}^2 - F(r) - 2G \left(\sqrt{\frac{r^2}{4} + z^2} \right)$$

By applying the Legendre Transform to our Lagrangian, we produce the Hamiltonian

$$H(r, \theta, z, p_r, p_\theta, p_z) := \frac{1}{2M_1} \left(p_r^2 + \frac{p_\theta^2}{r^2} \right) + \frac{p_z^2}{2M_2} + F(r) + 2G \left(\sqrt{\frac{r^2}{4} + z^2} \right) \quad (3.13)$$

with equations of motion

$$\dot{r} = \frac{p_r}{M_1} \quad \dot{p}_r = \frac{p_\theta^2}{M_1 r^3} - F'(r) - \frac{r}{2\sqrt{\frac{r^2}{4} + z^2}} G' \left(\sqrt{\frac{r^2}{4} + z^2} \right) \quad (3.14)$$

$$\dot{\theta} = \frac{p_\theta}{M_1 r^2} \quad \dot{p}_\theta = 0 \quad (3.15)$$

$$\dot{z} = \frac{p_z}{M_2} \quad \dot{p}_z = -2G' \left(\sqrt{\frac{r^2}{4} + z^2} \right) \frac{z}{\sqrt{\frac{r^2}{4} + z^2}} \quad (3.16)$$

From the general theory in Appendix B or by direct verification, we have that the energy of the system is conserved along any solution

$$\frac{d}{dt} H(r(t), \theta(t), z(t), p_r(t), p_\theta(t), p_z(t)) = 0 \quad (3.17)$$

and so

$$H(r(t), \theta(t), z(t), p_r(t), p_\theta(t), p_z(t)) = H(r(t_0), \theta(t_0), z(t_0), p_r(t_0), p_\theta(t_0), p_z(t_0)) =: h.$$

Also, since $\dot{p}_\theta = 0$ it follows that the angular momentum of the system is constant in time:

$$p_\theta(t) = p_\theta(t_0) =: c. \quad (3.18)$$

Using the above we can substitute c for p_θ in expression (3.13), and obtain the *reduced Hamiltonian*

$$H_{\text{red}}(r, z, p_r, p_z; c) = \frac{1}{2M_1} \left(p_r^2 + \frac{c^2}{r^2} \right) + \frac{1}{2M_2} p_z^2 + F(r) + 2G \left(\sqrt{\frac{r^2}{4} + z^2} \right) \quad (3.19)$$

or

$$H_{\text{red}}(r, z, p_r, p_z; c) = \frac{1}{2M_1}p_r^2 + \frac{1}{2M_2}p_z^2 \quad (3.20)$$

where V_{red} is

$$V_{\text{red}}(r, z; c) = \frac{c^2}{2M_1 r^2} + F(r) + 2G\left(\sqrt{\frac{r^2}{4} + z^2}\right). \quad (3.21)$$

The equations of motion are

$$\dot{r} = \frac{p_r}{M_1} \quad (3.22)$$

$$\dot{z} = \frac{p_z}{M_2} \quad (3.23)$$

$$\dot{p}_r = \frac{c^2}{M_1 r^3} - F'(r) - G'\left(\sqrt{\frac{r^2}{4} + z^2}\right) \frac{r}{2\sqrt{\frac{r^2}{4} + z^2}} \quad (3.24)$$

$$\dot{p}_z = -2G'\left(\sqrt{\frac{r^2}{4} + z^2}\right) \frac{z}{\sqrt{\frac{r^2}{4} + z^2}} \quad (3.25)$$

Solving system (3.22)-(3.25) yields the value of $r(t)$. Then since

$$\dot{\theta}(t) = \frac{d\theta}{dt} = \frac{c}{M_1 r^2(t)}$$

we have that

$$\theta(t) = \frac{c}{M_1} \int_{t_0}^t \frac{d\tau}{r^2(\tau)} + \theta(t_0).$$

which is also a known value.

The *relative equilibria* associated with H_{red} are found by letting the right hand

side of the system (3.22) - (3.25), equal zero. This yields

$$\frac{c^2}{M_1 r^3} - F'(r) - G' \left(\sqrt{\frac{r^2}{4} + z^2} \right) \frac{r}{2\sqrt{\frac{r^2}{4} + z^2}} = 0 \quad (3.26)$$

$$2G' \left(\sqrt{\frac{r^2}{4} + z^2} \right) \frac{z}{\sqrt{\frac{r^2}{4} + z^2}} = 0 \quad (3.27)$$

$p_r = p_z = 0$, and we define V_{eff} as

$$V_{\text{eff}}(r, z; c) := \frac{c^2}{2M_1 r^2} + F(r) + 2G \left(\sqrt{\frac{r^2}{4} + z^2} \right). \quad (3.28)$$

From the system above, we observe that there are two distinct cases:

1. $z = 0$, consisting of *planar relative equilibria*
2. $z \neq 0$, so $G' \left(\sqrt{\frac{r^2}{4} + z^2} \right) = 0$, then we have *spatial relative equilibria*.

Remark 3.2.1. *The third mass is irrelevant to the existence of equilibria. However, it impacts the stability of the existing equilibria.*

Recall that the *Hill regions of motion* are determined by

$$\mathcal{H}(h) := \{r \mid V_{\text{red}}(r; c) \leq h\},$$

where

$$V_{\text{red}}(r; c) := \frac{c^2}{2M_1 r^2} + F(r) + 2G \left(\frac{r}{2} \right) \leq h$$

for each energy level h .

We end this section by observing that the set

$$\mathcal{N} := \{(r, z, p_r, p_z) \mid z = p_z = 0\} \quad (3.29)$$

is an invariant manifold for the flow of H_{red} , that is, motions which start at $z(t_0) = p_z(t_0) = 0$ will have $z(t) = p_z(t) = 0$ for all t . Indeed, this follows directly from the uniqueness of the ODE solutions. Physically, this is when the system displays planar motions, where the mass-point m_3 is fixed at the midpoint of the segment defined by the equal masses. The dynamics of the system on \mathcal{N} is given by the one degree of freedom system

$$\dot{r} = \frac{p_r}{M_1} \quad (3.30)$$

$$\dot{p}_r = \frac{c^2}{M_1 r^3} - F'(r) - G'\left(\frac{r}{2}\right) \quad (3.31)$$

Chapter 4

Relative equilibria for molecular-type interactions

In this chapter we study the existence and stability of equilibria and relative equilibria of a triatomic isosceles molecule in classical approximation.

We assume that the inter-atomic potentials $m_1 - m_2$ and $m_i - m_3$, $i = 1, 2$, are given by two smooth molecular-type potentials $F : (0, \infty) \rightarrow \mathbb{R}$ and $G : (0, \infty) \rightarrow \mathbb{R}$, respectively. The shapes of F and G are sketched in Figure 1.1. In addition, we assume that if two atoms have the same mass, then they are of the same kind; that is, if $m_1 = m_2 = m_3$, then the inter-atomic interaction is described by one potential function. We denote the critical points of F and G by r_{cr}^F and r_{cr}^G , respectively. To

simplify notation, we introduce

$$M := \frac{m_1 m_2}{m_1 + m_2} = \frac{m^2}{2m} = \frac{m}{2}.$$

The equilibria and relative equilibria are found qualitatively by solving system (3.26) – (3.27) with parameters r_{cr}^F , r_{cr}^G and c . We continue by considering the case of the generalized Lennard-Jones potential. For atoms of the same kind (interaction of atoms of type “ $i - i$ ”) we define the generalized Lennard-Jones potential to be

$$F(r) = -\frac{A_{ii}}{r^a} + \frac{B_{ii}}{r^b}, \quad 2 < a < b. \quad (4.1)$$

In our case this applies to the $m_1 - m_2$ interaction. For atoms of two different species “ $i - i'$ ” and “ $j - j'$ ”, the coefficients of the potential are determined by the Lorentz-Berthelot rule (see [Lorentz (1881), Berthelot (1889), Kirchner & al. (2012)]) as follows:

$$A_{ij} = \frac{A_{ii} + A_{jj}}{2} \quad B_{ij} = \frac{B_{ii} + B_{jj}}{2}. \quad (4.2)$$

Thus for two atoms of species “ $i - i'$ ” and “ $j - j'$ ” the potential is

$$G(r) = -\frac{A_{ii} + A_{jj}}{2r^a} + \frac{B_{ii} + B_{jj}}{2r^b}, \quad 2 < a < b. \quad (4.3)$$

In our model this applies to the $m_1 - m_3$ and $m_2 - m_3$ interactions.

In the last Section we establish the stability criteria.

4.1 Planar equilibria and relative equilibria ($z = 0$)

From system (3.26)-(3.27) we have that planar equilibria and relative equilibria ($z = 0$) are solutions of

$$\frac{c^2}{Mr^3} - F'(r) - G'\left(\frac{r}{2}\right) = 0, \quad (4.4)$$

or, equivalently,

$$\frac{c^2}{Mr^3} = F'(r) + G'\left(\frac{r}{2}\right). \quad (4.5)$$

4.1.1 The qualitative approach

We determine equilibria and relative equilibria by a graphical method. Specifically, we determine the number of intersections of the curves $\frac{c^2}{Mr^3}$ and $F'(r) + G'\left(\frac{r}{2}\right)$ as they occur in the left and right-hand side of equation (4.5). Each intersection of the curves correspond to a root of (4.5). It is immediate that the number of solutions depends on the value of c .

Equilibria

The equilibria of the system occur when $c = 0$. To find these unique points, we solve

$$F'(r) + G'\left(\frac{r}{2}\right) = 0 \quad (4.6)$$

or equivalently,

$$F'(r) = -G'\left(\frac{r}{2}\right).$$

4.1. PLANAR EQUILIBRIA AND RELATIVE EQUILIBRIA ($Z = 0$) 37

Given the shape of $F(r)$ and $G(r)$ (see Figure 1.1), it follows immediately that Equation (4.6) has one root, resulting in one planar equilibrium.

Relative Equilibria

The relative equilibria (RE) of the system occur when $c \neq 0$ and

$$\frac{c^2}{Mr^3} = F'(r) + G'\left(\frac{r}{2}\right). \quad (4.7)$$

Since $F'(r)$ and $G'\left(\frac{r}{2}\right)$ each have one maximum, their sum has at least one (see

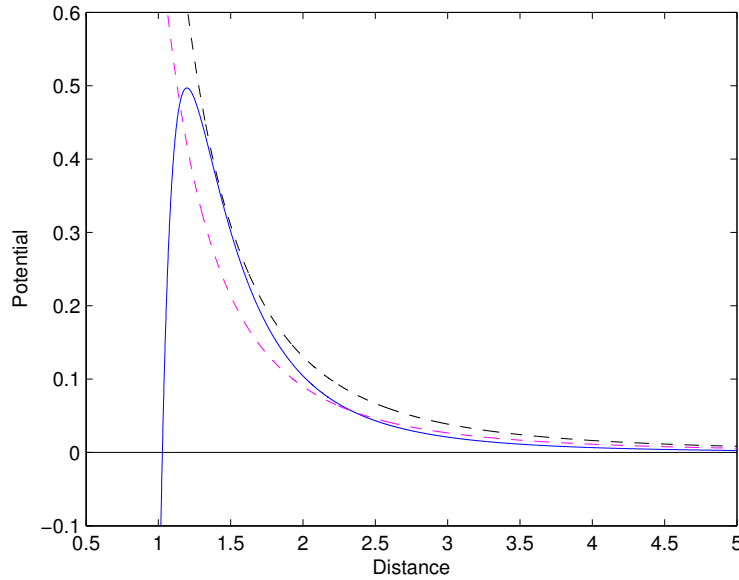


Figure 4.1: The sum $F'(r) + G'\left(\frac{r}{2}\right)$, pictured in dark blue, displaying one maximum.

The curves $\frac{c^2}{Mr^3}$ can intersect it in two points (the purple and light blue curves), which corresponds to angular momenta $0 < c < c_{0,p}$ or in one point (the black curve), which corresponds to an angular momentum $c = c_{0,p}$. For momenta $c > c_{0,p}$ there are no intersections.

Figure 4.1), and at most two maxima (see Figure 4.2). In the former case (Figure 4.1),

4.1. PLANAR EQUILIBRIA AND RELATIVE EQUILIBRIA ($Z = 0$) 38

there is some value $c_{0,p}$ such that solving Equation (4.7) yields two planar RE when $0 < c < c_{0,p}$, one unique planar RE when $c = c_{0,p}$, and no planar RE when $c > c_{0,p}$. The value $c_{0,p}$ is determined by the requiring that the curves $\frac{c^2}{Mr^3}$ and $F'(r) + G'\left(\frac{r}{2}\right)$ be tangent. Equivalently, $c_{0,p}$ and the coordinate $r(c_{0,p})$ at the tangency points must solve

$$\frac{c^2}{Mr^3} = F'(r) + G'\left(\frac{r}{2}\right) \quad (4.8)$$

$$-\frac{3c^2}{Mr^4} = F''(r) + \frac{1}{2}G''\left(\frac{r}{2}\right) . \quad (4.9)$$

In the latter case (Figure 4.2), we find that there can be a up to a maximum of

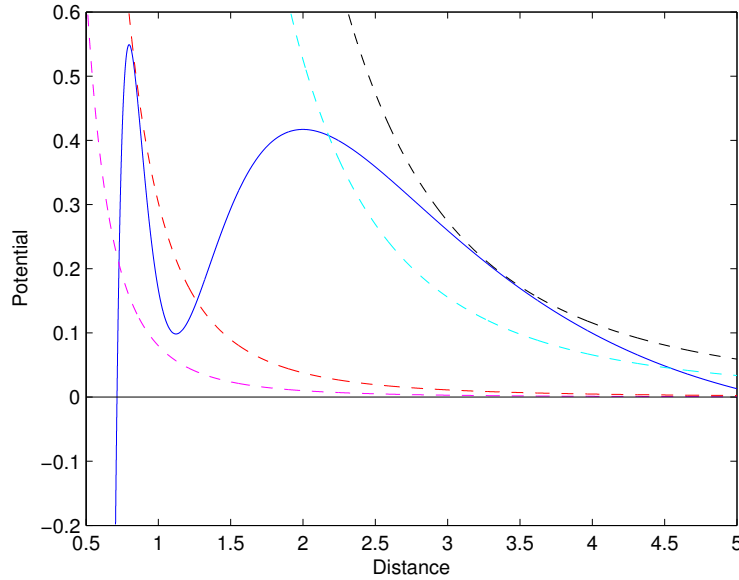


Figure 4.2: The sum $F'(r) + G'\left(\frac{r}{2}\right)$, pictured in dark blue, displaying two maxima. The curves $\frac{c^2}{Mr^3}$ can intersect it in four points, three points (the brown curve), two points (the light blue curve), or in one point (the black curve).

four planar RE; the number of solutions is determined by the value of the angular

momentum c .

4.1.2 The analytical approach

Now we further our analysis by applying the generalized Lennard-Jones potential with $F(r)$ and $G(r)$ defined by (4.1) and (4.3), respectively.

Equilibria

When $c = 0$, condition (4.6) becomes

$$\frac{a((1 + 2^{a-1})A_{ii} + 2^{a-1}A_{jj})}{r^{a+1}} - \frac{b((1 + 2^{b-1})B_{ii} + 2^{b-1}B_{jj})}{r^{b+1}} = 0. \quad (4.10)$$

Solving Equation (4.10), we verify that the system yields one planar equilibrium, with coordinate r given by

$$r_0 = \left(\frac{b((1 + 2^{b-1})B_{ii} + 2^{b-1}B_{jj})}{a((1 + 2^{a-1})A_{ii} + 2^{a-1}A_{jj})} \right)^{\frac{1}{b-a}}. \quad (4.11)$$

Relative Equilibria

When $c \neq 0$, Equation (4.7) becomes

$$c^2 = M \left(\frac{a((1 + 2^{a-1})A_{ii} + 2^{a-1}A_{jj})}{r^{a-2}} - \frac{b((1 + 2^{b-1})B_{ii} + 2^{b-1}B_{jj})}{r^{b-2}} \right) \quad (4.12)$$

Since $2 < a < b$, the function given by the right hand side of the equation above has one maximum as in Figure 4.1. The value $c_{0,p}$, and the corresponding $r(c_{0,p})$, which must solve (4.8) - (4.9), cannot be determined analytically.

4.2 Spatial equilibria and relative equilibria ($z \neq 0$)

In the previous section, we discussed the case when a molecule is in linear formation. Now we consider the case of a molecule in bent formation, i.e., when $z \neq 0$. The system (3.26) - (3.27) becomes

$$\frac{c^2}{Mr^3} - F'(r) = 0 \quad (4.13)$$

$$G' \left(\sqrt{\frac{r^2}{4} + z^2} \right) = 0 \quad (4.14)$$

To find the equilibria and relative equilibria of system we first solve (4.13)-(4.14) for r , then find the corresponding value for z .

4.2.1 The qualitative approach

Equilibria

When $c = 0$, Equation (4.13) reduces to $F'(r) = 0$, which is solved by $r = r_{cr}^F$. Then by using Equation (4.14), and the fact that $G'(r_{cr}^G) = 0$, we have

$$\sqrt{\frac{(r_{cr}^F)^2}{4} + z^2} = r_{cr}^G$$

which yields,

$$z^2 = (r_{cr}^G)^2 - \frac{(r_{cr}^F)^2}{4}. \quad (4.15)$$

4.2. SPATIAL EQUILIBRIA AND RELATIVE EQUILIBRIA ($Z \neq 0$) 41

Since $z^2 > 0$, then there are two spatial equilibria located at

$$(r, z) = \left(r_{cr}^F, \pm \sqrt{(r_{cr}^G)^2 - \frac{(r_{cr}^F)^2}{4}} \right). \quad (4.16)$$

provided $r_{cr}^F < 2r_{cr}^G$.

Relative Equilibria

We find the relative equilibria ($c \neq 0$) of system (4.13) - (4.14), through analyzing the curves in Figure 4.3, followed by a discussion on equation (4.14), which determines the corresponding z value.

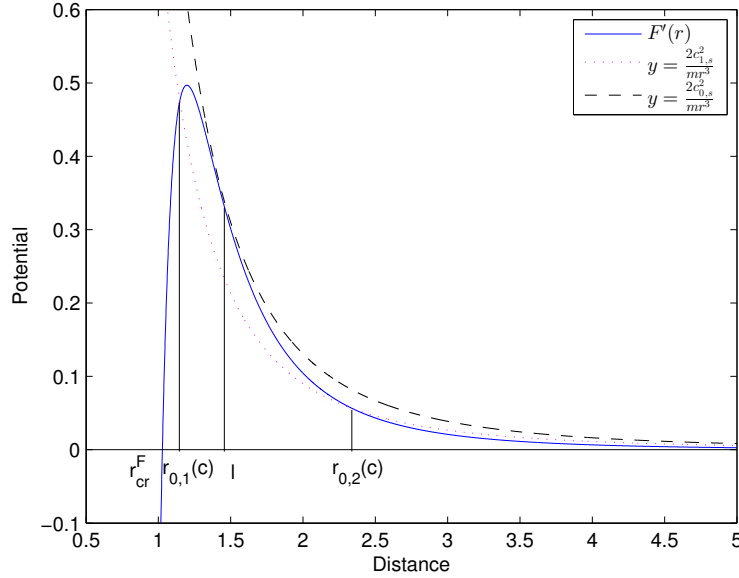


Figure 4.3: Diagram of $F'(r)$ depicting $\frac{c^2}{Mr^3}$ for $c = c_{0,s}$ and $c = c_{1,s}$.

Figure 4.3 portrays the components of Equation (4.13), where the solid line represents the curve $y = F'(r)$ and the dashed lines represent the curve $y = \frac{c^2}{Mr^3}$ for

4.2. SPATIAL EQUILIBRIA AND RELATIVE EQUILIBRIA ($Z \neq 0$) 42

different values of c . We observe that there is some value $c = c_{0,s} > 0$ and $r(c_{0,s}) = l$, such that

1. For $0 < c < c_{0,s}$, there exists two spatial RE denoted by $r_{0,i}(c)$, $i = 1, 2$ where

$$r_{cr}^F < r_{0,1}(c) < l < r_{0,2}(c). \quad (4.17)$$

Also, $\lim_{c \rightarrow c_{0,s}} r_{0,1}(c) = l = \lim_{c \rightarrow c_{0,s}} r_{0,2}(c)$, $\lim_{c \rightarrow 0} r_{0,1}(c) = r_{cr}^F$ and $\lim_{c \rightarrow 0} r_{0,2}(c) = \infty$;

2. For $c = c_{0,s}$, there exists one spatial RE at $r(c_{0,s}) = l$;

3. For $c > c_{0,s}$, no spatial RE exist.

The values $c = c_{0,s}$ and $r(c_{0,s}) = l$ is determined as the point of tangency of $y = \frac{c^2}{Mr^3}$ and $y = F'(r)$, that is, it is the solution $(l, c_{0,s})$ of the the system

$$\frac{c^2}{Mr^3} = F'(r) \quad (4.18)$$

$$-\frac{3c^2}{Mr^4} = F''(r). \quad (4.19)$$

Now we discuss Equation (4.14), which when reduced to (4.15), gives us the “height” z of the bent molecule. For this equation to admit real solutions we must have

$$r_{cr}^G \geq \frac{r_{0,1}(c)}{2} \quad \text{or} \quad r_{cr}^G \geq \frac{r_{0,2}(c)}{2},$$

which is equivalent to

$$r_{0,1}(c) \leq 2r_{cr}^G \quad \text{or} \quad r_{0,2}(c) \leq 2r_{cr}^G. \quad (4.20)$$

Using Figure (4.3), we observe the following

1. If $2r_{cr}^G \leq r_{cr}^F$, given the ordering in expression (4.17), there is no value of c which satisfies equation (4.20).
2. For $r_{cr}^F < 2r_{cr}^G \leq l$, there exists some threshold value $c_{1,s}$, given by

$$\frac{c_{1,s}^2}{M(2r_{cr}^G)^3} = F'(2r_{cr}^G), \quad \text{where } 0 < c_{1,s} \leq c_{0,s}. \quad (4.21)$$

For all $0 < c \leq c_{1,s}$ where $r_{0,1}(c) \leq 2r_{cr}^G < r_{0,2}(c)$, we have a single family of spatial RE with

$$z_{1,2} = \pm \sqrt{(r_{cr}^G)^2 - \frac{(r_{0,1}(c))^2}{4}}, \quad (4.22)$$

which ceases to exist when $c > c_{1,s}$.

Thus there is a family of isosceles spatial RE, which begins from a non-collinear equilibrium. As the angular momentum increases from zero, these RE persist up to the critical value $c_{1,s}$, then disappear for all $c > c_{1,s}$. At $c = c_{1,s}$ the “height” of the isosceles RE triangle is zero, and the isosceles RE degenerates to a planar collinear RE. Equivalently, when $c = 0$ there is a spatial equilibrium (r, z) , which is given by (4.16); as c increases from 0 to $c_{1,s}$, the height of the triangle decreases continuously. This occurs until $c = c_{1,s}$ where the collinear

(flat) REs are reached (when $z = 0$).

3. If $l < 2r_{cr}^G$ and $c_{1,s}$ is found using (4.21), then from Figure (4.3) we observe that

- If $c \in (0, c_{1,s})$ we have $r_{0,1}(c) < 2r_{cr}^G < r_{0,2}(c)$, which leads to one family of spatial RE where

$$z_{1,2} = \pm \sqrt{(r_{cr}^G)^2 - \frac{(r_{0,1})^2}{4}}. \quad (4.23)$$

- If $c \in [c_{1,s}, c_{0,s})$ we have $r_{0,1}(c) < r_{0,2}(c) \leq 2r_{cr}^G$, which leads to two families of spatial RE,

$$z_{1,2} = \pm \sqrt{(r_{cr}^G)^2 - \frac{(r_{0,1})^2}{4}} \quad z_{3,4} = \pm \sqrt{(r_{cr}^G)^2 - \frac{(r_{0,2})^2}{4}} \quad (4.24)$$

When $c = c_{1,s}$, the second family “ $z_{3,4}$ ” of spatial RE branches from the planar collinear RE. At $c = c_{0,s}$, the isosceles families join and there exists one unique spatial RE, $r(c_{0,s}) = l$. We observe from Figure 4.3, that no spatial RE exist for $c > c_{0,s}$.

To summarize our findings, we have proven:

Proposition 4.2.1. *Let $(l, c_{0,s})$ be the solution of the system (4.18) - (4.19) and $c_{1,s}$ the solution of (4.21). Then*

1. *If $r_{cr}^F > 2r_{cr}^G$ then there are no RE.*
2. *If $r_{cr}^F < 2r_{cr}^G \leq l$, then, for $c \in (0, c_{1,s})$, there is one spatial family of RE. At $c = c_{1,s}$ this family joins a planar family of RE.*

3. If $l < 2r_{cr}^G$ then

a) for $c \in (0, c_{1,s})$ there is one spatial family of RE;

b) for $c \in [c_{1,s}, c_{0,s})$ there are two spatial families of RE. At $c = c_{0,s}$ these families coincide;

c) for $c > c_{0,s}$, no spatial RE exist.

Identical Atoms

Remark 4.2.2 (H_3 molecules). *If the three atoms are identical, then $F(r) = G(r)$, and so $r_{cr}^F = r_{cr}^G$. In particular, $r_{cr}^F \leq 2r_{cr}^G$ and so the cases 2 and 3 of the preceding Proposition apply.*

4.2.2 The analytical approach

Now we further analyze our system by applying the generalized Lennard-Jones potentials defined in (4.1) and (4.3) to system (4.13) - (4.14), yielding

$$\frac{c^2}{Mr^3} - \frac{aA_{ii}}{r^{a+1}} + \frac{bB_{ii}}{r^{b+1}} = 0 \quad (4.25)$$

$$\frac{a(A_{ii} + A_{jj})}{2 \left(\sqrt{\frac{r^2}{4} + z^2} \right)^{a+1}} - \frac{b(B_{ii} + B_{jj})}{2 \left(\sqrt{\frac{r^2}{4} + z^2} \right)^{b+1}} = 0 \quad (4.26)$$

Recall that for $F(r)$ and $G(r)$, we denote the critical points as r_{cr}^F and r_{cr}^G

$$r_{cr}^F = \left(\frac{b}{a} \right)^{\frac{1}{b-a}} \left(\frac{B_{ii}}{A_{ii}} \right)^{\frac{1}{b-a}}, \quad r_{cr}^G = \left(\frac{b}{a} \right)^{\frac{1}{b-a}} \left(\frac{B_{ii} + B_{jj}}{A_{ii} + A_{jj}} \right)^{\frac{1}{b-a}}. \quad (4.27)$$

Equilibria

To find the equilibria of system (4.25)-(4.26), we let $c = 0$. Then (4.25) is solved by $r = r_{cr}^F$, and from (4.26) we get (4.15) or

$$z^2 = \left(\frac{b}{a}\right)^{\frac{2}{b-a}} \left[\left(\frac{B_{ii} + B_{jj}}{A_{ii} + A_{jj}}\right)^{\frac{2}{b-a}} - \frac{1}{4} \left(\frac{B_{ii}}{A_{ii}}\right)^{\frac{2}{b-a}} \right].$$

Since $z^2 > 0$, then there are two spatial equilibria when $r_{cr}^F < 2r_{cr}^G$, located at

$$(r, z) = \left(r_{cr}^F, \pm \left(\frac{b}{a}\right)^{\frac{1}{b-a}} \sqrt{\left(\frac{B_{ii} + B_{jj}}{A_{ii} + A_{jj}}\right)^{\frac{2}{b-a}} - \frac{1}{4} \left(\frac{B_{ii}}{A_{ii}}\right)^{\frac{2}{b-a}}} \right). \quad (4.28)$$

Relative Equilibria

For $c \neq 0$, we find the spatial RE of system (4.25)-(4.26). Recall that the cornerstone value for angular momentum $c = c_{0,s}$, and corresponding distance $r(c_{0,s}) = l$ is determined by the solution $(l, c_{0,s})$ of system (4.18)-(4.19). After some elementary calculations, we find

$$l = \left(\frac{b(b-2)B_{ii}}{a(a-2)A_{ii}}\right)^{\frac{1}{b-a}}, \quad c_{0,s} = \sqrt{M \left(\frac{aA_{ii}}{l^{a-2}} - \frac{bB_{ii}}{l^{b-2}}\right)}, \quad (4.29)$$

In the previous section, we found that a change in the number of existing spatial RE can occur with different positions (or values) of $2r_{cr}^G$, and angular momentum c . Threshold values for c include $c_{0,s}$, defined in (4.29), and $c_{1,s}$ where $0 < c_{1,s} \leq c_{0,s}$, defined as

$$c_{1,s} := 2\sqrt{2M \left(\frac{aA_{ii}}{(2r_{cr}^G)^{a-2}} - \frac{bB_{ii}}{(2r_{cr}^G)^{b-2}}\right)}. \quad (4.30)$$

Corollary 4.2.3. *Let l , $c_{0,s}$ and $c_{1,s}$ be as defined by (4.29) and (4.30), respectively.*

4.2. SPATIAL EQUILIBRIA AND RELATIVE EQUILIBRIA ($Z \neq 0$) 47

Applying the generalized Lennard-Jones potential to Proposition (4.2.1), we obtain the following three cases:

1. If $2r_{cr}^G \leq r_{cr}^F$, or equivalently, when

$$2^{b-a} \leq \frac{1 + \frac{A_{jj}}{A_{ii}}}{1 + \frac{B_{jj}}{B_{ii}}}, \quad (4.31)$$

there are no spatial RE.

2. If $r_{cr}^F < 2r_{cr}^G \leq l$, or equivalently, when

$$\frac{1 + \frac{A_{jj}}{A_{ii}}}{1 + \frac{B_{jj}}{B_{ii}}} < 2^{b-a} \leq \left(\frac{b-2}{a-2} \right) \left(\frac{1 + \frac{A_{jj}}{A_{ii}}}{1 + \frac{B_{jj}}{B_{ii}}} \right), \quad (4.32)$$

for $c \in (0, c_{1,s})$, there exists one family of spatial RE.

3. If $l < 2r_{cr}^G$, or equivalently, when

$$\left(\frac{b-2}{a-2} \right) \left(\frac{1 + \frac{A_{jj}}{A_{ii}}}{1 + \frac{B_{jj}}{B_{ii}}} \right) < 2^{b-a}, \quad (4.33)$$

then

a) for $c \in (0, c_{1,s})$ there is one spatial family of RE;

b) for $c \in [c_{1,s}, c_{0,s})$ there are two spatial families of RE. At $c = c_{0,s}$ these families coincide;

c) for $c > c_{0,s}$, no spatial RE exist.

Identical Atoms

When all three atoms are identical and we have a H_3 -type molecule, the three masses m_1, m_2, m_3 are equal, and the coefficients of the potential are $A_{ij} = \frac{A_{ii}+A_{jj}}{2} = \frac{A_{ii}+A_{ii}}{2} = A_{ii}$ and $B_{ij} = \frac{B_{ii}+B_{jj}}{2} = \frac{B_{ii}+B_{ii}}{2} = B_{ii}$. After substitution in conditions (4.32) - (4.32) and taking into account that $2 < a < b$, we obtain

1. If

$$2^{b-a} \leq \left(\frac{b-2}{a-2} \right) \quad (4.34)$$

then for $c \in (0, c_{1,s})$ there is one family of spatial RE.

2. If

$$\left(\frac{b-2}{a-2} \right) < 2^{b-a} \quad (4.35)$$

then for

a) for $c \in (0, c_{1,s})$ there is one spatial family of RE;

b) for $c \in [c_{1,s}, c_{0,s})$ there are two spatial families of RE. At $c = c_{0,s}$ these families coincide;

c) for $c > c_{0,s}$, no spatial RE exist.

Remark 4.2.4. *For the 12–6 Lennard-Jones potential the condition (4.35) is verified.*

4.3 Stability

In this section we state the stability conditions of the equilibria and relative equilibria following the definitions and criteria presented in Appendix B. In the next chapter we

apply them in the context of the Lennard-Jones potential and continue our analysis through numerical simulations.

4.3.1 Lyapunov stability

We determine if the equilibria and RE are stable by using a Lyapunov test. Let $(r_e, z_e; c)$ be a relative equilibrium. Given the structure of the reduced Hamiltonian “kinetic plus reduced (effective) potential” (see relation (3.20)), we need to determine whether or not the Hessian $D^2V_{\text{red}}(r_e, z_e; c)$ of the reduced potential V_{red} given by (3.21), is positive definite. In the affirmative case, the RE is stable. Otherwise, the stability cannot be determined in this way and we proceed to spectral analysis.

In our case, $D^2V_{\text{red}}(r_e, z_e; c)$ is positive definite if the values of the first position in the upper left corner and the determinant of the matrix $D^2V_{\text{red}}(r_e, z_e; c)$ are positive. We calculate the components of

$$D^2V_{\text{red}}(r, z; c) = \begin{pmatrix} \frac{\partial^2 V_{\text{red}}}{\partial r^2} & \frac{\partial^2 V_{\text{red}}}{\partial r \partial z} \\ \frac{\partial^2 V_{\text{red}}}{\partial z \partial r} & \frac{\partial^2 V_{\text{red}}}{\partial z^2} \end{pmatrix} \quad (4.36)$$

and find

$$\begin{aligned}\frac{\partial^2 V_{\text{red}}}{\partial r^2}(r, z; c) &= \frac{3c^2}{Mr^4} + F''(r) + r^2 \frac{G''\left(\sqrt{\frac{r^2}{4} + z^2}\right)}{2(r^2 + 4z^2)} + G'\left(\sqrt{\frac{r^2}{4} + z^2}\right) \left(\frac{4z^2}{(r^2 + 4z^2)^{\frac{3}{2}}}\right) \\ \frac{\partial^2 V_{\text{red}}}{\partial z \partial r}(r, z; c) &= \frac{2rz}{r^2 + 4z^2} \left[G''\left(\sqrt{\frac{r^2}{4} + z^2}\right) - \frac{2G'\left(\sqrt{\frac{r^2}{4} + z^2}\right)}{\sqrt{r^2 + 4z^2}} \right] = \frac{\partial^2 V_{\text{red}}}{\partial r \partial z}(r, z; c) \\ \frac{\partial^2 V_{\text{red}}}{\partial z^2}(r, z; c) &= \frac{4}{r^2 + 4z^2} \left[2z^2 G''\left(\sqrt{\frac{r^2}{4} + z^2}\right) + G'\left(\sqrt{\frac{r^2}{4} + z^2}\right) \left(\frac{r^2}{\sqrt{r^2 + 4z^2}}\right) \right].\end{aligned}$$

Planar equilibria and relative equilibria ($z = 0$)

When $z_e = 0$, we find $D^2 V_{\text{red}}(r_e, 0; c)$

$$D^2 V_{\text{red}}(r_e, 0; c) = \begin{pmatrix} \frac{3c^2}{Mr_e^4} + F''(r_e) + \frac{1}{2} G''\left(\frac{r_e}{2}\right) \left(\frac{2-r_e}{r_e^2}\right) & 0 \\ 0 & \frac{4}{r_e} G'\left(\frac{r_e}{2}\right) \end{pmatrix}. \quad (4.37)$$

Spatial equilibria and relative equilibria ($z \neq 0$)

For relative equilibria with $z_e \neq 0$ we have

$$D^2 V_{\text{red}}(r_e, z_e; c) = \begin{pmatrix} \frac{3c^2}{Mr_e^4} + F''(r_e) + r_e^2 \frac{G''\left(\sqrt{\frac{r_e^2}{4} + z_e^2}\right)}{2(r_e^2 + 4z_e^2)} & \frac{2r_e z_e}{r_e^2 + 4z_e^2} G''\left(\sqrt{\frac{r_e^2}{4} + z_e^2}\right) \\ \frac{2r_e z_e}{r_e^2 + 4z_e^2} G''\left(\sqrt{\frac{r_e^2}{4} + z_e^2}\right) & \frac{8z_e^2}{r_e^2 + 4z_e^2} G''\left(\sqrt{\frac{r_e^2}{4} + z_e^2}\right) \end{pmatrix} \quad (4.38)$$

Remark 4.3.1. From the expression (4.37) and (4.38), the RE Lyapunov stability does not depend on the third mass m_3 , but only on the two equal masses $m_1 = m_2 = m$

(via the reduced mass $M = \frac{m_1 m_2}{m_1 + m_2} = \frac{m}{2}$).

4.3.2 Spectral Stability

If the Lyapunov test fails, then the stability of the RE can not be determined by this method. Instead, we test for spectral stability. This is done by calculating the eigenvalues of the linearization matrix $\mathbb{J}D^2H_{\text{red}}(r_e, z_e, 0, 0; c)$, where

$$\mathbb{J} = \begin{pmatrix} 0 & 0 & 1 & 0 \\ 0 & 0 & 0 & 1 \\ -1 & 0 & 0 & 0 \\ 0 & -1 & 0 & 0 \end{pmatrix}. \quad (4.39)$$

$$D^2H_{\text{red}}(r_e, z_e, 0, 0; c) = \begin{pmatrix} \frac{\partial^2 H_{\text{red}}}{\partial r^2} & \frac{\partial^2 H_{\text{red}}}{\partial r \partial z} & \frac{\partial^2 H_{\text{red}}}{\partial r \partial p_r} & \frac{\partial^2 H_{\text{red}}}{\partial r \partial p_z} \\ \frac{\partial^2 H_{\text{red}}}{\partial z \partial r} & \frac{\partial^2 H_{\text{red}}}{\partial z^2} & \frac{\partial^2 H_{\text{red}}}{\partial z \partial p_r} & \frac{\partial^2 H_{\text{red}}}{\partial z \partial p_z} \\ \frac{\partial^2 H_{\text{red}}}{\partial p_r \partial r} & \frac{\partial^2 H_{\text{red}}}{\partial p_r \partial z} & \frac{\partial^2 H_{\text{red}}}{\partial p_r^2} & \frac{\partial^2 H_{\text{red}}}{\partial p_r \partial p_z} \\ \frac{\partial^2 H_{\text{red}}}{\partial p_z \partial r} & \frac{\partial^2 H_{\text{red}}}{\partial p_z \partial z} & \frac{\partial^2 H_{\text{red}}}{\partial p_z \partial p_r} & \frac{\partial^2 H_{\text{red}}}{\partial p_z^2} \end{pmatrix} \Big|_{(r,z,p_r,p_z;c)=(r_e,z_e,0,0;c)} \quad (4.40)$$

The matrix $\mathbb{J}D^2H_{\text{red}}(r_e, z_e, 0, 0; c)$ yields four eigenvalues. If all these eigenvalues are purely complex then the RE $(r_e, z_e; c)$ is spectrally stable. If there is at least one eigenvalue with non-zero real part, then the RE is unstable.

Chapter 5

Numerical Simulations for Lennard-Jones Type Interactions

5.1 General set-up

In what follows we investigate numerically the equilibria and relative equilibria of isosceles triatomic molecules of type D_2H , H_3 and H_2D . As noted previously, we assume that if two atoms have the same mass, then they are of the same kind. We consider the Lennard-Jones interactions as defined in Chapter 4 by formula (4.1) and (4.3) with $a = 6$ and $b = 12$.

The numerical explorations are performed in Matlab[®] code. The entries needed to run the code are $a, b, A_{ii}, B_{ii}, A_{jj}, B_{jj}$ and the masses m_1, m_2, m_3 .

The RE are solutions to system (3.26) - (3.27). We determine these as a function of

the angular momentum c , which varies from zero to its maximal (critical) value where the RE cease to exist. To test the stability of a RE $(r_e, z_e, 0, 0; c)$, we first test for Lyapunov stability by evaluating the Hessian of the reduced potential as given by (4.36). If this is found to be positive definite, then the solution is Lyapunov stable. If the Lyapunov criteria fails, then we determine spectral stability by calculating the entries of the linearization matrix $\mathbb{J}D^2H_{\text{red}}(r_e, z_e, 0, 0; c)$, where \mathbb{J} and $D^2H_{\text{red}}(r_e, z_e, 0, 0; c)$ are given by (4.39) and (4.40), respectively, and by finding the real part of each eigenvalue. If there exists at least one eigenvalue with non-zero real part, then the corresponding relative equilibrium is unstable; otherwise it is spectrally stable.

As a side note, we observe that the existence of RE, given by the solutions of (3.26) - (3.27), is independent of the third mass m_3 . Moreover, from Remark 4.3.1, the RE Lyapunov stability test is also independent of m_3 .

The output of the code consists of diagrams of the following two types:

1. Diagrams which depict the dependency of the distances between the atoms to the total angular momentum. For the planar case, we have only the diagram which shows of the dependency of the distance between m_1 and m_2 to the total angular momentum. For the spatial case an additional diagram displays the dependency of the distance between m_3 and the origin to the total angular momentum.
2. Energy-Momentum diagrams, that is, the RE in the total angular momentum - total energy (c, h) plane.

The diagrams are augmented by a legend with assigned symbols for the planar/spatial and stable/unstable cases.

5.2 Numerical Simulations

In this section we present:

1. Diagrams for a H_3 -type molecule, and
2. Diagrams for the three types of molecules. As mentioned, for atoms not of the same type, we use the Lorentz-Berthelot rule (4.2) for determining the potential parameters. The code was run with the fixed parameters

$$a = 6, \quad b = 12, \quad A_{ii} = B_{ii} = B_{jj} = 1. \quad (5.1)$$

1. Diagrams for a H_3 -type molecule.

To run the code for a H_3 -type molecule with parameters (5.1) as above, we further fix $m = m_3 = 1$, and $A_{jj} = A_{ii} = 1$ and $B_{jj} = B_{ii} = 1$. Then by Remark 4.2.4, for low angular momenta we expect one family of spatial RE. As the angular momentum increases, this family should bifurcate to two families of spatial RE. For high angular momenta only planar RE survive up to the dissociation of the molecule. The numerical experiments are in agreement with the theoretical predictions. Figures (5.1) - (5.3) portray the evolution of the inter-particle distance as the total angular momentum increases. Figure (5.4) displays the Energy-Momentum diagram, with a close-up

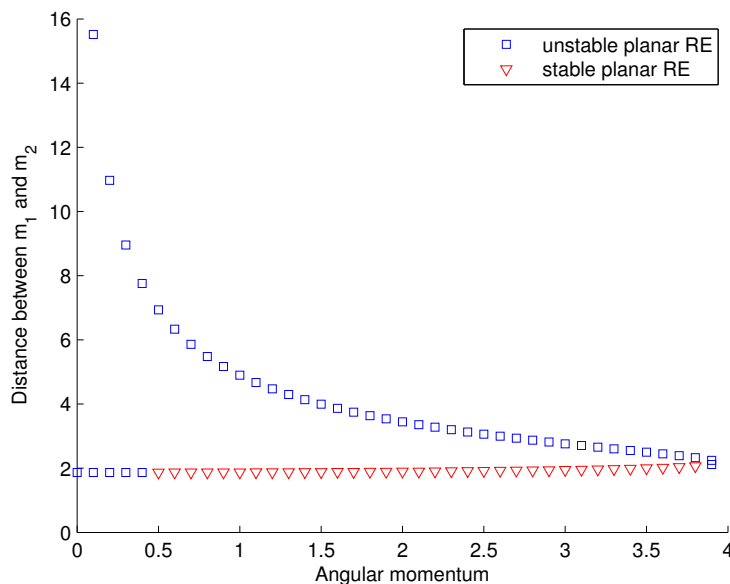


Figure 5.1: Dependency of the distance $m_1 - m_2$ on the angular momentum, for planar RE of an H_3 -type molecule.

of the bifurcation in Figure (5.5).

2. Diagrams for H_2D - and D_2H -type molecules obtained by varying m

We fix $A_{jj} = 5$ and $m_3 = 1$ and discuss molecules of the type H_2D and D_2H , by taking $m = 0.5$, and $m = 1.5$, respectively. For all these cases, we observe the presence of spatial RE. This is in agreement with the theoretical condition (4.33) of Corollary 4.2.3. Since the critical values c_0 and c_1 are directly proportional to $\sqrt{\frac{m}{2}} = \sqrt{M}$ (see formula (4.29) and (4.30)), we expect that they increase with m . The numerical experiments confirm this as well. Figures (5.6) - (5.11) show the evolution of the inter-particle distance as the total angular momentum increases. Figures (5.12) and (5.14) display the Energy-Momentum diagrams, with their respective bifurcations in Figures (5.13) and (5.15).

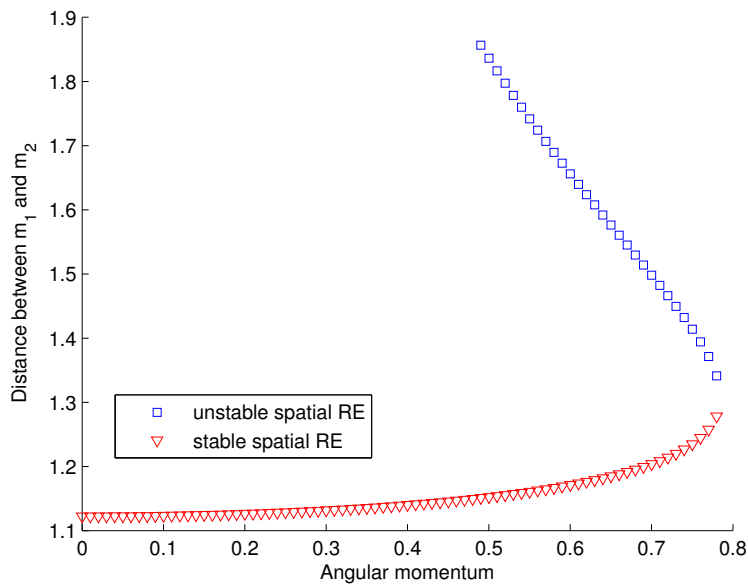


Figure 5.2: Dependency of the distance $m_1 - m_2$ on the angular momentum for spatial RE of an H_3 -type molecule.

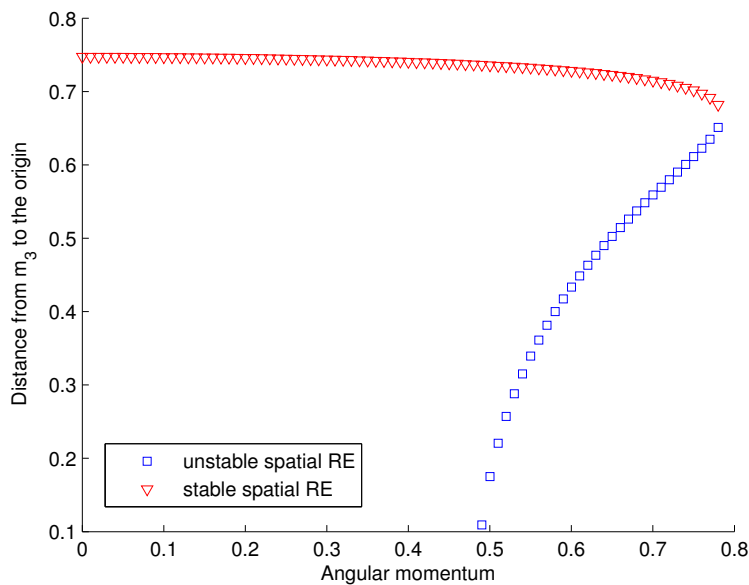


Figure 5.3: Dependency of the “height” distance m_3 to the origin on the angular momentum for spatial RE of an H_3 -type molecule.

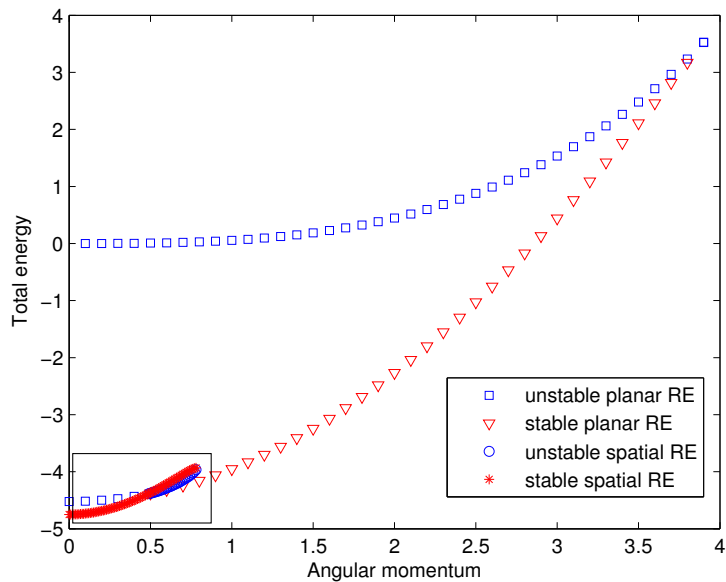


Figure 5.4: The Energy-Momentum diagram for H_3 -type molecules. At low momenta there are three families of RE: two planar and one spatial. As the momentum increases, the spatial family meets the planar family and it bifurcates

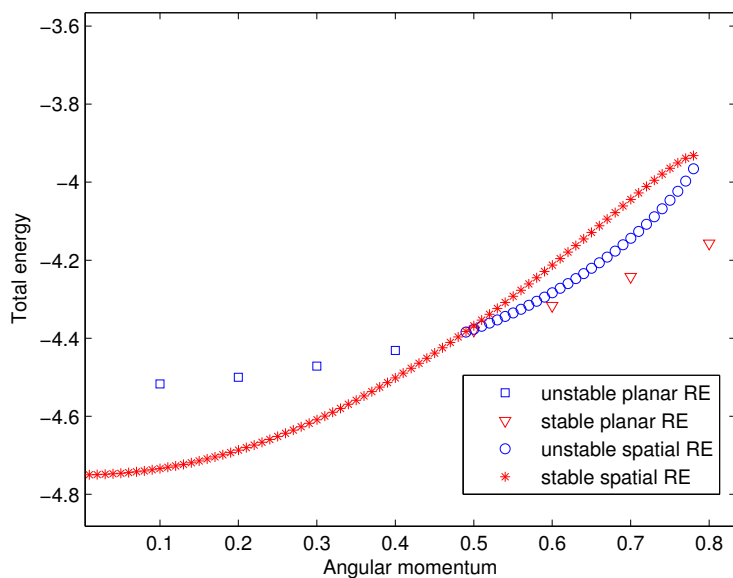


Figure 5.5: Close-up of the spatial RE bifurcation

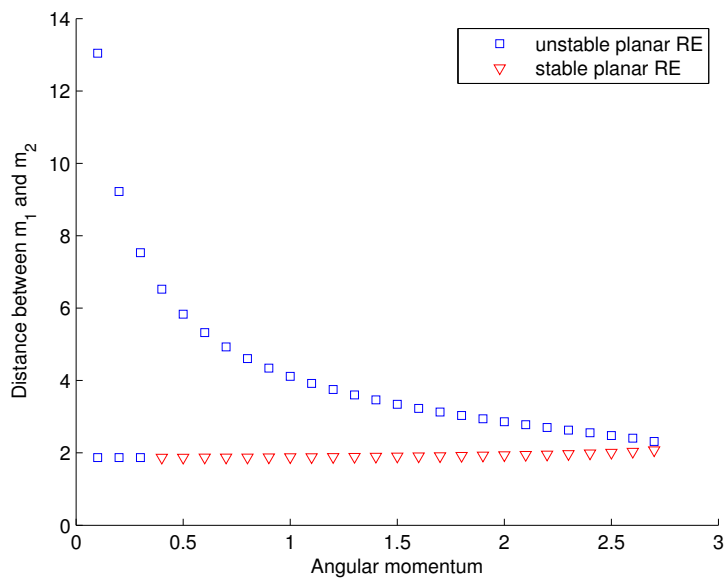


Figure 5.6: Dependency of the distance $m_1 - m_2$ on the angular momentum c , for planar RE molecules for an H_2D -type molecule ($m = 0.5$). As m increases, planar RE are present for higher momenta.

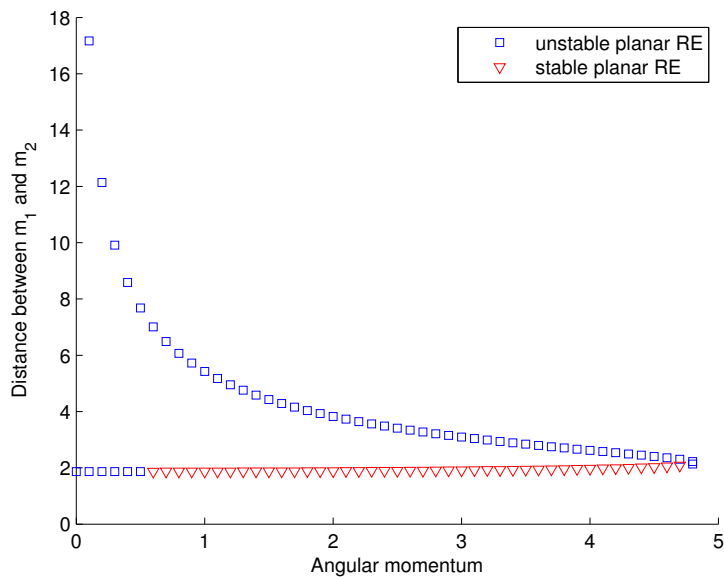


Figure 5.7: Dependency of the distance $m_1 - m_2$ on the angular momentum c , for planar RE molecules for an D_2H -type molecule ($m = 1.5$). As m increases, planar RE are present for higher momenta.

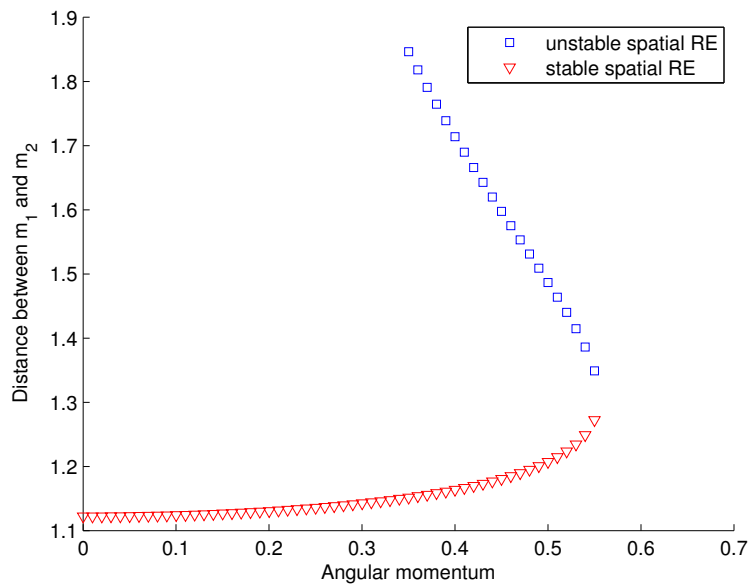


Figure 5.8: Dependency distance $m_1 - m_2$ on the angular momentum c for spatial RE of an H_2D -type molecule ($m = 0.5$)

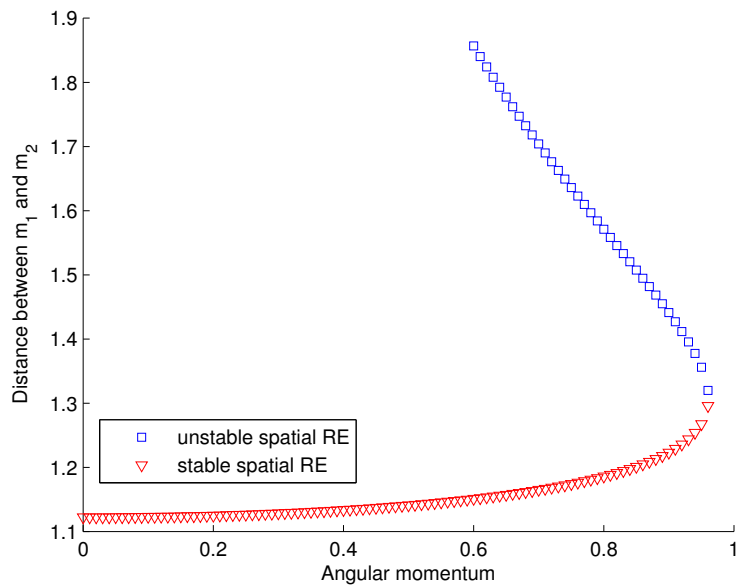


Figure 5.9: Dependency distance $m_1 - m_2$ on the angular momentum c for spatial RE of an D_2H -type molecule ($m = 1.5$)

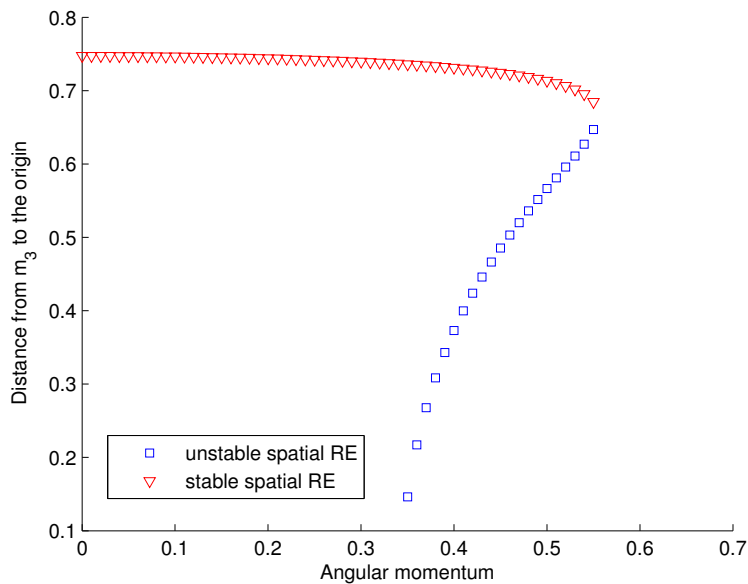


Figure 5.10: The dependency of the “height” distance m_3 to the origin on the angular momentum c for spatial RE of an H_2D -type molecule ($m = 0.5$)

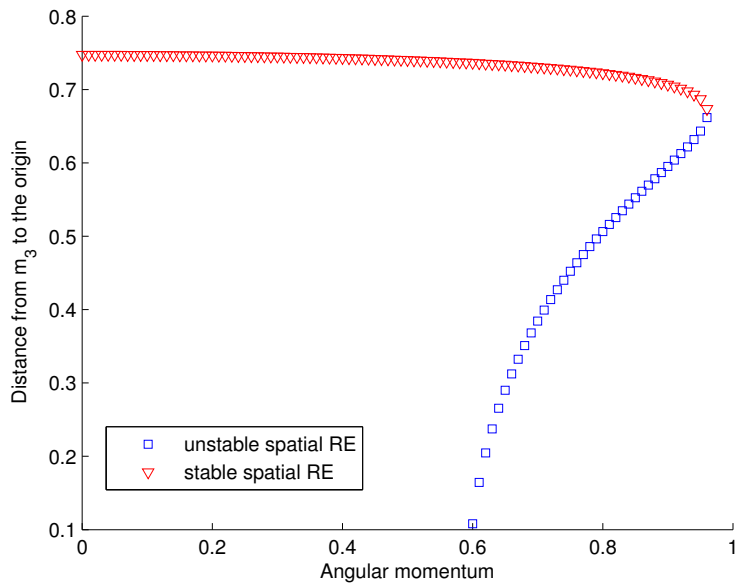


Figure 5.11: The dependency of the “height” distance m_3 to the origin on the angular momentum c for spatial RE of a D_2H -type molecule ($m = 1.5$)

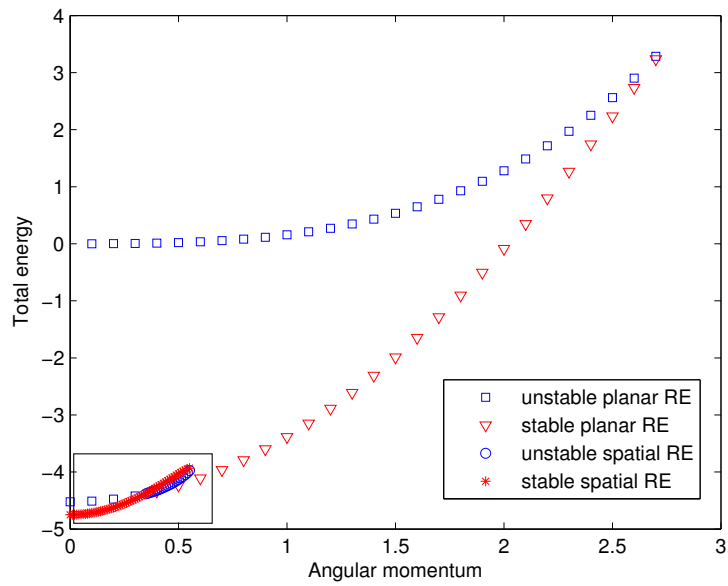


Figure 5.12: The Energy-Momentum diagram for H_2D -type molecule ($m = 0.5$)

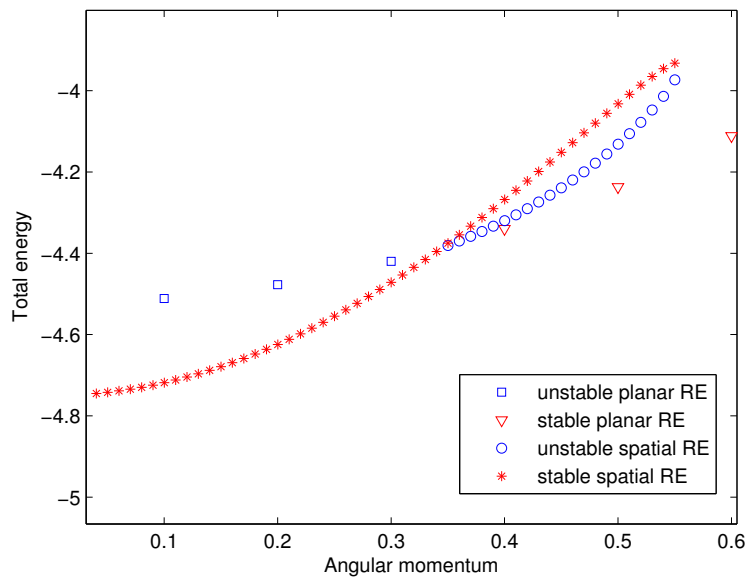


Figure 5.13: H_2D -type molecule ($m = 0.5$)

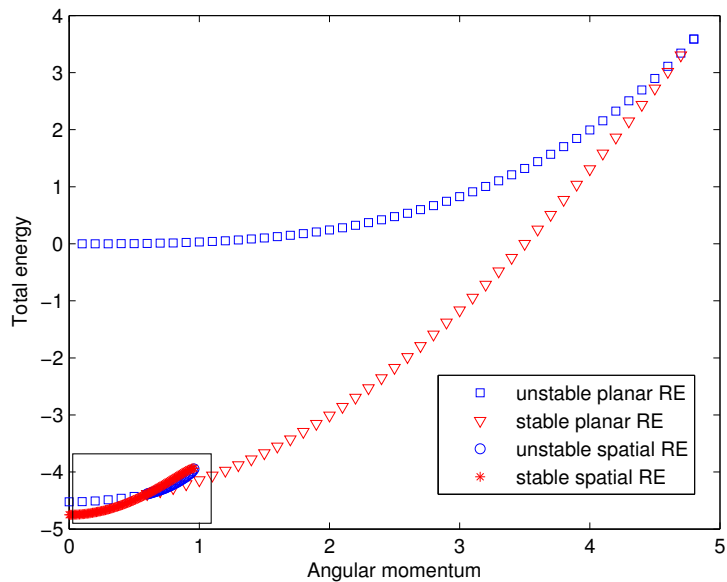


Figure 5.14: The Energy-Momentum diagram for D_2H -type molecule ($m = 1.5$)

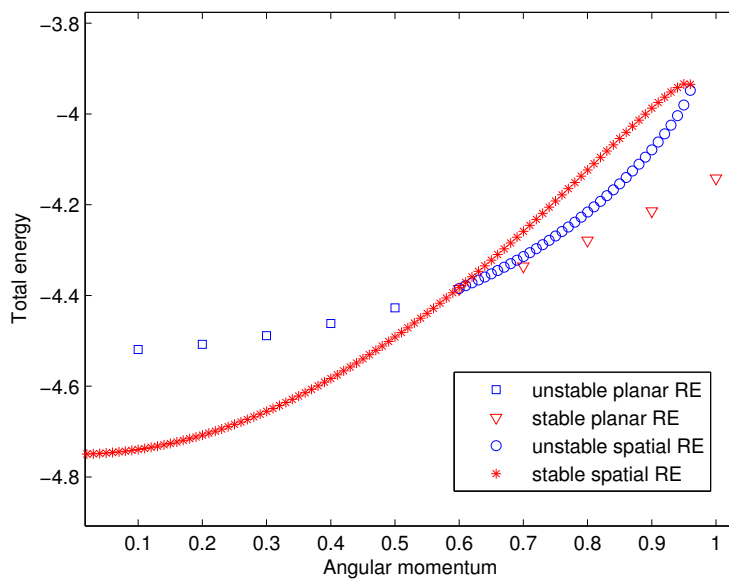


Figure 5.15: A close-up of the bifurcation for a D_2H -type molecule ($m = 1.5$)

Chapter 6

Conclusion

In this thesis, we study equilibria and relative equilibria of diatomic and isosceles triatomic molecule of the types D_2H , H_3 and H_2D in the framework of classical mechanics. Our research develops on three levels: first, we deduce results using qualitative analysis in which case the inter-particle interaction is modelled by a general repulsive-attractive “well”-shaped potential with parameters given by the coordinates of their critical points. Second, we perform an analytical investigation, in which case the inter-particle interaction is given by the generalized Lennard-Jones potential; third, we perform numerical experiments using the 12 – 6 Lennard-Jones potential.

For diatomic systems we retrieve known results (see [Kozin & al. (1999)]), including the description of the Hill regions of motion and the Energy-Momentum diagram.

For triatomic isosceles systems, we discuss qualitatively the number of planar and spatial families of RE as function of the total angular momentum. We observe that

the number of families RE is independent of the mass m_3 on the isosceles' triangle vertical. We find that there can be at least two and at most four families of planar RE. In Proposition (4.2.1) we establish the qualitative conditions which provide the number of families of spatial relative equilibria. To our knowledge, this is the first time such conditions are deduced. Further, we specialize the potential to the generalized Lennard-Jones potential (analytic form) and we prove that there are always two planar RE. In Corollary (4.2.3) we establish the analytic conditions equivalent to those in Proposition (4.2.1). In the stability analysis we observe that the Lyapunov stability criterion is independent of the mass m_3 .

We perform numerical experiments using a Matlab[®] code which we designed and implemented. We calculate diagrams for an H_3 -type molecule and compare H_2D - and D_2H -type molecules by varying the mass of the two identical atoms. We present the results in “distance versus angular momentum” and “Energy-Momentum diagrams.” The numerical experiments are all in agreement with the theoretical predictions.

The present investigation may be continued in a variety of directions. For instance, a further study is to find analytic conditions for RE stability, similar to those found here for RE existence. Another research direction could be the studying of the dependency of the RE stability with respect to the Lennard-Jones potential parameters. In a more involved investigation one may compare our Energy-Momentum diagrams to those in [Kozin & al. (1999)] and [Kozin & al. (2000)]. In these papers, the authors use an empirical (numerically deduced) molecular potential and perform the RE analysis in the full phase-space of the molecules (that is, the phase-space is not restricted to isosceles configurations). Consequently, the classical Hamiltonian model

of the molecule has additional degrees of freedom which could lead to different results on the RE stability (the additional degrees of freedom could correspond to unstable directions which in the isosceles restricted problem cannot be “seen”). It would be interesting to develop a comparison study, and detect the unstable directions in both isosceles restricted and non-restricted molecular configurations.

Appendix A

Equilibria and stability for autonomous ODEs

In this section we briefly review the standard theory on the existence and stability of equilibria of ODEs. The main references are [Glendinning (1994), Gross (2011), Dahleh & al. (2011), Meiss (2007), Nagle & al. (2008), Perko (2001)].

Definition A.0.1. *Consider the non-linear autonomous system*

$$\dot{x}(t) = f(x(t)), \quad x \in D \subset \mathbb{R}^n, \quad D \text{ open} \quad (\text{A.1})$$

*with $f : D \rightarrow \mathbb{R}^n$ is Lipschitz-continuous on its domain. A point $x_e \in D$ is called an **equilibrium point** for (A.1) if it is a solution of*

$$f(x(t)) = 0. \quad (\text{A.2})$$

It can be checked that a solution $x(t) = x_e$ for all t is valid, by verifying if (A.1) holds.

An equilibrium point x_e is said to be Lyapunov stable if solutions that start within a small neighbourhood stay within that neighbourhood. Additionally, if the solutions which start within a small neighbourhood tend to the equilibrium point, then they are called asymptotically stable. Formally,

Definition A.0.2. *An equilibrium point x_e is **Lyapunov stable** if and only if for all $\epsilon > 0$ there exists $\delta > 0$ such that if $|x(t_o) - x_e| < \delta$, then*

$$|x(t) - x_e| < \epsilon, \quad \forall t \geq t_o. \quad (\text{A.3})$$

Definition A.0.3. *An equilibrium point x_e is **asymptotically stable** if and only if it satisfies the following two conditions*

1. *the stability condition (A.3), as defined above, and*
2. *there exists $\delta > 0$ such that if $|x(t_o) - x_e| < \delta$, then*

$$\lim_{t \rightarrow \infty} |x(t) - x_e| = 0. \quad (\text{A.4})$$

From now on, without loss of generality, we will assume the equilibrium point $x_e = 0$, since this can be achieved by a linear change of coordinates.

Definition A.0.4. *Let $F(x)$ be a continuous function on some domain D containing the origin and assume that $F(0) = 0$. Then*

1. $F(x)$ is **positive definite** on D if $F(x) > 0, \forall x \in D \setminus \{0\}$
2. $F(x)$ is **positive semidefinite** on D if $F(x) \geq 0, \forall x \in D \setminus \{0\}$
3. $F(x)$ is **negative definite** on D if $F(x) < 0, \forall x \in D \setminus \{0\}$
4. $F(x)$ is **negative semidefinite** on D if $F(x) \leq 0, \forall x \in D \setminus \{0\}$

Definition A.0.5. Let $x_e = 0$ be the equilibrium point for the differential equation (A.1). Let D be an open neighbourhood surrounding the origin and $F(x)$ be a continuously differentiable function. Then $F(x)$ is a **Lyapunov Function** if it is continuously differentiable on D and

1. $F(0) = 0$
2. $F(x) \geq 0$ for all $x \in D \setminus \{0\}$
3. $\dot{F}(x(t)) \leq 0$ along any solution $x(t)$ with $x(t_0) \in D$.

Theorem A.0.6 (Lyapunov's First Stability Theorem). Suppose that a Lyapunov function $F(x)$ can be defined on a neighbourhood of the origin and $x_e = 0$. Then the origin is (Lyapunov) stable.

Theorem A.0.7 (Lyapunov's second stability theorem). Suppose that $x_e = 0$ is an equilibrium point for equation (A.1) and $F(x)$ is a Lyapunov function that is continuous on D , which contains the equilibrium point. If $\dot{F}(x) < 0$ for all $x \in D \setminus \{0\}$, then $x_e = 0$ is asymptotically stable.

If the Lyapunov test fails, then the stability of the equilibria cannot be determined by this method. Instead one resorts to studying the behaviour of the linear system at $x = x_e$.

Definition A.0.8. We call the **linearization** of (A.1) at the equilibrium x_e the linear system given by

$$\dot{x} = Ax, \tag{A.5}$$

where

$$A = Df(x_e) \tag{A.6}$$

The eigenvalues of matrix A determine the stability of the equilibrium point (see [Nagle & al. (2008)]).

Definition A.0.9. An equilibrium x_e of (A.1) is called **hyperbolic** if none of the eigenvalues of A have zero real part.

Proposition A.0.10. A hyperbolic equilibrium x_e of (A.1) is **unstable** if at least one of the eigenvalues of A has strictly positive real part.

Proposition A.0.11. A hyperbolic equilibrium x_e of (A.1) is **asymptotically stable** if all of the eigenvalues of A have strictly negative real part.

Definition A.0.12. A hyperbolic equilibrium x_e of (A.1) is **spectrally stable** if all of the eigenvalues of A have negative real part.

Note that a non-hyperbolic equilibrium may be spectrally stable. This is the case of conservative Hamiltonian systems which is discussed in Section B.5).

Definition A.0.13. For eigenvalues $\lambda_1, \dots, \lambda_n$ of A , if

1. all have negative real part, then x_e is called a **sink**;
2. all have positive real part, then x_e is called a **source**;

3. if at least one has positive real part and at least one has negative real part, then x_e is a **saddle**.

Appendix B

Mathematical formulation of conservative mechanical N -point mass systems

The following sections describe the classical dynamics prerequisites required for our study. The main sources of reference are [Holm & al. (2009), Meyer & al. (1992)].

B.1 Newtonian N -Body Systems

In this section we review some of the properties associated with N -bodies (each with mass m_i) with mutual (binary) interaction. We denote a fixed frame of reference by \mathbb{R}^d , where d is the spatial dimension ($d = 1, 2$ or 3), and each of the N -bodies is

represented by a single point mass.

Definition B.1.1. A *point mass* is an idealised zero-dimensional object that is completely described by its mass and spatial position. Its mass is assumed to be constant and its position varies as a function of time.

The *configuration* of a system containing N point masses that interact with one another is given by the multi-vector $\mathbf{q} = (\mathbf{q}_1, \mathbf{q}_2, \dots, \mathbf{q}_N) \in \mathbb{R}^{dN}$, where \mathbf{q}_i denotes the position vector of each of the point masses. The set of all possible configurations of this system is called the *configuration space*, where (in the absence of constraints), it is either \mathbb{R}^{dN} (if no collisions are possible) or an open subset of \mathbb{R}^{dN} . We denote the velocity and acceleration as function of time of each point mass by $\frac{d\mathbf{q}_i}{dt} = \dot{\mathbf{q}}_i(t)$ and $\frac{d^2\mathbf{q}_i}{dt^2} = \ddot{\mathbf{q}}_i(t)$, respectively.

Definition B.1.2. *Newton's second law for the system is*

$$m_i \ddot{\mathbf{q}}_i = \mathbf{F}_i \quad \text{for } i = 1, 2, \dots, N, \quad (\text{B.1})$$

where \mathbf{F}_i is the total force on the i^{th} point mass.

Definition B.1.3. A frame of reference in which Newton's second law applies is called an *inertial frame*.

Throughout, we assume an inertial frame of reference. We also assume that each \mathbf{F}_i is a smooth function of configurations only, i.e., $\mathbf{F}_i = \mathbf{F}_i(\mathbf{q}_1, \mathbf{q}_2, \dots, \mathbf{q}_N)$. Thus the system (B.1) is a second order autonomous ODE system with \mathbb{R}^{dN} equations and \mathbb{R}^{dN} unknowns.

The following dynamical quantities play central roles in the dynamics of the system preceding. In many situations, these quantities are conserved, that is, they are constant along any trajectory

$$\mathbf{q}(t) = (\mathbf{q}_1(t), \mathbf{q}_2(t), \dots, \mathbf{q}_N(t))$$

of the system (B.1), as long as it satisfies equation (B.1).

Definition B.1.4 (Dynamical quantities).

The **linear momentum** (or **impulse**) of a single point mass with position \mathbf{q}_i is

$$\mathbf{p}_i := m_i \dot{\mathbf{q}}_i$$

Then the **(total) linear momentum** of the system is the sum of the linear momenta of all of the point masses, that is

$$\mathbf{p} := \sum \mathbf{p}_i := \sum m_i \dot{\mathbf{q}}_i$$

The **centre of mass** is a unique location in space such that

$$c(t) = \frac{\sum_i^N m_i \mathbf{q}_i}{\sum_i^N m_i}. \quad (\text{B.2})$$

The **angular momentum**, about the origin of coordinates $\mathbf{q} = \mathbf{0}$, of a single point mass with position $\mathbf{q}_i \in \mathbb{R}^3$ is

$$\boldsymbol{\pi}_i := \mathbf{q}_i \times m_i \dot{\mathbf{q}}_i = \mathbf{q}_i \times \mathbf{p}_i, \quad (\text{B.3})$$

where \times denotes the three-dimensional vector cross-product. Then the **(total) angular momentum** of a spatial system ($d = 3$) of N point masses, taken about the origin of coordinates where $\mathbf{q} = \mathbf{0}$, is the sum of the angular momenta of all of the point masses, that is,

$$\boldsymbol{\pi} = \sum \boldsymbol{\pi}_i := \sum \mathbf{q}_i \times m_i \dot{\mathbf{q}}_i = \sum \mathbf{q}_i \times \mathbf{p}_i. \quad (\text{B.4})$$

Geometrically, this is the sum of the N oriented areas given by the cross-products of pairs of vectors \mathbf{q}_i and \mathbf{p}_i . For a planar system (with $d = 2$), the total angular momentum is the scalar defined by

$$\pi := \sum m_i (q_i^1 \dot{q}_i^2 - q_i^2 \dot{q}_i^1) = \sum q_i^1 p_i^2 - q_i^2 p_i^1, \quad (\text{B.5})$$

where $\mathbf{q}_i = (q_i^1, q_i^2)$ and $\mathbf{p}_i = (p_i^1, p_i^2)$. Note that if the vectors \mathbf{q}_i are embedded in \mathbb{R}^3 as $(q_i^1, q_i^2, 0)$, then π as defined above is the third component of the vector $\boldsymbol{\pi}$ as defined in (B.4). Also note that angular momentum is undefined for systems defined on a line ($d = 1$).

The **(total) kinetic energy** of the system of N point masses is

$$K := \frac{1}{2} \sum m_i \|\dot{\mathbf{q}}_i\|^2,$$

Where $\|\dot{\mathbf{q}}_i\|^2 = \dot{\mathbf{q}}_i \cdot \dot{\mathbf{q}}_i = \sum_j (\dot{q}_i^j)^2$ is the squared **Euclidean norm** of $\dot{\mathbf{q}}_i$.

Remark B.1.5. One can convert the total angular momentum and kinetic energy

into polar coordinates by performing a change in coordinates

$$\mathbf{q}_i = (r_i \cos \theta_i, r_i \sin \theta_i) \quad \text{for } i = 1, 2, \dots, N.$$

yielding

$$\begin{aligned} \pi &= \sum m_i (r_i \cos \theta_i, r_i \sin \theta_i) \times \left(\dot{r}_i \cos \theta_i - r_i \dot{\theta}_i \sin \theta_i, \dot{r}_i \sin \theta_i + r_i \dot{\theta}_i \cos \theta_i \right) \\ &= \sum m_i r_i^2 \dot{\theta}_i, \\ K &= \frac{1}{2} \sum m_i \left\| \left(\dot{r}_i \cos \theta_i - r_i \dot{\theta}_i \sin \theta_i, \dot{r}_i \sin \theta_i + r_i \dot{\theta}_i \cos \theta_i \right) \right\|^2 \\ &= \frac{1}{2} \sum m_i \left(\dot{r}_i^2 + r_i^2 \dot{\theta}_i^2 \right). \end{aligned}$$

Under specific conditions, we have conservation of linear momentum, angular momentum, as well as energy.

Theorem B.1.6 (Conservation of linear momentum). *If $\sum \mathbf{F}_i = \mathbf{0}$, then the total linear momentum is conserved.*

Before we state the second conservation law, we require the following definition.

Definition B.1.7. *The **torque** on a point mass with position $\mathbf{q} \in \mathbb{R}^3$ and force \mathbf{F} is $\mathbf{q} \times \mathbf{F}$. The **total torque** of a system of N point mass is $\sum \mathbf{q}_i \times \mathbf{F}_i$.*

Theorem B.1.8 (Conservation of angular momentum). *If $\sum \mathbf{q}_i \times \mathbf{F}_i = \mathbf{0}$, for a system, then its total angular momentum is conserved.*

Now we will consider the force being exerted on a single mass point by another mass point within the system.

Definition B.1.9 (Binary particle interaction).

In many systems, the only forces on the point masses are **forces of binary interaction** \mathbf{F}_{ij} , each parallel to the inter-particle position vector $\mathbf{d}_{ij} = \mathbf{q}_i - \mathbf{q}_j$, such that we always have $\mathbf{F}_{ij} = -\mathbf{F}_{ji}$, and the total force on each point mass i is $\mathbf{F}_i = \sum_j \mathbf{F}_{ij}$. This system is called a **closed system**. Moreover, such forces are called **internal**, and any other forces are **external**.

Proposition B.1.10. In any closed system, the total force and the total torque are both zero.

Corollary B.1.11. The total angular momentum of a closed system is conserved.

Example B.1.12. (Newtonian 2-body systems) Consider a system formed by two mass points m_1 and m_2 , with mutual interaction, so that the motion is described by:

$$m_1 \ddot{\mathbf{q}}_1 = -\mathbf{F}(\mathbf{q}_2 - \mathbf{q}_1) \quad (\text{B.6})$$

$$m_2 \ddot{\mathbf{q}}_2 = \mathbf{F}(\mathbf{q}_2 - \mathbf{q}_1) \quad (\text{B.7})$$

where $F : D \subset \mathbb{R}^d \rightarrow \mathbb{R}^d$ is a force which depends on the relative vector $(\mathbf{q}_2 - \mathbf{q}_1)$ only. Then, since the sum of forces is zero, the linear momentum is conserved and we have

$$m_1 \dot{\mathbf{q}}_1(t) + m_2 \dot{\mathbf{q}}_2(t) = \text{const.} =: \mathbf{c}_1 \quad (\text{B.8})$$

where the constant \mathbf{c}_1 is determined by the initial conditions. (The relation above can be also immediately observed from the equations of motion).

Equation (B.8) leads to

$$\mathbf{c}(t) = \frac{m_1 \mathbf{q}_1(t) + m_2 \mathbf{q}_2(t)}{m_1 + m_2} = \frac{\mathbf{c}_1}{m_1 + m_2} t + \mathbf{c}_2 \quad (\text{B.9})$$

where \mathbf{c}_2 is a constant determined by the initial conditions. Let

$$\mathbf{r} := \mathbf{q}_2 - \mathbf{q}_1 \quad (\text{B.10})$$

be the relative vector of m_1 and m_2 and consider the change of coordinates $(\mathbf{q}_1, \mathbf{q}_2) \rightarrow (\mathbf{r}, \mathbf{c})$

$$\mathbf{r} = \mathbf{q}_2 - \mathbf{q}_1 \quad (\text{B.11})$$

$$\mathbf{c} = \frac{m_1 \mathbf{q}_1 + m_2 \mathbf{q}_2}{m_1 + m_2}. \quad (\text{B.12})$$

Then \mathbf{r} is given by the equation

$$\begin{aligned} \mathbf{r}(t) &= \mathbf{q}_2(t) - \mathbf{q}_1(t) = \frac{m_1 + m_2}{m_2} \mathbf{c}(t) - \frac{m_1}{m_2} \mathbf{q}_1(t) - \mathbf{q}_1(t) \\ &= \frac{m_1 + m_2}{m_2} \mathbf{c}(t) - \frac{m_1 + m_2}{m_2} \mathbf{q}_1(t). \end{aligned} \quad (\text{B.13})$$

From the above we deduce that

$$\ddot{\mathbf{r}}(t) = \frac{m_1 + m_2}{m_1 m_2} \mathbf{F}(\mathbf{r}) \quad (\text{B.14})$$

where we used (B.6) to substitute $\ddot{\mathbf{q}}_1$. Let $\tilde{\mathbf{r}}(t)$ be a solution of the equation (B.14)

above. Then the motion $\mathbf{r}(t)$ is given by

$$\mathbf{r}(t) = \tilde{\mathbf{r}}(t) + \frac{m_1 + m_2}{m_2} \mathbf{c}(t) \quad (\text{B.15})$$

that is, $\mathbf{r}(t)$ is the sum of the relative vector dynamics $\tilde{\mathbf{r}}(t)$ and dynamics of centre of mass vector $\mathbf{c}(t)$. Since the dynamics of the centre of mass (B.2) is known from the initial conditions (see equation (B.9)), it is sufficient to solve only (B.14).

Thus, without loss of generality, in the case of Newtonian 2-body systems, one takes the constants $\mathbf{c}_1 = \mathbf{0}$ and $\mathbf{c}_2 = \mathbf{0}$ and studies only the dynamics of the relative vector given by (B.14). It is customary to write this equation under the form

$$M\ddot{\mathbf{r}} = \mathbf{F}(\mathbf{r}) \quad (\text{B.16})$$

and call $M := \frac{m_1 m_2}{m_1 + m_2}$ the relative mass.

Unlike linear and angular momenta, the kinetic energy of closed systems is not necessarily conserved. However, the total energy is conserved if no forces are present.

Definition B.1.13. A *Newtonian N -body potential system* is a mechanical system formed by N point masses where the force on each mass point is the gradient of a function. Specifically,

$$m_i \ddot{\mathbf{q}}_i = - \frac{\partial V}{\partial \mathbf{q}_i}, \text{ for } i = 1, \dots, N$$

where $V : D \subset \mathbb{R}^{dn} \rightarrow \mathbb{R}$ is a smooth function called the **potential energy**.

Definition B.1.14. A *central force problem* is a mechanical system where

$$F(\mathbf{q}) = F(|q|) \frac{\mathbf{q}}{|q|}. \quad (\text{B.17})$$

This system is a Newtonian potential system with potential given by

$$V(\mathbf{q}) := -U(|q|) \quad (\text{B.18})$$

where $U(|q|)$ is an anti-derivative of F .

Example B.1.15. (Newtonian 2-body systems cont.) In Example B.1.12, if we consider that \mathbf{F} depends only on the distance between m_1 and m_2 only, i.e.

$$\mathbf{F} = F(|\mathbf{q}_2 - \mathbf{q}_1|) \frac{\mathbf{q}_2 - \mathbf{q}_1}{|\mathbf{q}_2 - \mathbf{q}_1|} = F(r) \frac{\mathbf{r}}{r} \quad (\text{B.19})$$

then we find

$$V(\mathbf{r}) = -U(r) = \int (-F(\rho)) d\rho = - \int F(\rho) d\rho \quad (\text{B.20})$$

where $\int F(\rho) d\rho$ is an antiderivative of F . Thus equation (B.16) can be equivalently written as

$$M\ddot{\mathbf{r}} = - \frac{\partial V}{\partial \mathbf{r}} \quad (\text{B.21})$$

Example B.1.16 (The classical N -body problem). Consider the motion of N point masses under their mutual Newtonian gravitational forces (i.e., inverse-square law). This system is a Newtonian potential system, with

$$V(\mathbf{q}) = \sum_{1 \leq i < j \leq N} \frac{-Gm_i m_j}{\|\mathbf{q}_i - \mathbf{q}_j\|}. \quad (\text{B.22})$$

The general problem of solving this system or determining its characteristics is called the *Newtonian N -body problem*.

Definition B.1.17. The *total energy* of a Newtonian N -body potential system with potential energy V is

$$E := K + V \tag{B.23}$$

where K is kinetic energy.

Now we arrive at the third conservation law.

Theorem B.1.18 (Conservation of energy). *In any Newtonian N -body potential system, the total energy is conserved.*

Proof.

$$\begin{aligned} \frac{dE}{dt} &= \frac{d}{dt}(K + V) = \frac{d}{dt} \left(\frac{1}{2} \sum_{i=1}^N m_i \|\dot{\mathbf{q}}_i\|^2 + \sum_{i=1}^N V(\mathbf{q}_i) \right) \\ &= \frac{1}{2} \left(\sum_{i=1}^N m_i \dot{\mathbf{q}}_i \ddot{\mathbf{q}}_i + \sum_{i=1}^N m_i \ddot{\mathbf{q}}_i \dot{\mathbf{q}}_i \right) + \sum_{i=1}^N \frac{\partial V}{\partial \mathbf{q}_i} \frac{d\mathbf{q}_i}{dt} \\ &= \sum_{i=1}^N m_i \dot{\mathbf{q}}_i \ddot{\mathbf{q}}_i + \sum_{i=1}^N \frac{\partial V}{\partial \mathbf{q}_i} \frac{d\mathbf{q}_i}{dt} \\ &= \sum_{i=1}^N \dot{\mathbf{q}}_i \left(m_i \ddot{\mathbf{q}}_i + \frac{\partial V}{\partial \mathbf{q}_i} \right) = 0 \end{aligned}$$

□

Remark B.1.19. *For this reason, Newtonian N -body potential systems are also referred to as **conservative**.*

Theorem B.2.3. *The equations of motion of a Newtonian N -body potential system*

$$m_i \ddot{\mathbf{q}}_i = - \frac{\partial V}{\partial \mathbf{q}_i}, \quad i = 1, \dots, N$$

are equivalent to the **Euler-Lagrange equations**,

$$\frac{d}{dt} \left(\frac{\partial L}{\partial \dot{\mathbf{q}}} \right) - \frac{\partial L}{\partial \mathbf{q}} = 0, \quad i = 1, \dots, N \quad (\text{B.26})$$

for the **Lagrangian** L defined by formula (B.24).

Note that here, $\dot{\mathbf{q}}$ is considered as an independent variable, so that $L : \mathbb{R}^{2dN} \rightarrow \mathbb{R}$, and equation (B.24) has partial derivatives with respect to both \mathbf{q} and $\dot{\mathbf{q}}$. Yet, when evaluating (B.24) and its derivatives, we substitute $\dot{\mathbf{q}}(t) = \frac{d}{dt} \mathbf{q}(t)$.

Proof.

$$\frac{d}{dt} \left(\frac{\partial L}{\partial \dot{\mathbf{q}}} \right) - \frac{\partial L}{\partial \mathbf{q}} = \frac{d}{dt} (M \dot{\mathbf{q}}) + \frac{\partial V}{\partial \mathbf{q}} = M \ddot{\mathbf{q}} + \frac{\partial V}{\partial \mathbf{q}} = 0$$

□

Definition B.2.4. A **time-independent Lagrangian system** on a configuration space \mathbb{R}^{dN} is the system of ODEs in equation (B.26), i.e. the Euler-Lagrange equations, for some function $L : D \times \mathbb{R}^{dN} \rightarrow \mathbb{R}$, $D \subset \mathbb{R}^{dN}$ open, $L = L(\mathbf{q}, \dot{\mathbf{q}})$, called the **Lagrangian**.

Theorem B.2.5. *The Euler-Lagrange equations are coordinate-independent.*

Proof. Consider a change of coordinates $\mathbf{q} = \mathbf{q}(\mathbf{r})$, where $\mathbf{q}(\mathbf{r})$ is a smooth map with

a smooth inverse. Then

$$\dot{\mathbf{q}} = \frac{d\mathbf{q}}{dt} = \frac{\partial \mathbf{q}}{\partial \mathbf{r}} \cdot \frac{d\mathbf{r}}{dt} = \frac{\partial \mathbf{q}}{\partial \mathbf{r}} \cdot \dot{\mathbf{r}}, \quad \text{so} \quad \frac{\partial \dot{\mathbf{q}}}{\partial \mathbf{r}} = \frac{\partial^2 \mathbf{q}}{\partial \mathbf{r}^2} \cdot \dot{\mathbf{r}} \quad \text{and} \quad \frac{\partial \dot{\mathbf{q}}}{\partial \dot{\mathbf{r}}} = \frac{\partial \mathbf{q}}{\partial \mathbf{r}}.$$

If we also assume $\mathbf{q}(t)$ is smooth, then the equality of mixed partials gives

$$\frac{d}{dt} \left(\frac{\partial \mathbf{q}}{\partial \mathbf{r}} \right) = \frac{\partial \dot{\mathbf{q}}}{\partial \mathbf{r}}, \quad \text{so} \quad \frac{d}{dt} \left(\frac{\partial \dot{\mathbf{q}}}{\partial \dot{\mathbf{r}}} \right) = \frac{d}{dt} \left(\frac{\partial \mathbf{q}}{\partial \mathbf{r}} \right) = \frac{\partial \dot{\mathbf{q}}}{\partial \mathbf{r}}.$$

If the Euler-Lagrange equations hold for $(\mathbf{q}, \dot{\mathbf{q}})$ then

$$\begin{aligned} \frac{d}{dt} \left(\frac{\partial L}{\partial \dot{\mathbf{r}}} \right) - \frac{\partial L}{\partial \mathbf{r}} &= \frac{d}{dt} \left(\frac{\partial L}{\partial \dot{\mathbf{q}}} \cdot \frac{\partial \dot{\mathbf{q}}}{\partial \dot{\mathbf{r}}} \right) - \left(\frac{\partial L}{\partial \mathbf{q}} \cdot \frac{\partial \mathbf{q}}{\partial \mathbf{r}} + \frac{\partial L}{\partial \dot{\mathbf{q}}} \cdot \frac{\partial \dot{\mathbf{q}}}{\partial \mathbf{r}} \right) \\ &= \frac{d}{dt} \left(\frac{\partial L}{\partial \dot{\mathbf{q}}} \right) \cdot \frac{\partial \dot{\mathbf{q}}}{\partial \dot{\mathbf{r}}} + \frac{\partial L}{\partial \dot{\mathbf{q}}} \cdot \frac{d}{dt} \left(\frac{\partial \dot{\mathbf{q}}}{\partial \dot{\mathbf{r}}} \right) - \frac{\partial L}{\partial \mathbf{q}} \cdot \frac{\partial \mathbf{q}}{\partial \mathbf{r}} - \frac{\partial L}{\partial \dot{\mathbf{q}}} \cdot \frac{\partial \dot{\mathbf{q}}}{\partial \mathbf{r}} \\ &= \frac{d}{dt} \left(\frac{\partial L}{\partial \dot{\mathbf{q}}} \right) \cdot \frac{\partial \mathbf{q}}{\partial \mathbf{r}} + \frac{\partial L}{\partial \dot{\mathbf{q}}} \cdot \frac{\partial \dot{\mathbf{q}}}{\partial \mathbf{r}} - \frac{\partial L}{\partial \mathbf{q}} \cdot \frac{\partial \mathbf{q}}{\partial \mathbf{r}} - \frac{\partial L}{\partial \dot{\mathbf{q}}} \cdot \frac{\partial \dot{\mathbf{q}}}{\partial \mathbf{r}} \\ &= \left(\frac{d}{dt} \left(\frac{\partial L}{\partial \dot{\mathbf{q}}} \right) - \frac{\partial L}{\partial \mathbf{q}} \right) \cdot \frac{\partial \mathbf{q}}{\partial \mathbf{r}} + \frac{\partial L}{\partial \dot{\mathbf{q}}} \cdot \frac{\partial \dot{\mathbf{q}}}{\partial \mathbf{r}} - \frac{\partial L}{\partial \dot{\mathbf{q}}} \cdot \frac{\partial \dot{\mathbf{q}}}{\partial \mathbf{r}} \\ &= \left(\frac{d}{dt} \left(\frac{\partial L}{\partial \dot{\mathbf{q}}} \right) - \frac{\partial L}{\partial \mathbf{q}} \right) = 0. \end{aligned}$$

□

By Theorem B.2.5, we can perform a change of coordinates by expressing $L = K - V$ in the new coordinates in which we can compute the (new) Euler-Lagrange equations.

Example B.2.6. (*Newtonian 2-body potential systems*) Recall from Example B.1.15 the equation of motion (B.21) of the relative vector between two mass points with

binary interaction. The Lagrangian for this problem is:

$$L(\mathbf{r}, \dot{\mathbf{r}}) = \frac{1}{2}M\dot{\mathbf{r}}^2 - V(\mathbf{r}). \quad (\text{B.27})$$

or, in components

$$L(r_x, r_y, \dot{r}_x, \dot{r}_y) = \frac{1}{2}M(\dot{r}_x^2 + \dot{r}_y^2) - V\left(\sqrt{r_x^2 + r_y^2}\right). \quad (\text{B.28})$$

The Euler-Lagrange equations are given by

$$M\ddot{r}_x = -\frac{\partial V}{\partial r_x}, \quad M\ddot{r}_y = -\frac{\partial V}{\partial r_y}. \quad (\text{B.29})$$

Passing L to polar coordinates we have

$$L(r, \theta, \dot{r}, \dot{\theta}) = \frac{1}{2}M\left(\dot{r}^2 + (r\dot{\theta})^2\right) - V(r, \theta) \quad (\text{B.30})$$

with the Euler-Lagrange equations given by

$$\begin{aligned} \frac{d}{dt} \frac{\partial}{\partial \dot{r}} \left(\frac{1}{2}M\left(\dot{r}^2 + (r\dot{\theta})^2\right) - V(r) \right) &= \frac{\partial}{\partial r} \left(\frac{1}{2}M\left(\dot{r}^2 + (r\dot{\theta})^2\right) - V(r) \right) \\ \frac{d}{dt} \frac{\partial}{\partial \dot{\theta}} \left(\frac{1}{2}M\left(\dot{r}^2 + (r\dot{\theta})^2\right) - V(r) \right) &= \frac{\partial}{\partial \theta} \left(\frac{1}{2}M\left(\dot{r}^2 + (r\dot{\theta})^2\right) - V(r) \right). \end{aligned}$$

Calculating the above, the Euler-Lagrange equations become

$$\begin{aligned} M\ddot{r} &= Mr\dot{\theta}^2 - V'(r) \\ \frac{d}{dt}Mr^2\dot{\theta} &= 0. \end{aligned}$$

Remark that in this problem it is more convenient to use the equations in polar coordinates. Indeed, the second equation above gives the integral of motion:

$$Mr^2(t)\dot{\theta}(t) = \text{const.}$$

which can be used to reduce the system.

Definition B.2.7. The *energy function* for a Lagrangian $L(\mathbf{q}, \dot{\mathbf{q}})$ is

$$E := \frac{\partial L}{\partial \dot{\mathbf{q}}} \dot{\mathbf{q}} - L,$$

In particular, for Lagrangians of the form (B.24) we have the energy given by

$$E = \sum m_i \|\dot{\mathbf{q}}_i\|^2 - L = \frac{1}{2} \sum m_i \|\dot{\mathbf{q}}_i\|^2 + V = K + V.$$

Theorem B.2.8. In any time-independent Lagrangian system, the energy function is conserved.

Proof.

$$\begin{aligned} \frac{dE}{dt} &= \frac{d}{dt} \left(\frac{\partial L}{\partial \dot{\mathbf{q}}} \dot{\mathbf{q}} - L(\mathbf{q}, \dot{\mathbf{q}}) \right) = \frac{d}{dt} \left(\frac{\partial L}{\partial \dot{\mathbf{q}}} \dot{\mathbf{q}} \right) - \frac{dL(\mathbf{q}, \dot{\mathbf{q}})}{dt} \\ &= \frac{d}{dt} \left(\frac{\partial L}{\partial \dot{\mathbf{q}}} \right) \dot{\mathbf{q}} + \left(\frac{\partial L}{\partial \dot{\mathbf{q}}} \right) \ddot{\mathbf{q}} - \frac{\partial L}{\partial \mathbf{q}} \dot{\mathbf{q}} - \frac{\partial L}{\partial \dot{\mathbf{q}}} \ddot{\mathbf{q}} \\ &= \frac{\partial L}{\partial \mathbf{q}} \dot{\mathbf{q}} + \frac{\partial L}{\partial \dot{\mathbf{q}}} \ddot{\mathbf{q}} - \frac{\partial L}{\partial \mathbf{q}} \dot{\mathbf{q}} - \frac{\partial L}{\partial \dot{\mathbf{q}}} \ddot{\mathbf{q}} = 0 \end{aligned}$$

□

An alternative dynamical description for mechanical systems is provided by its Hamiltonian formulation. This will be discussed in the following section.

B.3 The Legendre transform and Hamiltonian mechanics

Definition B.3.1. The **Legendre transform** for a Lagrangian $L(\mathbf{q}, \dot{\mathbf{q}})$ is the change of variables $(\mathbf{q}, \dot{\mathbf{q}}) \mapsto (\mathbf{q}, \mathbf{p})$ given by

$$\mathbf{p} := \frac{\partial L}{\partial \dot{\mathbf{q}}}.$$

The new variables \mathbf{p} are called the **momenta**.

Remark B.3.2. If $L(\mathbf{q}, \dot{\mathbf{q}}) = \frac{1}{2}\mathbf{q}^T M \dot{\mathbf{q}} - V(\mathbf{q}) = \sum \frac{1}{2}m_i \|\dot{\mathbf{q}}_i\|^2 - V(\mathbf{q})$, then

$$\mathbf{p}_i = \frac{\partial L}{\partial \dot{\mathbf{q}}_i} = m_i \dot{\mathbf{q}}_i.$$

Definition B.3.3. A Lagrangian L is **hyperregular** if the Legendre transform for L is a diffeomorphism, that is, a differentiable map with a differentiable inverse.

Remark B.3.4. If $L(\mathbf{q}, \dot{\mathbf{q}}) = \sum \frac{1}{2}m_i \|\dot{\mathbf{q}}_i\|^2 - V(\mathbf{q})$, then the Legendre transform, defined by $\mathbf{p}_i := \frac{\partial L}{\partial \dot{\mathbf{q}}_i} = m_i \dot{\mathbf{q}}_i$, is hyperregular, since it is differentiable and has a differentiable inverse given by $\dot{\mathbf{q}}_i = \frac{1}{m_i} \mathbf{p}_i$.

Theorem B.3.5. *If $L : \mathbb{R}^{2dN} \rightarrow \mathbb{R}$ is any hyperregular Lagrangian, then the Euler-Lagrange equations,*

$$\frac{d}{dt} \left(\frac{\partial L}{\partial \dot{\mathbf{q}}_i} \right) - \frac{\partial L}{\partial \mathbf{q}_i} = 0, \quad i = 1, \dots, N,$$

are equivalent to **Hamilton's equations of motion**,

$$\dot{\mathbf{q}} = \frac{\partial H}{\partial \mathbf{p}}, \quad \dot{\mathbf{p}} = - \frac{\partial H}{\partial \mathbf{q}}, \quad (\text{B.31})$$

for the **Hamiltonian**

$$H(\mathbf{q}, \mathbf{p}) := \mathbf{p} \cdot \dot{\mathbf{q}}(\mathbf{q}, \mathbf{p}) - L(\mathbf{q}, \dot{\mathbf{q}}(\mathbf{q}, \mathbf{p})),$$

where $\dot{\mathbf{q}}(\mathbf{q}, \mathbf{p})$ is the second component of the inverse Legendre transform.

Proof. The Euler-Lagrange equations are second order ODEs in the variables $\mathbf{q} = (\mathbf{q}_1, \dots, \mathbf{q}_N)$, but they can also be interpreted as part of an equivalent first order system of ODEs in the variables $(\mathbf{q}, \dot{\mathbf{q}})$, with the extra equations $\frac{d}{dt} \mathbf{q} = \dot{\mathbf{q}}$. Applying the Legendre transform gives the equivalent system

$$\frac{d}{dt} \mathbf{q}_i = \dot{\mathbf{q}}_i(\mathbf{q}, \mathbf{p}), \quad \frac{d}{dt} \mathbf{p}_i - \frac{\partial L}{\partial \mathbf{q}_i} = 0$$

We now calculate the partial derivatives of H :

$$\begin{aligned}\frac{\partial H}{\partial \mathbf{q}_i} &= \mathbf{p}_i \cdot \frac{\partial \dot{\mathbf{q}}_i(\mathbf{q}_i, \mathbf{p}_i)}{\partial \mathbf{q}_i} - \frac{\partial L}{\partial \mathbf{q}_i} - \frac{\partial L}{\partial \dot{\mathbf{q}}_i} \cdot \frac{\partial \dot{\mathbf{q}}_i(\mathbf{q}_i, \mathbf{p}_i)}{\partial \mathbf{q}_i} = -\frac{\partial L}{\partial \mathbf{q}_i} \\ \frac{\partial H}{\partial \mathbf{p}_i} &= \dot{\mathbf{q}}_i(\mathbf{q}_i, \mathbf{p}_i) + \mathbf{p}_i \cdot \frac{\partial \dot{\mathbf{q}}_i(\mathbf{q}_i, \mathbf{p}_i)}{\partial \mathbf{p}_i} - \frac{\partial L}{\partial \dot{\mathbf{q}}_i} \cdot \frac{\partial \dot{\mathbf{q}}_i(\mathbf{q}_i, \mathbf{p}_i)}{\partial \mathbf{p}_i} = \dot{\mathbf{q}}_i(\mathbf{q}_i, \mathbf{p}_i).\end{aligned}$$

Consequently, the Euler-Lagrange equations are equivalent to

$$\frac{d}{dt} \mathbf{q}_i = \frac{\partial H}{\partial \mathbf{p}_i}, \quad \frac{d}{dt} \mathbf{p}_i = -\frac{\partial H}{\partial \mathbf{q}_i}.$$

□

Remark B.3.6. *Since the Euler-Lagrange equations are coordinate independent, then for any Hamiltonian deduced via hyperregular Legendre transform, Hamilton's equations are coordinate independent as well.*

Theorem B.3.7. *In any Hamiltonian system with a Hamiltonian $H(\mathbf{q}, \mathbf{p})$, the Hamiltonian is conserved.*

Proof.

$$\dot{H} := \sum_{i=1}^N \left(\frac{\partial H}{\partial \mathbf{q}_i} \cdot \dot{\mathbf{q}}_i + \frac{\partial H}{\partial \mathbf{p}_i} \cdot \dot{\mathbf{p}}_i \right) = \sum_{i=1}^N \left(\frac{\partial H}{\partial \mathbf{q}_i} \cdot \frac{\partial H}{\partial \mathbf{p}_i} - \frac{\partial H}{\partial \mathbf{p}_i} \cdot \frac{\partial H}{\partial \mathbf{q}_i} \right) = 0.$$

□

The Legendre transform applied to the Lagrangian of the Newtonian N -body potential system (B.24) leads to

$$\mathbf{p}_i = m_i \dot{\mathbf{q}}_i \tag{B.32}$$

and hence

$$H(\mathbf{q}, \mathbf{p}) = \mathbf{p} \cdot \dot{\mathbf{q}}(\mathbf{q}, \mathbf{p}) - L(\mathbf{q}, \dot{\mathbf{q}}(\mathbf{q}, \mathbf{p})) = \sum \frac{m_i}{2} \|\dot{\mathbf{q}}_i\|^2 + V(\mathbf{q}) = \sum \frac{1}{2m_i} \|\mathbf{p}_i\|^2 + V.$$

Thus the *Hamiltonian of a Newtonian N -body potential system* takes the form

$$H(\mathbf{q}, \mathbf{p}) = \frac{1}{2} \mathbf{p}^T M^{-1} \mathbf{p} + V(\mathbf{q}) \tag{B.33}$$

where M^{-1} is the inverse of the mass matrix (B.25).

Remark B.3.8. *The Hamiltonian in the above theorem is the energy function E expressed as a function of \mathbf{q} and \mathbf{p} .*

Example B.3.9. *(Newtonian 2-body potential systems in polar coordinates) Recall from Example B.2.6 the Lagrangian (B.30) giving the relative motion for a Newtonian 2-body potential system on polar coordinates. By applying the Legendre transform we obtain the corresponding Hamiltonian*

$$H(r, \theta, p_r, p_\theta) = \frac{1}{2M} \left(p_r^2 + \frac{p_\theta^2}{r^2} \right) + V(r). \tag{B.34}$$

for which the associated equations of motion are

$$\begin{aligned} \dot{r} &= \frac{p_r}{M} & \dot{p}_r &= \frac{p_\theta^2}{Mr^3} - V'(r) \\ \dot{\theta} &= \frac{p_\theta}{mr^2} & \dot{p}_\theta &= 0. \end{aligned}$$

For a Newtonian N -body potential system it can also be shown directly that Newton's equation of motion accept a Hamiltonian formulation:

Theorem B.3.10. *Every Newtonian N -body potential system*

$$m_i \ddot{\mathbf{q}}_i = - \frac{\partial V}{\partial \mathbf{q}_i}, \quad i = 1, \dots, N \quad (\text{B.35})$$

is equivalent to Hamilton's canonical equations, for the Hamiltonian (B.33). More precisely, $(\mathbf{q}(t), \mathbf{p}(t))$ is a solution to Equation (B.3) if and only if $\mathbf{q}(t)$ is a solution of equation (B.35) and $\mathbf{p}(t) = (\mathbf{p}_1(t), \dots, \mathbf{p}_N(t)) = (m_1 \dot{\mathbf{q}}_1(t), \dots, m_N \dot{\mathbf{q}}_N(t))$, where $\mathbf{p}(t)$ is linear momentum.

Proof. Recall that Hamilton's equations for (B.33) are

$$\dot{\mathbf{q}}_i = \frac{\partial H}{\partial \mathbf{p}_i} = \frac{1}{m_i} \mathbf{p}_i, \quad \dot{\mathbf{p}}_i = - \frac{\partial H}{\partial \mathbf{q}_i} = - \frac{\partial V}{\partial \mathbf{q}_i}, \quad i = 1, \dots, N. \quad (\text{B.36})$$

The second order system in Equation (B.35) is equivalent to the following first order system in variables $(\mathbf{q}, \dot{\mathbf{q}})$,

$$\frac{d}{dt} \mathbf{q}_i = \dot{\mathbf{q}}_i, \quad m_i \frac{d}{dt} \dot{\mathbf{q}}_i = - \frac{\partial V}{\partial \mathbf{q}_i}, \quad i = 1, \dots, N. \quad (\text{B.37})$$

Changing variables from $(\mathbf{q}, \dot{\mathbf{q}})$ to (\mathbf{q}, \mathbf{p}) , with $\mathbf{p}_i = m_i \dot{\mathbf{q}}_i$ gives the system

$$\dot{\mathbf{q}}_i = \frac{1}{m_i} \mathbf{p}_i = \frac{\partial H}{\partial \mathbf{p}_i}, \quad \dot{\mathbf{p}}_i = m_i \ddot{\mathbf{q}}_i = - \frac{\partial V}{\partial \mathbf{q}_i}, \quad i = 1, \dots, N.$$

□

In many applications of classical mechanics, such as our problem, one usually begins with a Lagrangian model and then converts this to a Hamiltonian system, provided

the Lagrangian is hyperregular. The benefit for using the Hamiltonian approach is that it is particularly suitable for studying conserved quantities.

B.4 Cyclic Coordinates

Definition B.4.1. Consider a smooth Lagrangian $L : D \times \mathbb{R}^N \rightarrow \mathbb{R}$, $D \subset \mathbb{R}^N$ open:

$$L = L(q_1, q_2, \dots, q_N, \dot{q}_1, \dot{q}_2, \dots, \dot{q}_N) \quad (\text{B.38})$$

A coordinate q_i for some $i = 1, \dots, N$ is called **cyclic** if it does not appear explicitly in the Lagrangian expression.

Without loss of generality, let q_1 be a cyclic coordinate. Then the Lagrangian takes the form

$$L = L(q_2, q_3, \dots, q_N, \dot{q}_1, \dot{q}_2, \dot{q}_3, \dots, \dot{q}_N) \quad (\text{B.39})$$

Using the Legendre Transform, the corresponding Hamiltonian is

$$H = H(q_2, q_3, \dots, q_N, p_1, p_2, \dots, p_N). \quad (\text{B.40})$$

We have

$$\dot{q}_1 = \frac{\partial H}{\partial p_1} \quad (\text{B.41})$$

$$\dot{p}_1 = -\frac{\partial H}{\partial q_1} \quad (\text{B.42})$$

$$\dot{q}_i = \frac{\partial H}{\partial p_i} \quad (\text{B.43})$$

$$\dot{p}_i = -\frac{\partial H}{\partial q_i} \quad \text{for } i = 2, \dots, N. \quad (\text{B.44})$$

Given some initial conditions $(q_1(t_0), q_2(t_0), q_3(t_0), \dots, q_N(t_0), p_1(t_0), p_2(t_0), \dots, p_N(t_0))$, equation (B.42) leads to the momentum conservation

$$p_1(t) = \text{const.} = p_1(t_0) =: c. \quad (\text{B.45})$$

Further, provided the system given by $H(q_2, q_3, \dots, q_N, p_1, p_2, \dots, p_N) \Big|_{p_1=c}$ is solved, and so explicit expressions for $q_i(t; c)$ and $p_i(t; c)$, $i = 2, 3, \dots, N$ are found, then one can determine

$$q_1(t) = q_1(t_0) + \int_{t_0}^t \frac{\partial H}{\partial p_1}(q_2(\tau), \dots, q_N(\tau), p_2(\tau), \dots, p_N(\tau); c) d\tau. \quad (\text{B.46})$$

So the presence of a cyclic coordinate implies that the corresponding momentum is constant along the motion (the constant being fixed by the initial conditions) and the number of degrees of freedom drops by one.

Definition B.4.2. *The **Reduced Hamiltonian** is*

$$H_{red}(q_2, q_3, \dots, q_N, p_2, \dots, p_N; c) := H(q_2, q_3, \dots, q_N, p_1, p_2, \dots, p_N) \Big|_{p_1=c}. \quad (\text{B.47})$$

In H_{red} , the constant c may be treated as a parameter, which is allowed to take all the values permitted by the initial conditions.

In the particular case of Newtonian N -body potential systems with a Hamiltonian of the form

$$H = H(q_2, q_3, \dots, q_N, p_1, p_2, \dots, p_N) = \sum_{i=1}^N \frac{1}{2m_i} p_i^2 + V(q_2, q_3, \dots, q_N). \quad (\text{B.48})$$

we have

$$H_{\text{red}}(q_2, q_3, \dots, q_N, p_2, \dots, p_N; c) := \frac{1}{2m_1} c^2 + \sum_{i=2}^N \frac{1}{2m_i} p_i^2 + V(q_2, q_3, \dots, q_N) \quad (\text{B.49})$$

where $c = p_1(t) = \text{const.} = p_1(t_0)$.

Example B.4.3. (*Newtonian 2-body potential systems cont.*) Recall from the Examples (B.2.6) and (B.3.9) that the Lagrangian is (B.30), with corresponding Hamiltonian (B.34). For reader's convenience we re-write these below

$$L(r, \theta, \dot{r}, \dot{\theta}) = \frac{1}{2} M \left(\dot{r}^2 + (r^2 \dot{\theta})^2 \right) - V(r),$$

and

$$H(r, \theta, p_r, p_\theta) = \frac{1}{2M} \left(p_r^2 + \frac{p_\theta^2}{r^2} \right) + V(r),$$

We observe that θ is cyclic in L , as this coordinate is missing from the expression.

Consequently, the corresponding momentum p_θ is a conserved quantity. This is immediate from the Hamiltonian equations of motion:

$$\begin{aligned} \dot{r} &= \frac{p_r}{M} & \dot{p}_r &= \frac{p_\theta^2}{Mr^3} - V'(r) \\ \dot{\theta} &= \frac{p_\theta}{mr^2} & \dot{p}_\theta &= 0. \end{aligned}$$

Indeed, from the last equation above we have $p_\theta(t) = \text{const.} = p(t_0) =: c$. The reduced Hamiltonian is

$$H_{\text{red}}(r, p_r; c) = \frac{1}{2M} p_r^2 + \frac{c^2}{2Mr^2} + V(r).$$

B.5 Equilibria and relative equilibria

Definition B.5.1. *Given a Hamiltonian*

$$H = H(\mathbf{q}, \mathbf{p}) = H(q_1, q_2, q_3, \dots, q_N, p_1, p_2, \dots, p_N), \quad (\text{B.50})$$

a Hamiltonian **equilibrium** is an equilibrium $(\mathbf{q}_e, \mathbf{p}_e)$ point of the Hamiltonian system of equations associated to H .

The method for studying the stability of each equilibrium point, as outlined in Appendix A, are used for studying the stability of a Hamiltonian equilibrium. However, some specific features of the analysis occur due to the structure of the Hamiltonian equations. Let $(\mathbf{q}_e, \mathbf{p}_e)$ be an equilibrium for (B.50).

To apply the Lyapunov Method, we define the Lyapunov function

$$F(\mathbf{q}, \mathbf{p}) := H(\mathbf{q}, \mathbf{p}) - H(\mathbf{q}_e, \mathbf{p}_e)$$

where we use identical notation to Definition A.0.5. Then

1. $F(\mathbf{q}_e, \mathbf{p}_e) = H(\mathbf{q}_e, \mathbf{p}_e) - H(\mathbf{q}_e, \mathbf{p}_e) = 0$
2. For any solution $(\mathbf{q}(t), \mathbf{p}(t))$,

$$\frac{d}{dt}F(\mathbf{q}(t), \mathbf{p}(t)) = \frac{d}{dt}H(\mathbf{q}(t), \mathbf{p}(t)) = 0,$$

since the Hamiltonian is conserved along solutions.

So the first and the third conditions of Lyapunov's First Stability Theorem A.0.6 are satisfied for any Hamiltonian system. The second condition is satisfied if $(\mathbf{q}_e, \mathbf{p}_e)$ is a local minimum point of the Hamiltonian. So we have

Theorem B.5.2 (Lyapunov's Stability Theorem for Hamiltonian systems). *An equilibrium of a Hamiltonian system is stable if it is a local minimum point of the Hamiltonian.*

Recall that a Newtonian N -body potential system, with Hamiltonian $H(\mathbf{q}, \mathbf{p})$ defined by (B.33) has the equations of motion

$$\dot{\mathbf{q}} = M^{-1}\mathbf{p}, \quad \dot{\mathbf{p}} = -\frac{\partial V}{\partial \mathbf{q}}. \quad (\text{B.51})$$

It follows that equilibria are always of the form $(\mathbf{q}_e, \mathbf{p}_e) = (\mathbf{q}_{\text{cr}}, \mathbf{0})$, where \mathbf{q}_{cr} is a critical point of the potential $V(\mathbf{q})$. Further,

$$H(\mathbf{q}_e, \mathbf{p}_e) = H(\mathbf{q}_{\text{cr}}, \mathbf{0}) = \frac{1}{2} \mathbf{0}^T M^{-1} \mathbf{0} + V(\mathbf{q}_{\text{cr}}) = V(\mathbf{q}_{\text{cr}}). \quad (\text{B.52})$$

Since the diagonal of the matrix M has strictly positive entries, the matrix M^{-1} has strictly positive entries as well, and so for any vector \mathbf{p} , we have $\mathbf{p} M^{-1} \mathbf{p} \geq 0$. Hence,

$$H(\mathbf{q}, \mathbf{p}) = \frac{1}{2} \mathbf{p} M^{-1} \mathbf{p} + V(\mathbf{q}) \geq V(\mathbf{q}) \quad \text{for all } (\mathbf{q}, \mathbf{p}). \quad (\text{B.53})$$

If \mathbf{q}_{cr} is a local minimum for $V(\mathbf{q})$, then using (B.52) and (B.53) we obtain

$$H(\mathbf{q}, \mathbf{p}) - H(\mathbf{q}_e, \mathbf{p}_e) \geq V(\mathbf{q}) - V(\mathbf{q}_{\text{cr}}) \geq 0 \quad \text{for all } (\mathbf{q}, \mathbf{p}). \quad (\text{B.54})$$

and so $(\mathbf{q}_e, \mathbf{p}_e) = (\mathbf{q}_{\text{cr}}, \mathbf{0})$ is a local minimum for the Hamiltonian. So we have

Proposition B.5.3 (Lyapunov's Stability Theorem for Newtonian N -body potential systems). *If \mathbf{q}_{cr} is a local minimum point of the potential then the equilibrium $(\mathbf{q}_{\text{cr}}, \mathbf{0})$ of a Newtonian N -body potential system is stable.*

Corollary B.5.4. *If the Hessian $D^2V(\mathbf{q}_e)$ is positive definite, then the equilibrium $(\mathbf{q}_{\text{cr}}, \mathbf{0})$ is stable.*

If the Lyapunov criterion fails, then we resort to spectral analysis. It can be shown [Meyer & al. (1992)] that the eigenvalues of the linearization matrix of a Hamiltonian system always form conjugate quadruplets, i.e. they take on the form

$$\lambda_{1,2,3,4} = \pm\alpha \pm i\beta.$$

This implies that asymptotic stability (where $Re(\lambda) < 0$ for all λ) is not possible in any Hamiltonian system, but only spectral stability. The latter is insured by

$$Re \lambda = 0 \quad \text{for all } \lambda.$$

In the presence of a cyclic coordinate, the dynamics is reduced by one degree of freedom and the reduced Hamiltonian depends on a parameter.

Definition B.5.5. *An equilibrium point of the reduced Hamiltonian H_{red} is a **relative equilibrium** of the un-reduced Hamiltonian H .*

Note that equilibria of H_{red} depend parametrically on c . The methods for studying Hamiltonian equilibria may now be applied to the case of relative equilibria, with the distinction that the existence and stability of relative equilibria depend on c .

Remark B.5.6. *An equilibrium of H_{red} with $c = 0$ is an equilibrium of H .*

For mechanical systems, in the presence of a cyclic coordinate with physical meaning (e.g. angular momentum), the dynamics is dependent on two *internal* parameters: the total energy, h , and the momentum level, c . The **energy-momentum diagrams** display the relative equilibria and their stability in the (c, h) plane, such that every plotted point represents a relative equilibrium with momentum c and energy h . In this way, one observes for what levels of energy and momentum the number of relative equilibria in the system changes.

B.6 Hill regions of motion

Consider a Hamiltonian of a Newtonian N -body potential system as given by equation (B.33). Since the total energy is conserved, along any solution $(\mathbf{q}(t), \mathbf{p}(t))$

$$H(\mathbf{q}, \mathbf{p}) = \frac{1}{2}\mathbf{p}^T M^{-1}\mathbf{p} + V(\mathbf{q}) = h \quad (\text{B.55})$$

where we suppressed the dependency of t . The constant h is fixed by the initial conditions. Since the inverse of the mass matrix M^{-1} has only diagonal entries which are strictly positive, we have $\mathbf{p}^T(t)M^{-1}\mathbf{p} \geq \mathbf{0}$ for any values \mathbf{p} , the equality being attained for $\mathbf{p} = \mathbf{0}$. Then we must have

$$0 \leq \frac{1}{2}\mathbf{p}^T(t)M^{-1}\mathbf{p}(t) = h - V(\mathbf{q}(t)) \quad (\text{B.56})$$

Thus, for any solution $(\mathbf{q}(t), \mathbf{p}(t))$ with initial conditions $(\mathbf{q}(t_0), \mathbf{p}(t_0))$ we obtain the following inequality:

$$V(\mathbf{q}(t)) \leq h \quad (\text{B.57})$$

where $h = H(\mathbf{q}(t_0), \mathbf{p}(t_0))$. Hence, in a Newtonian N -body potential system, for each fixed energy level, the configurations $\mathbf{q}(t)$ are constrained by the inequality (B.57).

Definition B.6.1. *Given a Hamiltonian of the form (B.55), the configuration space accepts a partition of the form*

$$\mathcal{H}(h) := \{\mathbf{q} \mid V(\mathbf{q}) \leq h\}, \quad h \in \mathbb{R} \quad (\text{B.58})$$

The domains $\mathcal{H}(h)$ are called the **Hill regions of motion**.

Appendix C

Matlab code used for Numerical Simulations

Full Matlab® code for the *Diatomic* system can be found at github.com/DamarisMcKinley/Diatomic_Code, and for the *Triatomic* system at github.com/DamarisMcKinley/Triatomic_Code. Here we present the code used for the *Triatomic* system.

The main process is as follows,

```
1 %Clear all previous information
2 clc;
3 clear;
4
```

```
5 %Begin timing the process
6 tic;
7
8 %Define variables
9 syms C x R z pr pz real
10
11 %GatherUserInput
12
13 %Define value of parameters
14 a=1; %A_ii from the thesis
15 b=5; %A_jj from the thesis
16 d=1; %B_ii from the thesis
17 e=1; %B_jj from the thesis
18 alpha=6; %a from the thesis
19 beta=12; %b from the thesis
20 m=3/4; %M from the thesis
21 n=3/4; %M_2 from the thesis
22
23 %Define arrays
24 howmanycs=[];
25 Cvalue=[];
26 Rvalue=[];
27 zvalue=[];
28 allpossolR=[];
29 allpossolz=[];
30 allpossolx=[];
31 H=[]; X=[]; Y=[]; Z=[];
32 T=[]; U=[]; V=[]; W=[];
33 S=[]; P=[]; Q=[]; O=[];
```

```
34 ZS=[]; ZSP=[]; ZU=[];
35 HP=[]; XP=[]; YP=[]; ZP=[];
36 TP=[]; UP=[]; VP=[]; WP=[];
37 SP=[]; PP=[]; QP=[]; OP=[];
38 Hredarray=[];
39
40
41 JJ=[zeros(2) eye(2); -1*eye(2) zeros(2)];
42
43 %Define lower and upper bounds for angular momentum in planar case,
44 %as well as step size
45 lb=0;
46 ub=60;
47 stpp=0.1;%0.1
48
49 %Derivatives of our potentials, w.r.t. z and R
50 diffF=diff(f_fcn(R,a,d,alpha,beta),R,1);
51 diffG=diff(subs(g_fcn(R,z,a,b,d,e,alpha,beta),z,0),R,1);
52 diffFt=diff(diffF,R,1);
53 diffGt=diff(diffG,R,1);
54 diffGz=diff(g_fcn(R,z,a,b,d,e,alpha,beta),z,1);
55 diffGzz=diff(g_fcn(R,z,a,b,d,e,alpha,beta),z,2);
56
57
58 %%%%%%%%%%%%%%%%%%%%%%%%%%%%%%%%%%%%%%%%%%%%%%%%%%%%%%%%%%%%%%%%%%%%%%%%% PLANAR CASE %%%%%%%%%%%%%%%%%%%%%%%%%%%%%%%%%%%%%%%%%%%%%%%%%%%%%%%%%%%%%%%%%%%%%%%%%
59
60 %Find all planar relative equilibria
61 for c=lb:stpp:ub;
62
```

```

63     howmanycs=[howmanycs c];
64
65     %Find all possible values for R, given the value for c
66     allsolnsforRplanar
67
68     %Determine current amount of RE found
69     sizeRvalue=max(size(Rvalue));
70
71     %Separate all values of R,and pick only the real positive ones
72     allpossolforRplanar
73
74     %If no more values for R are found, stop looking
75     if sizeRvalue==max(size(Rvalue)) && max(size(howmanycs))>4
76         break;
77     end
78
79 end
80
81
82 %Find the stability of the RE
83 if isequal(max(size(Rvalue)),max(size(Cvalue))) && max(size(Rvalue))>0
84
85     %Define the Hessian of the potential and reduced Hamiltonian
86     HessVeff=[subs((3*C^2)/(m*R^4)+diff(f_fcn(R,a,d,alpha,beta),...
87         R,2)+2*(subs(diff(g_fcnxs(x,a,b,d,e,alpha,beta),x,2),x,...
88         (R^2/4+z^2))*(diff((R^2/4+z^2),R,1))^2+(diff((R^2/4+z^2)...
89         ,R,2))*subs(diff(g_fcnxs(x,a,b,d,e,alpha,beta),x,1),x,...
90         (R^2/4+z^2))),z,0) 0;0 subs(2*(subs(diff(g_fcnxs(x,a,b,...
91         d,e,alpha,beta),x,2),x,(R^2/4+z^2))*(diff((R^2/4+z^2),...

```



```

92     z,1)^2)+diff((R^2/4+z^2),z,2)*subs(diff(g_fcnxs(x,a,b,...
93     d,e,alpha,beta),x,1),x,(R^2/4+z^2)),z,0)];
94     HessHred=[
95     subs((3*C^2)/(m*R^4)+diff(f_fcn(R,a,d,alpha,beta),R,2)+2*...
96     (subs(diff(g_fcnxs(x,a,b,d,e,alpha,beta),x,2),x,(R^2/4+z^2...
97     ))*(diff((R^2/4+z^2),R,1))^2+(diff((R^2/4+z^2),R,2))*subs...
98     (diff(g_fcnxs(x,a,b,d,e,alpha,beta),x,1),x,(R^2/4+z^2))),...
99     z,0) 0 0 0;0 subs(2*(subs(diff(g_fcnxs(x,a,b,d,e,alpha,...
100     beta),x,2),x,(R^2/4+z^2)))*(diff((R^2/4+z^2),z,1)^2)+diff...
101     ((R^2/4+z^2),z,2))*subs(diff(g_fcnxs(x,a,b,d,e,alpha,beta),...
102     x,1),x,(R^2/4+z^2)),z,0) 0 0;0 0 1/m 0;0 0 0 1/n];
103
104     for p=1:max(size(Cvalue));
105         %Find the Hessian of Veff, at R, C and z=0
106         A=subs(HessVeff,{R,z,C},{Rvalue(p),0,Cvalue(p)});
107
108         %Find the total energy of the system for each RE
109         plugRredHplanar
110
111         %Classify each RE as stable, unstable or spectrally stable
112         Stabilityplanar
113
114     end
115
116 else
117     warning('Rvalue array is empty');
118 end
119
120 %Keep track of all planar solutions

```

```
121 UP=U; VP=V; WP=W; XP=X; YP=Y; ZP=Z; SP=S; PP=P; QP=Q;
122
123
124 %%%%%%%%%%%%%%%%%%%%%%%%%% SPATIAL CASE %%%%%%%%%%%%%%%%%%%%%%%%%%
125
126 %Reset all arrays for the spatial case
127 howmanycs=[];
128 Cvalue=[];
129 Rvalue=[];
130 zvalue=[];
131 allpossolR=[];
132 allpossolz=[];
133 allpossolx=[];
134 H=[]; X=[]; Y=[]; Z=[];
135 T=[]; U=[]; V=[]; W=[];
136 S=[]; P=[]; Q=[]; O=[];
137 Hredarray=[];
138
139 %Derivatives of our potentials, w.r.t. z and R
140 diffF=diff(f_fcn(R,a,d,alpha,beta),R,1);
141 diffG=diff(g_fcn(R,z,a,b,d,e,alpha,beta),R,1);
142 diffx=diff(g_fcnx(x,a,b,d,e,alpha,beta),x,1);
143 diffGz=diff(g_fcn(R,z,a,b,d,e,alpha,beta),z,1);
144 diffGzz=diff(g_fcn(R,z,a,b,d,e,alpha,beta),z,2);
145 diffGzR=diff(diffG,z,1);
146 diffGRR=diff(diffG,R,1);
147 diffFRR=diff(diffF,R,1);
148
149 %Define lower and upper bounds for angular momentum, as well as step
```

```
150 %size
151 lbs=0.0001;
152 ubs=2;
153 ints=0.01; %0.01
154
155
156 for c=lbs:ints:ubs;
157
158     howmanycs=[howmanycs c];
159
160     %Find all possible values for R, given the value for c
161     allsolnsforR
162
163     %Determine current amount of RE found
164     sizeRvalue=max(size(Rvalue));
165
166     %Separate all values of R,and pick only the real positive ones
167     allpossolforR
168
169     %If no more values for R are found, stop looking
170
171     %     while c~=0
172     %         if sizeRvalue==max(size(Rvalue))
173     %             break;
174     %         end
175     %     end
176 end
177
178
```

```

179 %Define the Hessian of the potential and reduced Hamiltonian
180 HessVeff=[(3*C^2)/(m*R^4)+diff(f_fcn(R,a,d,alpha,beta),R,2)+2*(subs...
181     (diff(g_fcnxs(x,a,b,d,e,alpha,beta),x,2),x,(R^2/4+z^2))*...
182     (diff((R^2/4+z^2),R,1))^2)+2*(subs(diff(g_fcnxs(x,a,b,d,e,alpha...
183     ,beta),x,2),x,(R^2/4+z^2))*(diff((R^2/4+z^2),z,1))*(diff((R^2/4...
184     +z^2),R,1)))+2*(subs(diff(g_fcnxs(x,a,b,d,e,alpha,beta),x,2),x,...
185     R^2/4+z^2))*(diff((R^2/4+z^2),z,1))*(diff((R^2/4+z^2),R,1)))+2*...
186     (subs(diff(g_fcnxs(x,a,b,d,e,alpha,beta),x,2),x,(R^2/4+z^2))*...
187     (diff((R^2/4+z^2),z,1)^2)]);
188 HessHred=[
189     (3*C^2)/(m*R^4)+diff(f_fcn(R,a,d,alpha,beta),R,2)+2*(subs(diff...
190     (g_fcnxs(x,a,b,d,e,alpha,beta),x,2),x,(R^2/4+z^2))*(diff((R^2/4...
191     +z^2),R,1))^2)+2*(subs(diff(g_fcnxs(x,a,b,d,e,alpha,beta),x,2),...
192     x,(R^2/4+z^2))*(diff((R^2/4+z^2),z,1))*(diff((R^2/4+z^2),R,1)))+...
193     0 0;2*(subs(diff(g_fcnxs(x,a,b,d,e,alpha,beta),x,2),x,(R^2/4+...
194     z^2))*(diff((R^2/4+z^2),z,1))*(diff((R^2/4+z^2),R,1)))+2*(subs...
195     (diff(g_fcnxs(x,a,b,d,e,alpha,beta),x,2),x,(R^2/4+z^2))*(diff(...
196     (R^2/4+z^2),z,1)^2)+0 0;0 0 1/m 0;0 0 0 1/n];
197
198 %Find the stability of the RE
199 if isequal(max(size(Rvalue)),max(size(Cvalue)),max(size(zvalue)))&&...
200     max(size(Rvalue))>0
201
202     for p=1:max(size(Cvalue));
203
204         %Find the Hessian of Veff, at R and z=0
205         A=subs(HessVeff,{R,z,C},{Rvalue(p),zvalue(p),Cvalue(p)});
206
207         %Find the total energy of the system for each RE

```

```
208         plugRedH
209
210         %Classify each RE as stable, unstable or spectrally stable
211         Stability
212
213     end
214
215 else
216     warning('Rvalue array for spatial solutions is empty');
217 end
218
219
220 %Output 1: Energy-Momentum Diagram
221 figure(1)
222 %planar unstable
223 if max(size(UP))>1
224     h_1=plot(UP,WP,'bs','MarkerSize',5);
225     hold on;
226 end;
227 %planar stable
228 if max(size(XP))>1
229     h_2=plot(XP,ZP,'rv','MarkerSize',5);
230     hold on;
231 end;
232 %planar spectrally stable
233 if max(size(SP))>=1
234     hold on;
235     h_3=plot(SP,QP,'yd','MarkerSize',5);
236 end;
```

```
237 %spatial unstable
238 if max(size(U))>=1 && max(size(W))>0
239     hold on;
240     h_4=plot(U,W,'bo','MarkerSize',5);
241 end;
242 %spatial stable
243 if max(size(X))>=1 && max(size(Z))>0
244     hold on;
245     h_5=plot(X,Z,'r*','MarkerSize',5);
246 end;
247 %spatial spectrally stable
248 if max(size(S))>=1
249     hold on;
250     h_6=plot(S,Q,'y-','MarkerSize',5);
251 end;
252 if max(size(UP))>=1 && max(size(XP))>=1 && max(size(SP))>=1 && ...
253     max(size(U))>=1 && max(size(X))>=1 && max(size(S))>=1
254     legend([h_1,h_2,h_3,h_4,h_5,h_6],'unstable planar RE',...
255         'stable planar RE','spectrally stable planar RE',...
256         'unstable spatial RE','stable spatial RE',...
257         'spectrally stable spatial RE');
258 elseif max(size(U))>=1 && max(size(X))>=1 && max(size(S))>=1
259     legend([h_1,h_2,h_4,h_5,h_6],'unstable planar RE',...
260         'stable planar RE','unstable spatial RE',...
261         'stable spatial RE','spectrally stable spatial RE');
262 elseif max(size(U))>=1 && max(size(X))>=1
263     legend([h_1,h_2,h_4,h_5],'unstable planar RE',...
264         'stable planar RE','unstable spatial RE','stable spatial RE');
265 elseif max(size(U))>=1
```

```
266     legend([h_1,h_2,h_4], 'unstable planar RE', 'stable planar RE', ...
267             'unstable spatial RE');
268 elseif max(size(X))>=1
269     legend([h_1,h_2,h_5], 'unstable planar RE', 'stable planar RE', ...
270             'stable spatial RE');
271 else max(size(UP))>=1 && max(size(XP))>=1
272     legend([h_1,h_2], 'unstable planar RE', 'stable planar RE');
273 end %Otherwise add more options for legend before end.
274 xlabel('Angular momentum')
275 ylabel('Total energy')
276 hold off;
277
278 %Output 2: C-R diagram for planar
279 figure(2)
280 %planar unstable
281 if max(size(UP))>=1 && max(size(WP))>0
282     hold on;
283     h_7=plot(UP,VP, 'bs', 'MarkerSize', 5);
284 end;
285 %planar stable
286 if max(size(XP))>=1 && max(size(ZP))>0
287     hold on;
288     h_8=plot(XP,YP, 'rv', 'MarkerSize', 5);
289 end;
290 %planar spectrally stable
291 if max(size(SP))>=1
292     hold on;
293     h_9=plot(SP,PP, 'yd', 'MarkerSize', 5);
294 end;
```

```
295 if max(size(UP))>=1 && max(size(XP))>=1 && max(size(SP))>=1
296     legend([h_7,h_8,h_9], 'unstable planar RE', 'stable planar RE', ...
297         'spectrally stable planar RE');
298 elseif max(size(UP))>=1 && max(size(XP))>=1
299     legend([h_7,h_8], 'unstable planar RE', 'stable planar RE');
300 elseif max(size(UP))>=1
301     legend([h_7], 'unstable spatial RE');
302 elseif max(size(XP))>=1
303     legend([h_8], 'unstable spatial RE');
304 end
305 xlabel('Angular momentum')
306 ylabel('Distance between m_1 and m_2')
307 hold off;
308
309
310 %Output 3: If spatial solutions exist, this is the diagram for CR
311 if max(size(U))>=1 || max(size(X))>=1 || max(size(S))>=1
312     % % C-R diagram for spatial
313     figure(3)
314     %spatial unstable
315     if max(size(U))>=1 && max(size(W))>=1
316         hold on;
317         h_14=plot(U,V, 'bs', 'MarkerSize', 5);
318     end;
319     %spatial stable
320     if max(size(X))>=1 && max(size(Z))>=1
321         hold on;
322         h_15=plot(X,Y, 'rv', 'MarkerSize', 5);
323     end;
```



```

324 %spatial spectrally stable
325 if max(size(S))>=1
326     hold on;
327     h_16=plot(S,P,'yd','MarkerSize',5);
328 end;
329 if max(size(U))>=1 && max(size(X))>=1 && max(size(S))>=1
330     legend([h_14,h_15,h_16],'unstable spatial RE',...
331           'stable spatial RE','spectrally stable spatial RE');
332 elseif max(size(U))>=1 && max(size(X))>=1
333     legend([h_14,h_15],'unstable spatial RE','stable spatial RE');
334 elseif (size(U))>=1
335     legend([h_14],'unstable spatial RE');
336 elseif max(size(X))>=1
337     legend([h_15],'stable spatial RE');
338 end
339 xlabel('Angular momentum')
340 ylabel('Distance between m_1 and m_2')
341 hold off;%%add spect to legend
342 end
343
344 %Output 4: If spatial solutions exist, this is the diagram for CZ
345 if max(size(ZU))>=1 || max(size(ZS))>=1 || max(size(ZSP))>=1
346     figure(4)
347     %spatial unstable
348     if max(size(U))>=1 && max(size(W))>0
349         hold on;
350         h_10=plot(U,ZU,'bs','MarkerSize',5);
351     end;
352     %spatial stable

```

```
353     if max(size(X))>=1 && max(size(Z))>0
354         hold on;
355         h_11=plot(X,ZS,'rv','MarkerSize',5);
356     end;
357     %spatial spectrally stable
358     if max(size(S))>=1
359         hold on;
360         h_12=plot(S,ZSP,'yd','MarkerSize',5);
361     end;
362     if max(size(ZU))>=1 && max(size(ZS))>=1 && max(size(ZSP))>=1
363         legend([h_10,h_11,h_12],'unstable spatial RE',...
364             'stable spatial RE','spectrally stable spatial RE');
365     elseif max(size(ZU))>=1 && max(size(ZS))>=1
366         legend([h_10,h_11],'unstable spatial RE','stable spatial RE');
367     elseif max(size(ZU))>=1
368         legend([h_10],'unstable spatial RE');
369     elseif max(size(ZS))>=1
370         legend([h_11],'stable spatial RE');
371     end
372     xlabel('Angular momentum')
373     ylabel('Distance from m_3 to the origin')
374     hold off;
375 end
376
377 TimeSpent=toc;
```

Using the functions

```

1
2 function f = f.fcn(R,a,d,alpha,beta)
3
4     f=-a./R.^alpha + d./R.^beta;
5
6 end

```

```

1 function g = g.fcn(R,z,a,b,d,e,alpha,beta)
2
3     g=-(a+b)./(2.*(R.^2./4.+z.^2).^ (alpha/2)) + ...
4         (d+e)./(2.*(R.^2./4.+z.^2).^ (beta/2));
5
6 end

```

We find all values for r_e

```

1 eqn=(c^2/(m.*R.^3)-diffF);
2
3 %Find all solutions for R numerically
4 allsolutionsR=(feval(symengine, 'numeric::solve', eqn,R));

```

We ensure the distance between the atoms (r_e) is positive

```

1 %Find all of the real and positive values
2
3 for q=1:max(size(allsolutionsR));

```

```

4     p(q)=imag(allsolutionsR(q));
5     if p(q)==0; %If the value is real
6         if allsolutionsR(q)>0; %distance must be positive
7
8             allsolnsforx
9
10            %determine how many z values are real and positive and
11            %satisfy the equation, then store the individual values
12            allpossolforx
13        end;
14    end;
15 end;

```

We find all values for z_e

```

1 eqn=diffx;
2
3 allsolutionsx=(feval(symengine, 'numeric::solve', eqn,x));

```

We ensure these values are valid

```

1 for j=1:max(size(allsolutionsx));
2     k(j)=imag(allsolutionsx(j));
3     if k(j)==0; %If the value is real
4         if allsolutionsx(j)>0; %must be positive
5             if (allsolutionsx(j)^2-allsolutionsR(q)^2/4)>=0
6                 next=(allsolutionsx(j)^2-allsolutionsR(q)^2/4)^(1/2);

```

```

7
8         Rvalue=[Rvalue allsolutionsR(q)];
9         Cvalue=[Cvalue c];
10        zvalue=[zvalue next];
11        end
12    end;
13 end;
14 end;

```

We find the total energy of the system at each solution $(r_e, z_e, 0, 0; c)$

```

1 %Find the energy corresponding to each RE and angular momentum
2 HredR=Hred(Rvalue(p), zvalue(p), 0, 0, Cvalue(p), m, n, a, b, d, e, alpha, beta);
3 Hredarray=[Hredarray HredR];

```

The stability of each solution is determined

```

1 %Value is stable if V is pos def, i.e. |A|>0 and if A(1,1)>0 If
2 %neither of the above properties are met, then look at the
3 %eigenvalues of the linearization matrix. If each eigenvalue has
4 %real part equal to zero, then spectrally stable. Otherwise
5 %the solution is unstable
6
7 if det(A)>0 && A(1,1)>0
8     %the point is Lyapunov stable
9     X=[X Cvalue(p)];
10    Y=[Y Rvalue(p)];

```

```
11     Z=[Z Hredarray(p)];
12     ZS=[ZS zvalue(p)];
13
14
15 elseif det(A)<=0 || A(1,1)<=0
16     %Linearization Matrix and corresponding eigenvalues
17     HessHredproc
18
19     %If all eigenvalues are purely complex, then spect stable.
20     if real(lambda(1,1))==0 && real(lambda(2,1))==0 && ...
21         real(lambda(3,1))==0 && real(lambda(4,1))==0
22         S=[S Cvalue(p)];
23         P=[P Rvalue(p)];
24         Q=[Q Hredarray(p)];
25         ZSP=[ZSP zvalue(p)];
26         warning('This is a good sign.');
```

%If at least one of them are not purely complex, then unstable

```
27
28 else
29     U=[U Cvalue(p)];
30     V=[V Rvalue(p)];
31     W=[W Hredarray(p)];
32     ZU=[ZU zvalue(p)];
33 end
34 end
```

Bibliography

- [Abraham & al. (1988)] R. ABRAHAM, J. E. MARSDEN AND T. RATIU, *Manifolds, Tensor Analysis, and Applications, Second Edition*, Applied Mathematical Sciences 75 **12**, Springer-Verlag New York Inc, (1988).
- [Berblinger & al. (1988)] M. BERBLINGER, E. POLLAK AND CH. SCHLIER, *Bound states embedded in the continuum of H_3* , Journal of Chemical Physics **88**, 5643, (1988).
- [Berthelot (1889)] D. BERTHELOT, *Sur le Melange des Gaz*, Comptes Rendus de L'Academie des Sciences **126**, 1703-1706, (1889).
- [Bird & al. (1967)] R.B. BIRD, C.F. CURTISS, J.O. HIRSCHFELDER, *Molecular Theory of Gases and Liquids*, Wiley, **2nd Edition**, (1967).
- [Brush (1970)] S.G. BRUSH, *Interatomic forces and gas theory from Newton to Lennard-Jones*, Archives of Rational Mechanics and Analysis **39**, 1-29, (1970).
- [Chambers & al. (1988)] A.V. CHAMBERS AND M.S. CHILD, *Barrier effects on the vibrational predissociation of HD_2^+* , Journal of Molecular Physics **65**, 1337-1344, (1988).

- [Dahleh & al. (2011)] M. DAHLEH, M. DAHLEH, G. VERGHESE, *Lectures on Dynamic Systems and Control, Chapter 13 - Internal (Lyapunov) Stability*, MIT OpenCourseWare: Massachusetts Institute of Technology, (2011).
- [Glendinning (1994)] P. GLENDINNING, *Stability, Instability and Chaos: an introduction to the theory of nonlinear differential equations*, Cambridge Texts in Applied Mathematics **12**, Cambridge University Press, (1994).
- [Gross (2011)] H. GROSS, *Calculus Revisited: Complex Variables, Differential Equations, and Linear Algebra*, MIT OpenCourseWare: Massachusetts Institute of Technology, (2011).
- [Harter & al. (1984)] W.G. HARTER, C.W. PATTERSON, *Rotational Energy Surfaces and High- J Eigenvalue Structure of Polyatomic-Molecules*, Journal of Chemical Physics **80**, 4241-4261, (1984).
- [Harter & al. (1993)] W.G. HARTER, *Principles of Symmetry, Dynamics and Spectroscopy*, Wiley, New York (1993).
- [Holm & al. (2009)] D.D. HOLM, T. SCHMAH AND C. STOICA, *Geometric Mechanics and Symmetry: From Finite to Infinite Dimensions*, Oxford Texts in Applied Mathematics and Engineering, Oxford University Press, **12**, (2009).
- [Kirchner & al. (2012)] B. KIRCHNER, J. VRABEC, *Multiscale Molecular Methods in Applied Chemistry*, Topics in Current Chemistry **307**, Springer-Verlag, (2012).
- [Kozin & al. (1996)] I. N. KOZIN AND I. M. PAVLICHENKOV, *Bifurcation in rotational spectra of nonlinear AB_2 molecules*, Journal of Chemical Physics **104**, No. 1, 4105, (1996).

- [Kozin & al. (1999)] I. N. KOZIN, R.M. ROBERTS AND J. TENNYSON, *Symmetry and structure of rotating H_3* , Journal of Chemical Physics **111**, No. 1, 140-150, (1999).
- [Kozin & al. (2000)] I. N. KOZIN, R.M. ROBERTS AND J. TENNYSON, *Relative equilibria of D_2H^+ and H_2D^+* , Molecular Physics **98**, No. 5, 295-307, (2000).
- [Lim (2003)] T. C. LIM, *The Relationship between Lennard-Jones (12-6) and Morse Potential Functions*, Zeitschrift für Naturforschung **58a**, 615-617, (2003).
- [Lohr (1996)] L. L. LOHR, *Energies and Structures of Rotating Argon Clusters: Analytic Descriptions and Numerical Simulations*, International Journal of Quantum Chemistry **57**, 707-714, (1996).
- [Lorentz (1881)] H.A. LORENTZ, *Über die Anwendung des Satzes vom Virial in der kinetischen Theorie der Gase* Annals of Physics **248**, 127-136, (1881).
- [Meiss (2007)] J.D. MEISS, *Differential Dynamical Systems*, SIAM, (2007).
- [Meyer & al. (1992)] K.R. MEYER AND G.R. HALL, *Introduction to Hamiltonian Dynamical Systems and the N-Body Problem*, Applied Mathematical Sciences **90** **12**, Springer-Verlag New York Inc, (1992).
- [Michel & al. (1997)] L. MICHEL AND B. ZHILINSKII, *Rydberg states of atoms and molecules*, Institut des Hautes Etudes Scientifique (1997).
- [Miller & al. (1996)] M.A. MILLER AND D.J. WALES, *Structure, rearrangements and evaporation of rotating atomic clusters*, Journal of Molecular Physics **89**, 533-554, (1996).

- [Nagle & al. (2008)] R. NAGLE, E. SAFF, A. SNIDER, *Fundamentals of Differential Equations and Boundary Value Problems*, Pearson Education, Inc, **12**, 5th Edition, Pearson Education, (2008).
- [Pavlichenkov & al. (1988)] I.M. PAVLICHENKOV, B. I. ZHILINSKII, *Critical phenomena in rotational spectra*, Annals of Physics **184**, 1-32, (1988).
- [Percival & al. (1982)] I. PERCIVAL AND D. RICHARDS, *Introduction to Dynamics*, Cambridge University Press, **12**, Cambridge University Press, (1982).
- [Perko (2001)] L. PERKO, *Differential Equations and Dynamical Systems*, Texts in Applied Mathematics, **7**, Springer Science + Business Media, LLC, (2001).
- [Schmah & al. (2006)] T. SCHMAH AND C. STOICA, *Stability for Lagrangian relative equilibria of three-point-mass systems*, Institute of Physics Publishing; Journal of Physics: Mathematical and General **39**, 14405-14425, (2006).